



# Integrative characterisation of the Northwestern European species of *Anacharis* Dalman, 1823 (Hymenoptera, Cynipoidea, Figitidae) with the description of three new species

Jonathan Vogel<sup>1</sup>, Mattias Forshage<sup>2</sup>, Saskia B. Bartsch<sup>1</sup>, Anne Ankermann<sup>1</sup>,  
Christoph Mayer<sup>1</sup>, Pia von Falkenhausen<sup>1</sup>, Vera Rduch<sup>1</sup>, Björn Müller<sup>1</sup>,  
Christoph Braun<sup>1</sup>, Hans-Joachim Krammer<sup>1</sup>, Ralph S. Peters<sup>1</sup>

**1** Leibniz Institute for the Analysis of Biodiversity Change, Museum Koenig Bonn, Adenauerallee 127, 53113 Bonn, North Rhine-Westphalia, Germany **2** Swedish Museum of Natural History, Department of Zoology, P.O. Box 50007, 104 05 Stockholm, Stockholms län, Sweden

Corresponding author: Jonathan Vogel (j.vogel@leibniz-lib.de, jvogel.hym@gmail.com)

---

Academic editor: Miles Zhang | Received 5 July 2024 | Accepted 24 July 2024 | Published 29 August 2024

---

<https://zoobank.org/EA190992-B01B-4F1B-A362-A4549C725580>

---

**Citation:** Vogel J, Forshage M, Bartsch SB, Ankermann A, Mayer C, von Falkenhausen P, Rduch V, Müller B, Braun C, Krammer H-J, Peters RS (2024) Integrative characterisation of the Northwestern European species of *Anacharis* Dalman, 1823 (Hymenoptera, Cynipoidea, Figitidae) with the description of three new species. Journal of Hymenoptera Research 97: 621–698. <https://doi.org/10.3897/jhr.97.131350>

---

## Abstract

The genus *Anacharis* Dalman, 1823 comprises parasitoid wasps that target early instars of brown lacewing larvae (Neuroptera: Hemerobiidae). So far, five species were recognised from the Western Palaearctic region, of which four are reported from Northwestern Europe.

In this study, we address the Northwestern European species diversity of the genus with an extended integrative taxonomy toolkit. A total of 700 specimens were examined for their external morphology, including the relevant type specimens. For 354 specimens, we obtained CO1 barcode sequences and applied three molecular species delimitation methods. All DNA barcode data are made publicly available via the German Barcode of Life (GBOL) and Barcode of Life Data system (BOLD) database. In addition, we examined images of Wing Interference Patterns (WIPs), examined the male genitalia and performed multivariate morphometric analyses.

The analyses revealed two clusters which we describe as the *immunis* and *eucharioides* species groups based on differences in DNA barcode, external morphology, WIPs and size of the male genitalia. Furthermore, we complement the diagnosis of the genus *Anacharis* and describe three new species,

*Anacharis martinae* Vogel, Forshage & Peters, **sp. nov.**, *Anacharis maxima* Vogel, Forshage & Peters, **sp. nov.** and *Anacharis minima* Vogel, Forshage & Peters, **sp. nov.** Finally, we synonymise *A. fergussoni* Mata-Casanova & Pujade-Villar, 2018, **syn. nov.** with *A. eucharoides* (Dalman, 1818), and we reinstate *A. ensifer* Walker, 1835, **stat. rev.**, *A. typica* Walker, 1835, **stat. rev.** and *A. petiolata* Zetterstedt, 1838, **stat. rev.** as valid species. In total, we recognise nine Northwestern European species to which we provide an identification key.

The species of *Anacharis* are morphologically very variable. Morphometric analyses alone did not provide information sufficient to delimit species, neither did analyses of WIPs and male genitalia, with few notable exceptions. Analyses of molecular sequence data proved crucially helpful to reliably delimit species and to find morphological diagnostic characters in a reverse taxonomy approach. For delimiting species groups, all included analyses proved helpful, and we show that exploring an extended integrative taxonomy toolkit can be beneficial for a comprehensive characterisation of species. We acknowledge that a complete overview of species distributions, and characterisation of ecological niches & host records is still required to deeply understand the genus as a whole, yet our results already allow broad access to and inclusion of *Anacharis* species in downstream biodiversity research.

## Keywords

CO1 barcoding, integrative taxonomy, male genitalia, morphometrics, Western Palaearctic, WIPs

## Introduction

*Anacharis* Dalman, 1823 (Figitidae: Anacharitinae) is a genus of parasitoid wasps that target early instar larvae of brown lacewings (Neuroptera: Hemerobiidae) as hosts. Specimens of the genus *Anacharis* can be quite common in Malaise trap or sweep net samples and are clearly the most common representatives of Anacharitinae in the Western Palaearctic region. They are typically found on or near vegetation in various habitats (herbs, shrubs, canopy of deciduous and coniferous trees) in which their hosts occur (Walker 1835; Handlirsch 1886; Aspöck et al. 1980; Miller and Lambdin 1985; Cave and Miller 1987; label data, own experience).

Until recently, only two species were recognised as valid for the Western Palaearctic region: *A. eucharoides* (Dalman, 1818) and *A. immunis* Walker, 1835, with a large number of names regarded as junior-synonyms of either of the two (Fergusson 1986). In 2018, the Palaearctic (and Indomalayan) species were revised, leading to a more detailed picture of the studied region's fauna (Mata-Casanova et al. 2018). Three new species, *A. belizini* Mata-Casanova & Pujade-Villar, 2018, *A. fergussoni* Mata-Casanova & Pujade-Villar, 2018 and *A. norvegica* Mata-Casanova & Pujade-Villar, 2018 were described and the already known species re-described. All treated taxa were integrated in a new dichotomous key that was based on previously unrecognised diagnostic characters. With this addition to the taxonomic knowledge of Western Palaearctic species, the total number of species in Western Palaearctic *Anacharis* was raised to five (*A. immunis*, *A. norvegica*, *A. eucharoides*, *A. fergussoni*, *A. parapsidalis*), of which four (all except *A. parapsidalis*) occur in Northwestern Europe. In addition, Mata-Casanova et al. (2018) treated two species, *A. antennata* and *A. belizini*, from the Indomalayan region. The revision was based on morphological data only.

In this study, we re-target the Northwestern European fauna of *Anacharis* by examining several hundred specimens, including relevant type specimens. For the first time for this genus we analyse CO1 barcode data in addition to examination of external morphology, and also include analyses of wing interference patterns, examination of dissected male genitalia and multivariate morphometrics. We aimed to characterise the species present in the study region but also to explore an extended integrative taxonomy toolkit in this challenging parasitoid wasp taxon, following the principle of a unified species concept as described by De Queiroz (2007).

We generated high quality DNA barcode data in the framework of the GBOL III: Dark Taxa project (Awad et al. 2020; Hausmann et al. 2020). The sequences and the respective metadata of the specimens are made publicly available at the GBOL (<https://data.bolgermany.de/ergebnisse/results>) and BOLD reference database (boldsystems.org). We applied automated species delimitation methods, namely ASAP (Puillandre et al. 2021), multirate PTP (Kapli et al. 2017), and objective clustering by using species identifier (Meier et al. 2006) on the barcode data and used the results as taxonomic orientation in a reversed taxonomy approach (Markmann and Tautz 2005). This allowed us to draw informed conclusions about species limits and connect these integratively composed species hypotheses with historical names by comparing our voucher specimens to type specimens.

The first character we explored in addition to morphological examination and analyses of DNA barcodes, are Wing Interference Patterns (WIPs), which are a property of insect wings. Especially wings of smaller insects show a remarkable array of colourful patterns on their wing membranes if the lighting conditions are right. The differences in colour and extent of each pattern is largely determined by the thickness and texture of the wings. Shevtsova and Hansson (2011) investigated WIPs for their potential in species delimitation within the genus *Achrysocharoides* Girault, 1913 (Chalcidoidea: Eulophidae), and the patterns were shown to be consistent within species. In the past decade, taxonomic studies of different parasitoid wasp taxa occasionally included WIPs in their species treatments (e.g. Buffington and Condon 2013; Buffington and Forshage 2014; Moser et al. 2023), while other studies highlighted their use for species delimitation in combination with machine-based analyses (Hosseini et al. 2019; Cannet et al. 2022, 2023; Jin et al. 2023). In Cynipoidea, the WIPs were shown to exhibit phylogenetically conserved patterns and their use for species delimitation was proposed for *Ganaspidium* Weld, 1952 (Figitidae) and *Andricus* Hartig, 1840 (Cynipidae) but never tested (Buffington and Sandler 2011). Here, we present the first larger-scale analysis of WIPs in Cynipoidea.

Little is known about the function of WIPs and their role might vary from group to group. They are hypothesised to be used for communication with conspecifics in, for example, courtship and mating of *Drosophila* Fallén, 1823 (Katayama et al. 2014; Hawkes et al. 2019) and *Pteromalus cassotis* Howard, 1889 (Shevtsova et al. 2011), and for signalling habitat occupation in fig wasps (Shevtsova et al. 2011).

The second character complex we explored here is the morphology of male genitalia. In recent years, the analysis of male genitalia of parasitoid wasps went through a renais-

sance. Studies made progress in describing genitalia morphology, facilitating comparison between various lineages, for example, Ceraphronoidea and Ichneumonoidea (Mikó et al. 2013; Dal Pos et al. 2023) and identifying homologous structures to the more complex ancestral apparatus of the Symphyta (Schulmeister et al. 2002). The male genitalia of parasitoid wasp taxa have been used as diagnostic character complexes in parasitoid wasp taxonomy, for example in Ceraphronoidea (Mikó et al. 2013; Trietsch et al. 2018; Salden and Peters 2023), Chalcidoidea: Trichogrammatidae (Hayat 2009; Polaszek et al. 2022) and Ichneumonoidea: Braconidae: Agathidinae (Žikić et al. 2011). The male genitalia of the superfamily Cynipoidea (e.g. Ronquist and Nordlander 1989; Fontal-Cazalla et al. 2002) are less complex than those of Ceraphronoidea (e.g. Salden and Peters 2023) and Symphyta (e.g. Schulmeister et al. 2002). The morphology of the male genitalia was used in a cladistic analysis of the figtitid subfamily Eucoilinae (Fontal-Cazalla et al. 2002). However, the potential of male genitalia for species or species group delimitation in Cynipoidea has not been evaluated yet and is explored here for the first time.

As a third line of enquiry, we explored multivariate analyses of morphometric characters. Morphometric characters and ratios are routinely applied by taxonomists to complement species' diagnoses and descriptions (e.g. van Achterberg and Shaw 2016; Mata-Casanova et al. 2018). Further, multivariate morphometric analysis can be used to extract the character ratios with the most diagnostic value and proved therefore invaluable to characterise species (e.g. Baur 2015; Janšta et al. 2020). Here, we apply multivariate morphometric analyses following Baur and Leuenberger (2011) for delimitation of species and species groups in *Anacharis*.

With this study we contribute to a clearer picture of the diversity of the North-western European *Anacharis* species, their intraspecific morphological variability, and show the potential of still relatively unexplored character traits for their use in alpha-taxonomical studies. Moreover, we refine the diagnosis of the genus and diagnose two species groups. The results of this work convey the release of the currently most comprehensive and taxonomically evaluated CO1 DNA barcode sequence dataset of *Anacharis* worldwide.

## Material and methods

### Institutional abbreviations

<b>CNC</b>	Canadian National Collection of Insects, Arachnids and Nematodes, Ottawa, Canada
<b>MGAB</b>	Muzeul Național de Istorie Naturală Grigore Antipa, Bucharest, Romania
<b>MHNG</b>	Muséum d'Histoire Naturelle, Genève, Switzerland
<b>MZLU</b>	Zoological Museum Lund, Sweden
<b>NHMUK</b>	Natural History Museum, London, United Kingdom
<b>NHRS</b>	Naturhistoriska riksmuseet, Stockholm, Sweden
<b>NMBE</b>	Naturhistorisches Museum Bern, Switzerland

<b>SDEI</b>	Senckenberg Deutsches Entomologisches Institut, Müncheberg, Germany
<b>ZFMK</b>	Leibniz Institute for the Analysis of Biodiversity Change, Museum Koenig Bonn, Germany
<b>ZMHB</b>	Museum für Naturkunde, Berlin, Germany
<b>ZMUC</b>	University of Copenhagen, Zoological Museum, Copenhagen, Denmark
<b>ZSM</b>	Zoologische Staatssammlung München, Germany

## Specimens and identification

In total, we acquired 394 fresh ethanol-preserved specimens in the course of the German Barcode of Life project (GBOL III: Dark Taxa) (see Suppl. material 1 for details). In addition, we examined 306 dry-mounted specimens from museum collections. For preparation, mounting and examination, a Leica M205 C stereomicroscope was used. We tentatively identified the specimens following Mata-Casanova et al. (2018) and identified the sexes by the presence of the female ovipositor or male genitalia in cases they were exerted. When they were retracted or obscured because of other reasons, we counted the number of antennomeres (13 in ♀, 14 in ♂). Additionally, the sexes were differentiated by the shape of the 7st metasomal sternite (7st) and tergite (7tg) as follows: The 7st of the female (hypopygium) is keel-shaped and has a longitudinal line of setae directly lateral to the ventral edge on each side. It is laterally overlapping the 7tg, which is dorsally more or less straight so that 6tg seamlessly transitions into 7tg in lateral view. The 7st of the male is ventrally flattened with a setal patch covering the surface. It is not overlapping the 7tg, which is distinctly sloping posteriorly. In consequence the male metasoma appears more “loaf-shaped” with a straight ventral delimitation and an almost even posteroventral angle with a sharp posterior slope; and the female metasoma appears more lens-shaped with a convex ventral side and posteriorly a somewhat sharp angle. Also, the female metasoma is relatively larger, and the petiole is distinctly shorter than in males of the same species. Beyond these characters, males and females of *Anacharis* look remarkably similar and can be treated together in diagnoses and descriptions.

We cite the label information of the historical type specimens verbatim in congruence with the Example 1 of the Darwin Core term “verbatimLabel” (i.e. citing one label per line, with personal interpretations of ambiguous label contents in square brackets, see <https://dwc.tdwg.org/examples/verbatimLabel> for details). All other specimens are cited as recommended by the journal’s author guidelines and separated into 1. type material, 1.1 primary type specimen(s), 1.2 secondary type specimen(s) and 2. other material, 2.1 DNA barcode vouchers, 2.2 Material without DNA Barcode.

All specimens are deposited at the ZFMK if not indicated otherwise. The specimen database, using Darwin Core terms, is attached as Suppl. material 1.

For the vertical distribution of each species we only accounted for the specimens where either elevation, coordinates or both were given on the labels and are likely biased when extreme statements are made. Especially those statements about lowland preference are affected due to the Swiss specimens that usually lack this information.

## Terminology

The terminology used herein follows Ronquist and Nordlander (1989) for external morphological terms and Harris (1979) for surface sculpture terms.

One character is newly defined here:

posteroventral hypocoxal furrow = The posteroventral groove of the mesopleuron that is located just before the insertion of the mid coxa (e.g. Fig. 17B).

## Imaging

For imaging of the specimens, we used a Canon EOS 7D<sup>®</sup> camera mounted on a P-51 Cam-Lift (Dun, Inc.). For lighting, we used a bidirectional flashlight arrangement set to medium intensity for habitus- and maximum intensity for detail-shots. We placed a sandwich paper-coated acrylic glass tube (ca. 6 cm diameter) around the specimen for light diffusion. The aperture was set as high as possible without underexposing the specimen. The image series were evaluated in ADOBE LIGHTROOM<sup>®</sup> v.5.6 and stacked with HELICON FOCUS<sup>®</sup> v.8.2.2.

For the SEM imaging, we mounted the heads of two specimens (*Anacharis petiolata*: ZFMK-HYM-00039676 and *Aegilips* sp.: ZFMK-HYM-00039677) on specimen holder stubs for gold coating with a Cressington Sputtercoater 108auto. The SEM images were then generated using a Zeiss Sigma 300VP system with the settings shown in Fig. 4A–D respectively. After the imaging, we mounted the gilded heads to the side of the cardboard of the corresponding specimens.

## DNA sequencing and molecular species delimitation

We performed non-destructive full-body DNA extractions from our specimens at the Center for Molecular Biodiversity Research (ZMB) at the ZFMK. The mtDNA barcode region of the CO1 gene was amplified by using the LCO1490-JJ forward and HCO2198-JJ reverse primer (Astrin and Stüben 2008) and the PCR protocol as described in Jafari et al. (2023). The sequences of both reads were assembled to a consensus sequence in GENEIOUS Prime v.2022.1.1 (Biomatters Ltd.). We kept and used those sequences for downstream analyses if they fulfilled the GBOL gold standard (i.e. consensus sequences have 1.  $\geq$  500 base pairs sequence length, 2. a high quality bin assignment, and 3.  $\leq$  1% disagreements and ambiguities, see Jafari et al. 2023 for more details). In addition to our own sequences (tagged with “ZFMK-TIS-...”), we accessed 71 *Anacharis* spp. CO1 sequences from BOLD (Ratnasingham and Hebert 2007), which were at least 500 bp long. They originate from Germany (65), Belarus (3), and Norway (3). We aligned the sequences using the built-in MUSCLE alignment algorithm with a maximum of 8 iterations (Edgar 2004) in GENEIOUS. The herein produced DNA barcode sequences can be accessed via bolgermany.de (German Barcode of Life Consortium 2011) and on boldsystems.org. Respective BOLD-IDs of all

sequences we used can be found in Suppl. material 1 for the specimens that were studied morphologically as well and Suppl. material 2 for the sequences that we accessed via BOLD and did not study the morphology of the respective specimens.

Using IQ-TREE v2.2.2.6 (Minh et al. 2020), we reconstructed a maximum likelihood tree and calculated ultrafast bootstrap support with 1000 replicates (Hoang et al. 2018) without further specifications. For species delimitation, the ASAP species delimitation algorithm (via <https://bioinfo.mnhn.fr/abi/public/asap/>, default settings, accessed 26<sup>th</sup> February 2024; Puillandre et al. 2021) and the Clustering function of Species Identifier v.1.6.2 (Meier et al. 2006) set to a 3% threshold (hereafter referenced as SpID) was applied to our alignment and multirate PTP (hereafter referenced as mPTP, Kapli et al. 2017) via a web server (<https://mptp.h-its.org/#/tree>, 26<sup>th</sup> February 2024) was applied to the tree file that was previously rooted with an outgroup sequence (*Aegilips* sp., BOLD-ID: CNKLH2372-15) in Figtree v1.4.4 (Andrew Rambaut, available at <http://tree.bio.ed.ac.uk/software/figtree/>). Fig. 1 was then composed in INKSCAPE v.1.3 (Inkscape project) by combining the final tree and the species delimitation results.

For the molecular characterisation of species (see species treatments), we analysed the distance matrix from the alignment provided in GENEIOUS to extract maximum intraspecific distances and minimum interspecific distances, stating the name of the closest species in parentheses. The consensus sequence was generated by aligning the sequences of each species separately in GENEIOUS. For the molecular characterisation we only used the sequences of those specimens that we also studied morphologically, i.e. excluding the sequences downloaded from BOLD.

## WIPs analysis

We performed all steps of a WIP preparation and imaging protocol for small ethanol-preserved insect (wasp) specimens (DOI: [dx.doi.org/10.17504/protocols.io.bp2l6xxy1lqe/v1](https://doi.org/10.17504/protocols.io.bp2l6xxy1lqe/v1)) published along with this manuscript. In short, the protocol covers instructions for the following steps:

### Section 1 - Slide preparation

Descriptions of how to dissect the wings, get fore and hind wing centrally positioned on a microscopic slide for better standardisation and prepare the slide for long term storage in a natural history collection.

### Section 2 - Imaging

Information on the camera system we used, the settings and how the raw images of the WIPs were acquired.

### Section 3 - Image processing

All steps to manually adjust the image values to make the WIPs stand out (cf. Fig. 2) and to automatically remove the background, left-align and position the fore and hind wing in standardised angles to each other to make the series of images utilisable for, e.g. machine learning applications.

In this study, we applied the following specifications to the protocol:

We used an Olympus SZX12 for a first batch of 179 preparations and a Leica M205 C for stereo microscope for a second batch of 37 preparations.

The first 179 wing dissections were done prior to DNA lysis and the wings were kept in ethanol tubes until further processing.

As background for imaging the WIPs, we used a cardboard painted with “ultrablack” Musou black from KOYO Orient Japan Co., Ltd., which absorbs up to 99.4% of light (according to the manufacturer).

The steps of section 3 (image processing) were followed only for the WIPs images shown in Fig. 2. Re-sizing the images to put them to scale was not necessary as the magnification during photography and the resulting resolution was the same for the entire series. For all other images, the raw images were used to compare WIPs within and between the species by eye.

By publishing the protocol for wing preparation and WIPs imaging from ethanol-preserved (small) insect specimens, we tried to provide standardisation for the necessary steps, specifically to a) produce standardised, artifact-free and high-quality WIP images, b) secure long-term-storage of the specimens, c) make the prepared wings re-traceable to the specimens they have been taken from, d) secure reproducibility of the imaging even decades after preparation (i.e. easy cleaning of the wing specimens prior to imaging), and to e) allow reproduction of the protocol with minimal financial resources. In all these aspects, there is undeniably room for improvement, yet we deliberately published the protocol on protocols.io. All interested parties are thereby invited to contribute to an optimised protocol. This will allow integration of WIPs in further applications such as advanced statistical or machine learning methods aiming at automated species identification.

## Male genitalia

We dissected the genitalia of 21 male specimens. The first 15 genitalia were extracted from metasomas that were dissected prior to the DNA lysis. The remaining six were extracted post-lysis without dissecting the entire metasoma. The genitalia were removed from the metasomas by fixating the metasomas with forceps and scooping out the genital with a minuten pin mounted on a skewer. In most cases, the apical half of the metasoma needed to be cut off as squeezing it did not let the genital capsule extrude. In those cases, we disintegrated the gaster to lay bare the genital. The “remaining” fragments of the gaster were discarded.

We used a Zeiss Axio Imager.Z2m. to produce multi-focus images that were later stacked with Helicon Focus v.8.2.2 (Helicon Soft Ltd.). For the genitalia shown in Fig. 3, the backgrounds of the stack images were removed in GNU image manipulation program v.2.10.34 (GIMP development team, available at [www.gimp.org](http://www.gimp.org)). The genital width and length were determined using these images.

## Morphometrics

Of a total of 115 specimens, consisting of 68 males and 47 females, we measured 48 external morphological characters. The selection of characters is mainly based on the measurements implemented in Mata-Casanova et al. (2018). The characters measured are listed in Table 1.

For the measurements, a calibrated scale ocular on a Leica M205 C stereomicroscope was used. Of those specimens that lacked wings due to the preparation of WIPs images, the wing length & marginal cell dimensions were measured on the WIPs images digitally using GIMP. As many male metasomas were dissected and/or destroyed prior to the measurements, no metasomal measurements for those specimens could be obtained, except the petiole length in most cases. The complete raw data is attached in Suppl. material 3.

We applied the imputation function of the mice R package (Buuren and Groothuis-Oudshoorn 2011) to account for missing data. For the multivariate morphometric analyses, the measurements of the metasoma, except the petiole length, the antennal measurements, and the male genitalia measurements were excluded (see characters marked with asterisk in Table 1). As 51 of the 68 male gasters could not be measured due to the destruction of the gaster during the extraction of the male genitalia, the resulting gap in the data was too large to be reliably imputed. We excluded the antennal and male genitalia measurements because the deviating number of segments between males (14) and females (13) complicated the downstream analysis and the male genitalia measurements due to both sex-specificity and relatively few measured individuals (21 of 68 males), causing a gap too large to be reliably imputed. The imputed dataset is supplied in Suppl. material 4.

We applied multivariate morphometric analysis based on Baur and Leuenberger (2011, 2020) and Baur et al. (2015) and performed principal component analysis (PCA), linear discriminant analysis (lda) and allometry analyses using R 4.3.3 and the R scripts provided by Baur and Leuenberger (2020).

## Results

### Molecular analyses

We obtained the CO1 barcode sequences of 354 out of 394 specimens (90% success rate). 348 sequences had the full 658 bp DNA barcode length, 6 had shorter sequences with a minimum length of 645 bp.

The numbers of species suggested by the automated species delimitation approaches ranges from seven (spID with 97% similarity threshold and mPTP) to nine (ASAP) (Fig. 1). Only few incongruencies with morphological data are

apparent (Fig. 1); these are presented and discussed in the integrative species treatments below.

Two species groups are apparent from the analyses of the DNA barcode data (see also taxonomic section), with a minimum distance of 16%.

**Table I.** Characters marked with asterisk were excluded from the morphometric analyses..

Character	Orientation	Description
Head length	Lateral	Distance from below the toruli in a right angle to the vertical head axis until the posterior edge of the head
Head width	Frontal and dorsal	Longest distance between the outer delimitation of the eyes.
Head height	Frontal	Distance from ventral clypeal margin to top of ocellar triangle
Malar space length	Frontal	Shortest distance between most dorsal corner of mandibular base to the eye
Eye height	Frontal	Longest distance between ventral margin of eye and the eye dorsally
Eye-to-eye distance	Frontal	= transfacial line in Mata-Casanova et al. (2018) = Shortest distance between eyes
Torulus diameter	Frontal	Diameter of an individual torulus, either left or right
Toruli distance	Frontal	Shortest distance between the toruli
Torulus eye distance	Frontal	Shortest distance between torulus and eye, left or right
Post ocellar line (POL)	Dorsal	Shortest distance between margins of median ocellus and lateral ocellus, either left or right
Ocular ocellar line (OOL)	Dorsal	Shortests distance between margins of lateral ocellus, left or right, and eye
Lateral ocellar line (LOL)	Dorsal	Shortest distance between margins of lateral ocelli
Ocellar Diameter (OD)	Dorsal	Diameter of the median ocellus
Antenna length*	Lateral or dorsal, depending on the positioning of the antenna	Distance from basal margin of scape to the apex of the last antennomere, measured on left or right antenna; in some cases calculated from the sum of the individual segments, as the antennae were too strongly bent
Antennomere length*	Lateral or dorsal, depending on the positioning of the antenna, scape always measured in lateral view	Distance from the basal margin of an antennomere to its apex, measured medially on left or right antenna
Length of mesosoma	Lateral	Distance between most anterior point of pronotum to the most posterior point of the nucha
Mesoscutum length	Dorsal	Longest distance between anterior and posterior margin of the mesoscutum
Mesoscutum width	Dorsal	Longest distance between the lateral margins of the mesoscutum
Mesoscutellum length	Dorsal	Longest median distance from anterior to posterior margin of the mesoscutellum
Fore wing marginal cell length	Dorsal	Distance between transversal section of front wing vein R1 and the intersection of R1 and Rs
Fore wing marginal cell width	Dorsal	Shortest distance between intersection of vein r and Rs and the marginal section of vein R1
Hind coxa length	Lateral	Longest distance between basal annular girdle and apical margin of the metacoxa
Length of metasoma*	Lateral	Longest distance between posterior margin of nucha and posterior margin of the 7 <sup>th</sup> metasomal sternite
Petiole length	Lateral	Distance between anterior constriction of petiole to anterior margin of the 2 <sup>nd</sup> metasomal tergite
Metasomal tergite 2 length*	Lateral	Longest median distance between anterior and posterior margin of the tergite
Metasomal tergite 2 length*	Dorsal	Longest median distance between anterior and posterior margin of the tergite
Metasomal tergite 3 length*	Lateral	Longest median distance between anterior and posterior margin of the tergite
Metasomal tergite 3 length*	Dorsal	Longest median distance between anterior and posterior margin of the tergite
Metasomal tergite 4 length*	Lateral	Longest median distance between anterior and posterior margin of the tergite
Metasomal tergite 4 length*	Dorsal	Longest median distance between anterior and posterior margin of the tergite
Male genital length*	Ventral	Median distance between the anterior parameral plate and the apex of the aedeagus
Male genital aedeagus width*	Ventral	Longest distance between lateral margins of the vertical penis valves

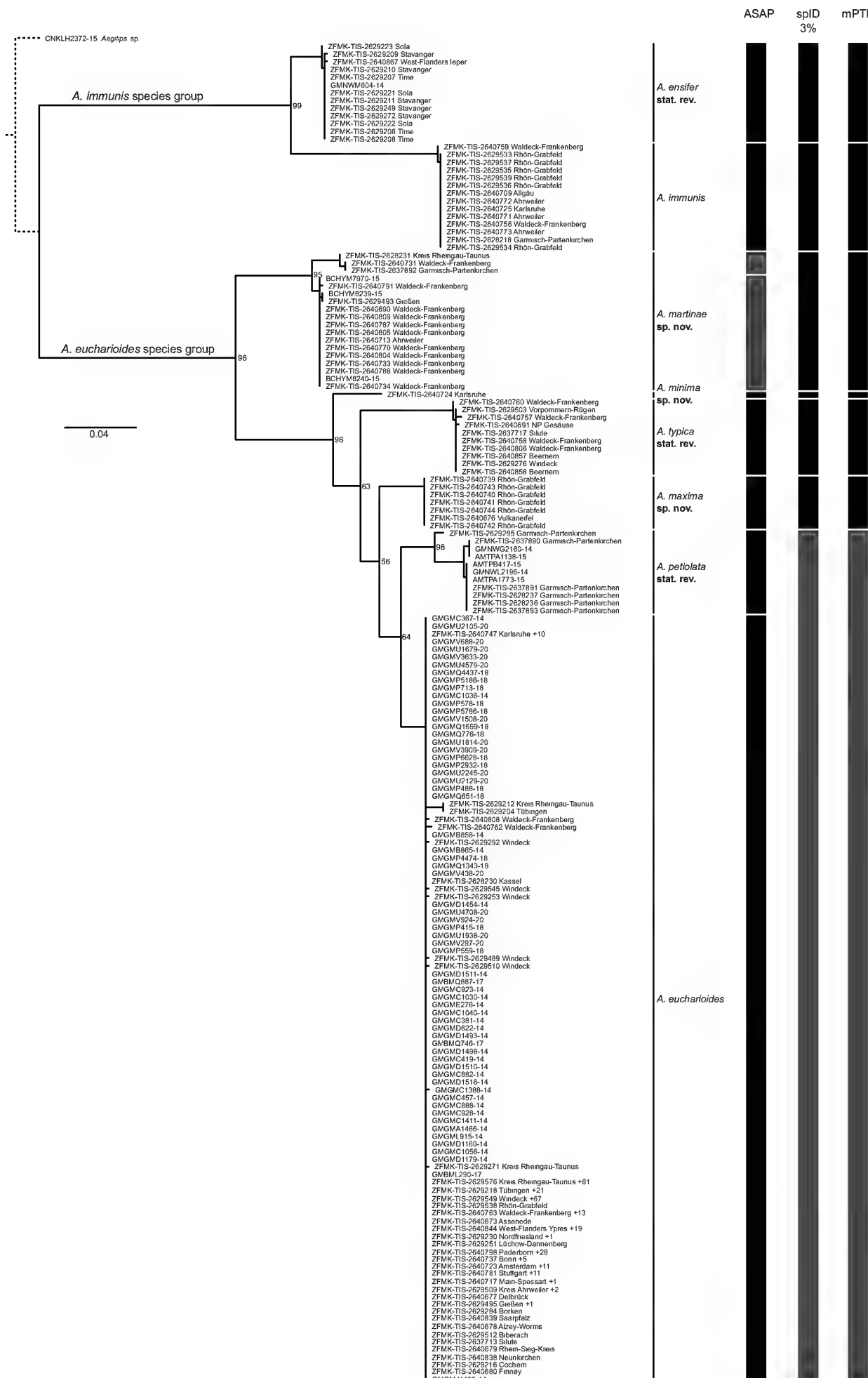


**Figure 1.** Maximum likelihood tree based on DNA barcode data, constructed with IQ Tree. The results of the species delimitation analyses are summarised on the right. Black boxes indicate congruence with our morphological examinations, while the red boxes highlight disagreements. Species and species groups are named according to the results of our integrative taxonomy approach (see corresponding treatments). The dotted line is connecting the outgroup, *Aegilips* sp., to the remaining tree and is not to scale. Identical sequences from the same sites are combined in respective tip labels and are indicated with a (+ n). Ultrafast-bootstrap support is shown on the nodes.

## WIPs

In total, we prepared 186 images of WIPs (145 *A. eucharioides*, 14 *A. norvegica*, 9 *A. martiniae*, 7 *A. immunis*, 6 *A. typica*, 4 *A. maxima*, 1 *A. petiolata*). We could not obtain any image for *A. minima*.

The WIPs exhibit the following general characteristics. The basal and marginal cell of the fore wing is largely pattern-free. The radial area (defined by wing margin, vein  $Rs$ , and the non-sclerotised vein  $M$ ) has an absent to faint pattern of straight to curved purple bands that does not reach the wing apex. How close the band-pattern extends towards the wing apex varies slightly between species. The patterns on the median area (defined by the wing margin and the non-sclerotised veins  $Rs+M$ ,  $M$ ,  $Cu_1$  and  $Cu_{1a}$ ) vary inter- and intraspecifically.

The basal cell of the hind wing is pattern-free. The radial, medial and cubital areas are fused to an apical area (defined by vein  $R1$ ,  $Rs\&1r-m$ , its shortest distance to the wing's hind margin and the wing margin). The pattern of the apical area consists of a

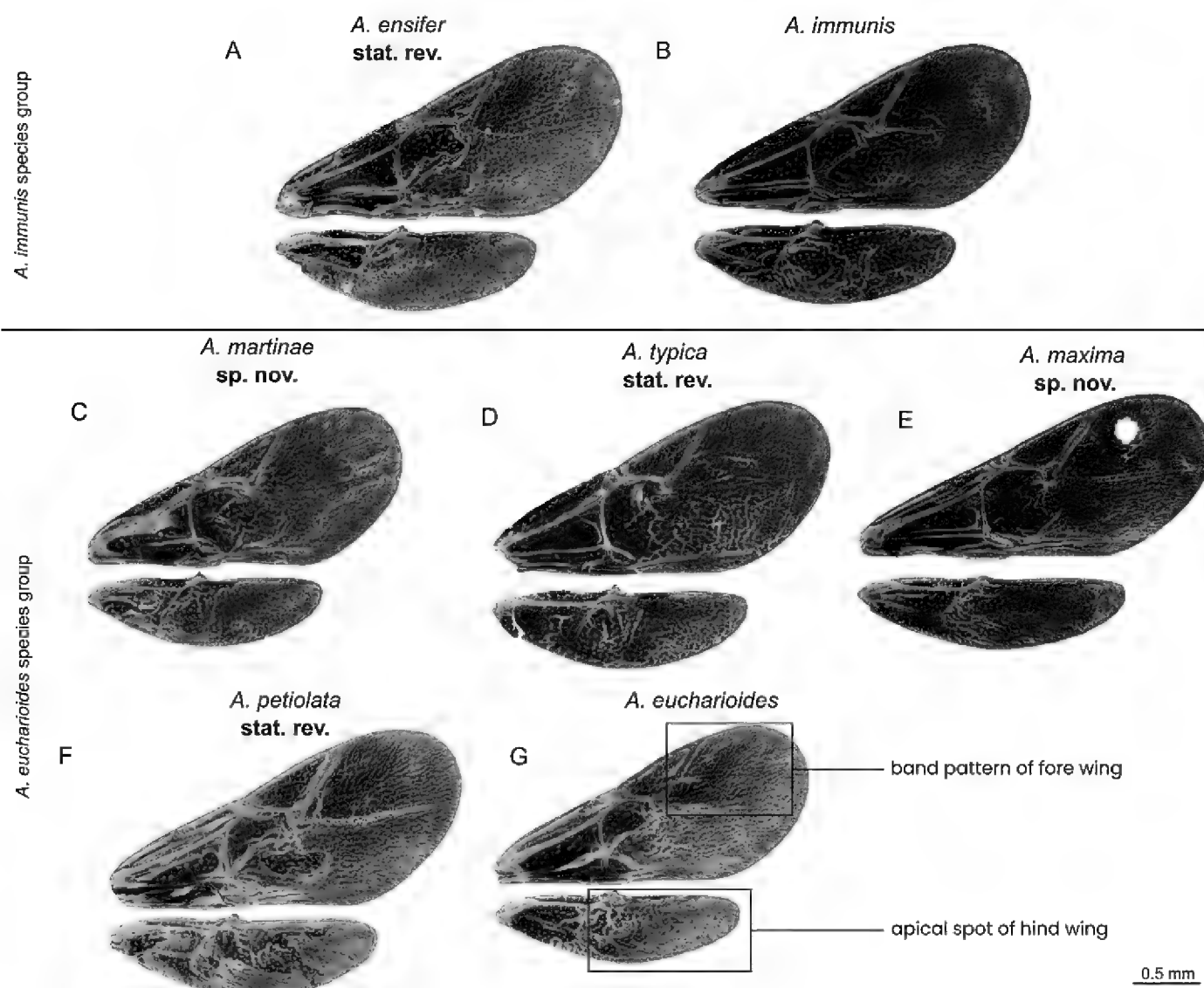


**Figure 2.** Fore and hind wings of different species of *Anacharis* showing the WIPs **A** *A. ensifer* stat. rev. male (ZFMK-TIS-2629206) **B** *A. immunis* male (ZFMK-TIS-2629539) **C** *A. martiniae* sp. nov. female holotype (ZFMK-TIS-2640787) **D** *A. typica* stat. rev. female (ZFMK-TIS-2640857) **E** *A. maxima* sp. nov. male paratype (ZFMK-TIS-2640676) **F** *A. petiolata* stat. rev. female (ZFMK-TIS-2629285) **G** *A. eucharioides* male (ZFMK-TIS-2629201).

spot that is situated at the apex of the wings which is surrounded by colour that does not follow an intraspecifically consistent pattern. The spot is running along the hind margin of the wing to an extent that varies between species groups. The dimensions, i.e. how much of the apical area is filled with the apical spot, partly varies between species (see descriptions of *A. martinae* sp. nov. and *A. maxima* sp. nov.). The basiocubital area (defined by the shortest distance of  $Rs\&1r-m$  to the wing's hind margin,  $M+Cu1$  and the wing margin) is often pattern-free or shows variable patterns.

### Male genitalia

The male genitalia of 21 specimens, representing all species except *A. petiolata* and *A. minima*, were dissected and measured. The post-DNA-lysis genitalia (Fig. 3C–E) turned out more transparent than the non-lysed genitalia (Fig. 3A, B, F). This greatly enhanced the visibility of the sclerotised structures and setae and eliminates the need for an extra maceration step.

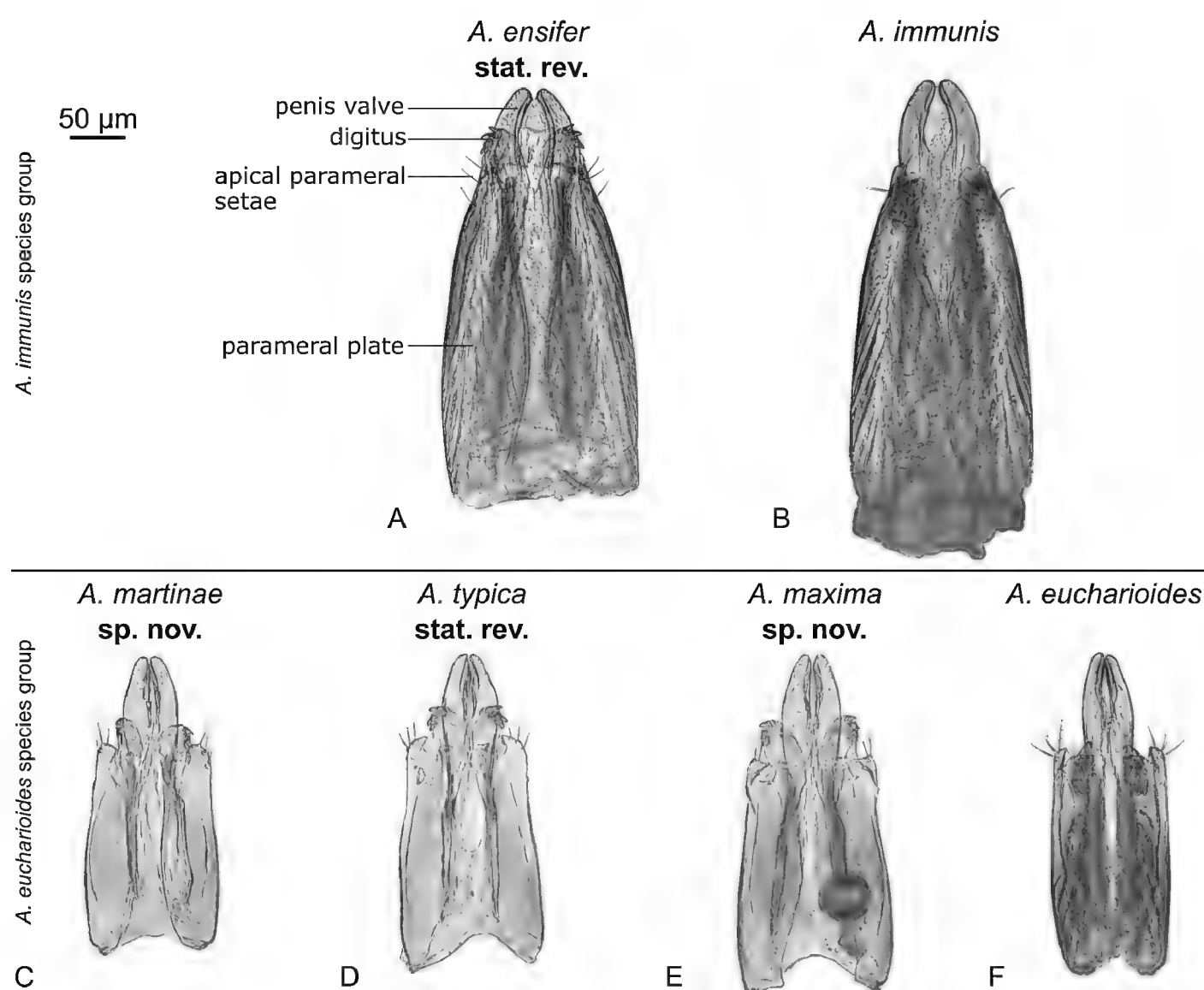


**Figure 3.** Comparison of *Anacharis* male genitalia in ventral view **A** *A. ensifer* stat. rev. (ZFMK-TIS-2629209) **B** *A. immunis* (ZFMK-TIS-2629539) **C** *A. martinae* sp. nov. male paratype (ZFMK-TIS-2640733) **D** *A. typica* stat. rev. (ZFMK-TIS-2640757) **E** *A. maxima* sp. nov., male paratype (ZFMK-TIS-2640741) **F** *A. eucharoides* (ZFMK-TIS-2629243) **A, B, F** were dissected prior to DNA lysis **C, D, E** after lysis.

The overall shape of the genitalia of *Anacharis* is very similar between species (Fig. 3). The genitalia are elongate with clearly protruding penis valves. The digitae are protruding beyond the parameres when stretched out and not protruding when bent. The digitae have two to four apical spines each. Note that due to the often concealed positioning of the digitae, our attempts to determine the absolute number of spines remained inconclusive for most genitalia. The apex of the parameral plate usually has three setae with differences in their respective positions (see diagnoses of the species groups).

The genitalia are 243–423  $\mu\text{m}$  in length, with a distinct difference between the species groups (see treatment section below). We observe consistent species-specific traits in *A. euchariooides* (Fig. 3F) and *A. maxima* sp. nov. (Fig. 3E).

## Multivariate morphometrics

On species group-level, the morphometric analyses almost fully separate two groups in a PCA (Fig. 5 left), and provide two extracted ratios that fully separate the two groups (Fig. 5 right). These results and ratios are used and discussed in the taxonomic treatment of the two species groups below.

On species-level, restricted to the *euchariooides* species group, all species overlap in a PCA when included in the same analyses (Fig. 7). To make interspecific differences better visible and to potentially extract delimitating ratios, we performed pairwise species-level PCA and ratio extractor analyses. Results of three analyses are shown in Fig. 8, representing different levels of separation between species. First, the PCA of *A. euchariooides* against the remaining species of the *euchariooides* group shows wide overlap and no ratios that can reliably separate the species (Fig. 8A). Second, the PCA of *A. martiniae* sp. nov. against the remaining species of the *euchariooides* species groups shows partial overlap and ratios that can separate at least most of the specimens of the two groups (Fig. 8B). Finally, the PCA of *A. maxima* sp. nov. against the remaining species of the *euchariooides* species group shows almost full separation of the species, and the ratio extractor provided two ratios which in combination can fully separate *A. maxima* sp. nov. from all other species (Fig. 8C). The results of the PCA and ratio extractor are used and discussed in the diagnoses and remarks of the species treatments below.

The PCA and ratio extractor results of the additional species-level analyses as well as the results of the allometry tests of all species group- and species-level comparisons are given in Suppl. material 5.

## Taxonomic section

### *Anacharis* Dalman, 1823

*Anacharis* Dalman, 1823 - Type species: *Cynips euchariooides* Dalman, 1818.

*Megapelmus* Hartig, 1840 - Type species: *Megapelmus spheciformis* Hartig, 1840 (= *Anacharis eucharoides* (Dalman, 1818)).

*Synapsis* Förster, 1869 - Type species: *Synapsis aquisgranensis* Förster, 1869 (= *Anacharis immunis* Walker, 1835), homonymous with beetle genus *Synapsis* Bates, 1868.

*Prosynapsis* Dalla Torre & Kieffer, 1910 - Type species: *Prosynapsis aquisgranensis* (Förster, 1869) (= *Anacharis immunis* Walker, 1835) - replacement name for *Synapsis* Förster, 1869, due to the aforementioned homonymy.

**Diagnosis.** The genus *Anacharis* is characterised by an elongate, smooth petiole (sometimes with some vague longitudinal striae, but never sculptured as in *Aegilips* Walker, 1835 and *Xyalaspis* Hartig, 1843). The mesoscutellum does not overhang the propodeum (as sometimes in *Aegilips* and always in *Xyalaspis*). The mesoscutellum is posteriorly rounded, never extended apically (usually pointed in *Aegilips*, pointed or extended into a spine in *Xyalaspis*). The mesoscutellum always possesses a posterior carina that separates the mesoscutellum into a dorsal and posterior surface (circumscutellar carina absent, indistinct or present in *Aegilips* and *Xyalaspis*). The circumscutellar carina is sometimes posteriorly flanged upwards, appearing tooth-like in lateral view (never flanged upwards in *Aegilips* and *Xyalaspis*, if carina is present). The mesopleural line is exhibited as a rugose and/or striate furrow, often extending from the anterior to close to the posterior margin of the mesopleuron (mesopleural sculpture in *Aegilips* and *Xyalaspis* not concentrated in any sort of furrow but equally spread out along anterior margin, sometimes reduced to the anterior half of mesopleuron or totally absent). The metasoma is apically pointed, especially in females (metasoma apically ending more abruptly in *Aegilips* and *Xyalaspis*). The occiput is either smooth, striolate, or striate (smooth in *Aegilips* and *Xyalaspis*). The upper face has a usually shallow to sometimes more distinct median dent (Fig. 4C, usually absent in *Aegilips* and *Xyalaspis* Fig. 4D).

**Etymology and grammatical gender.** Derived from Greek “Ana (ἀνά, up, back, against, above, across, throughout, again, counter)” and “charis (Χάρις, grace, beauty, favour, loveliness)”. Dalman describes *Anacharis* as looking similar to eucharitids (Dalman 1823) and arguably wanted to emphasise them as at least a “counterbeauty” to the eucharitids.

The grammatical gender of *Anacharis* is female (as used in Westwood 1833 and discussed in Reinhard 1860).

**Remarks.** The most recent diagnoses of the genus are presented in van Noort et al. (2015) and Mata-Casanova et al. (2016). The differential diagnosis presented here is a complemented version of the previous diagnoses. It aims to characterise the genus in the Western Palaearctic fauna by differentiating it against *Aegilips* and *Xyalaspis*, which are the only other anacharitine genera known from the Western Palaearctic. The added characters have not been evaluated as to their diagnostic value for the anacharitine fauna outside the Western Palaearctic.

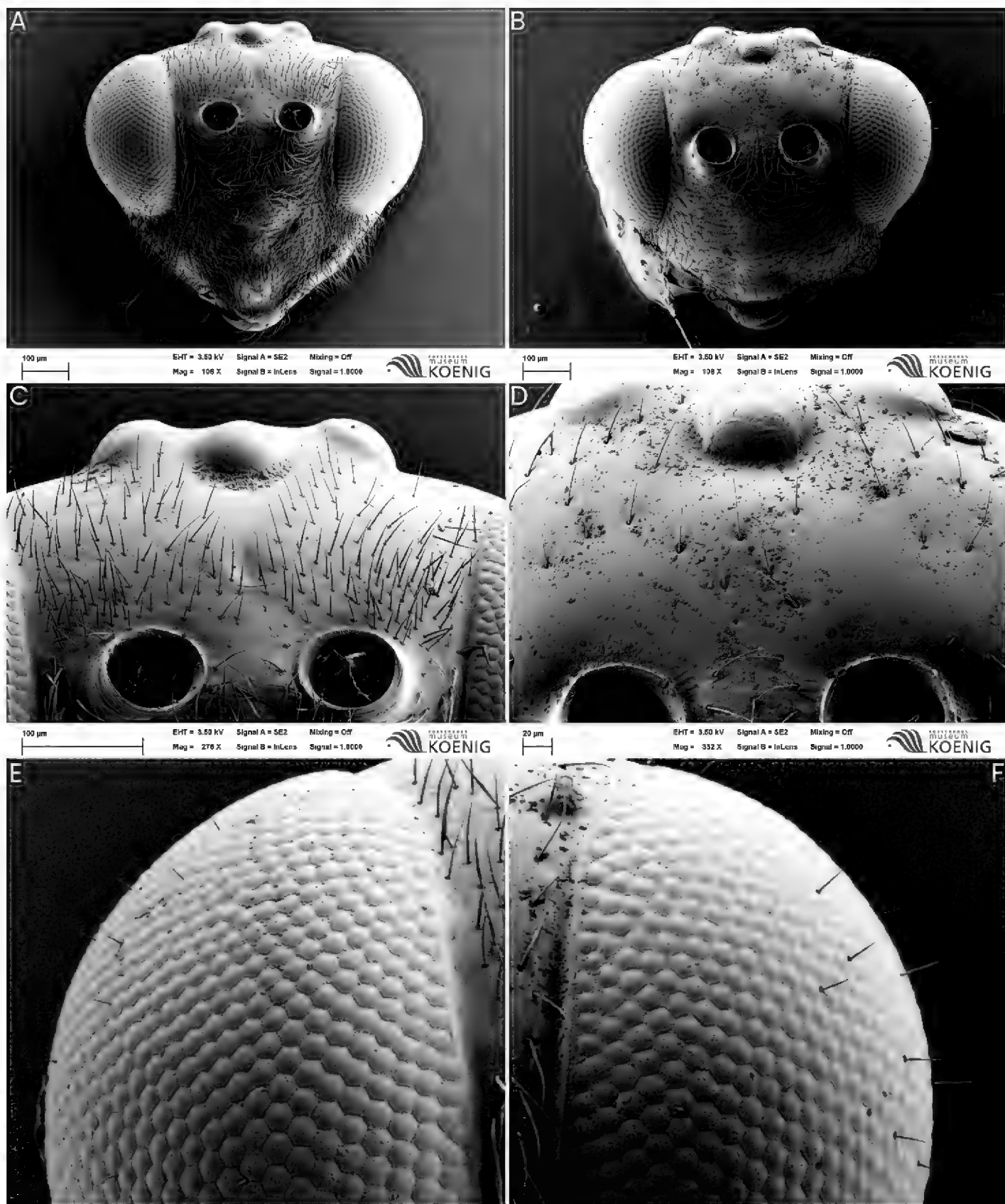


**Figure 4.** SEM images of the heads of *Anacharis typica*: ZFMK-HYM-00039676 (left: **A, C, E**) and *Aegilips* sp.: ZFMK-HYM-00039677 (right: **B, D, F**) with the specifications used for the SEM imaging shown at the bottom of each image (**A–D**) **A, B** overview of the head in frontal view **C, D** Upper face, frontal, showing the median dent typical for *Anacharis* (**C**) and its absence in *Aegilips* sp. (**D**) **E, F** the compound eyes with scattered setae (cropped images from **A** and **B** respectively).

## The species groups

The presence of two groups within *Anacharis* is corroborated by all methods applied here, i.e. the molecular analysis (Fig. 1), differences in WIPs (Fig. 2), differences in male genitalia proportions (Fig. 3) and the multivariate morphometric analysis (Fig. 5).

The description of two species groups is well-suited to classify the Western Palaearctic fauna. Species from outside this region are currently not considered and species groups and their diagnoses might need revision after treatment of the *Anacharis* world fauna. For example, the placement of the Nearctic *A. melanoneura* into one of the species groups might be problematic, as females of the species are reported to have placodeal sensillae starting at flagellomere two (Mata-Casanova et al. 2018), while they start at flagellomere one (*eucharioides* group) or three (*immunis* group) in the Western Palaearctic species.

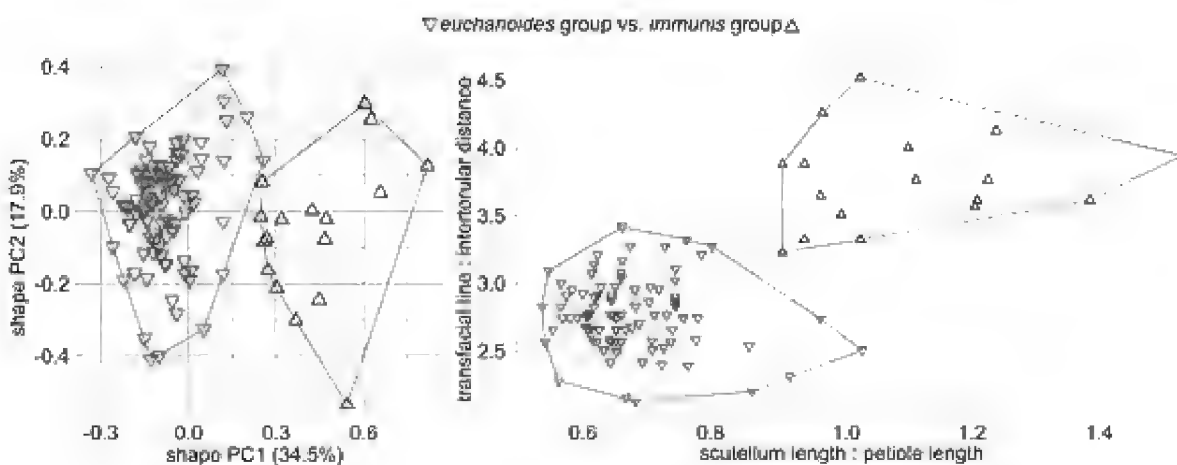


**Figure 5.** Results of morphometric analyses of the *eucharioides* species group against the *immunis* species group shape PCA shows almost full separation between species groups (Fig. 5 left) lda-ratio extractor suggests two ratios to fully separate the two species groups, which are included in the diagnoses of the respective groups groups (Fig. 5 right).

### *immunis* species group

**Diagnosis.** The genal carina is at a right angle to the vertical axis of the face in facial view (Figs 9C, 11C). The coriaceous texture of the malar area is meeting the eye only on its ventral margin. The occiput is smooth (Fig. 18A). The placodeal sensilla in the female antenna are starting at the fourth flagellomere. The eye-to-eye distance is 3.2 to 4.5 times longer than the intertorular distance (Figs 5 right, 9C, 11C). The notauli are weak, fading to absence anteriorly, inside without transversal carinae (Figs 9D, 11D). The mesopleural line is posteriorly fading and points to the posterior margin submedially (Figs 9B, 11B). The nuchal collar is slim and is either dorsomedially confluent with the median carina of the propodeum or it is dorsally bilobed, but never projecting dorsomedially (Fig. 6A, B). The inner side of the hind coxa has an equally distributed pubescence on its entire length (Fig. 11B). The mesoscutellum is 0.9–1.5 times longer than the petiole (Figs 5 right, 9A, 11A). In the WIPs, the apical spot of the hind wing is not restricted to the apical area but distinctly extending into the basiocubital area (Fig. 2A, B). The genitalia of the *immunis* species group are 374–423 (mean 401)  $\mu\text{m}$  long (Fig. 3A, B). The male genitalia have one of the apical parameral setae situated sub-apically.

**Species included.** *Anacharis ensifer* Walker, 1835, stat. rev., *A. immunis* Walker, 1835 and *A. norvegica* Mata-Casanova & Pujade-Villar, 2018.

**Remarks.** Previously, the species of *Anacharis* were grouped by their petiole length relative to the hind coxa length. Fergusson (1986), for example, separates his *A. immunis* and *A. euchariooides* by stating that the former has a petiole that is shorter than the hind coxa and the latter having it longer than the hind coxa. Mata-Casanova et al. (2018) changed the state of the species *A. immunis* and *A. norvegica* (i.e. what we call the *immunis* species group) to “petiole as long as hind coxa”. We found the ratio of the petiole length to the metacoxa length to be quite variable inter- and intraspecifically. The morphometric analysis revealed that instead the ratio of mesoscutellum length and petiole length is better suited to characterise the species groups (Fig. 5B). In addition to the relative petiole length, we propose a manifold of mainly qualitative characters that can be used more reliably to separate the two species groups.

The multivariate morphometrics on species group- level resulted in the addition of two diagnostic characters that are – in particular when combined – suited to separate specimens from either species group. Accordingly, the addition of morphometric analyses proved useful for separating *Anacharis* specimens on species group- level.

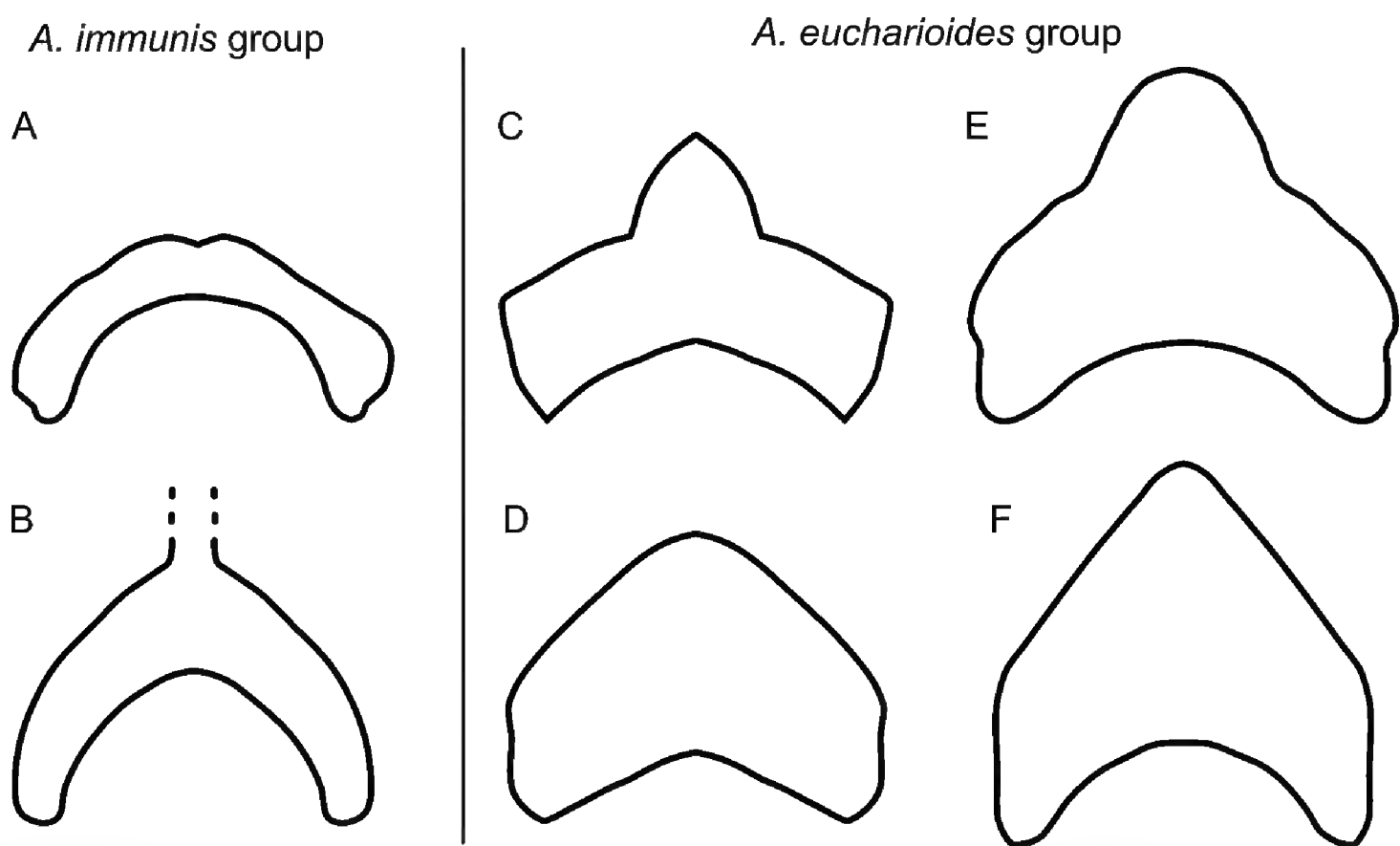


**Figure 6.** Variation of the nuchal collar within the two species groups **A** bilobed **B** confluent with median carina of propodeum **C** dorsomedial narrow tooth (as typical but not exclusive for *A. martinae* sp. nov.) **D** broad projection **E** blunt tooth **F** broad and high projection.

### *euchariooides* species group

**Diagnosis.** The genal carina within the *euchariooides* species group is not at a right angle to the vertical axis of the face in facial view (e.g. Fig. 10C). The coriaceous texture of the malar area is meeting the eye along its ventral and inner margin. The occiput has at least some noticeable transversal striolation to striation laterally to medially (Fig. 18B).

The placodeal sensilla in the female antenna are starting at the first flagellomere. The eye-to-eye distance is 2.1–3.4 times longer than the intertorular distance (Fig. 5 right, e.g. Fig. 10C). The notauli are weak and smooth (Fig. 14D) to strong and with distinct transversal carinae inside, never fading anteriorly (e.g. Fig. 10D). The mesopleural line is not distinctly fading posteriorly (except in *A. petiolata* & *A. typica*), and abruptly sloping towards posteroventral hypocoxal furrow in posterior quarter (e.g. Fig. 14B). The nuchal collar is broader and has a broad or narrow dorsomedial projection or tooth, which is not confluent with the median carina of the propodeum (Fig. 6C–F). The inner side of the hind coxa has no continuous pubescence along its entire length; it has some few setae dorsally or is entirely glabrous and has a patch of pubescence ventrally. The mesoscutellum is 0.5–1 times longer than the petiole (Fig. 5 right, e.g. Fig. 10A). In the WIPs, the apical spot of the hind wing is restricted to the apical area (Fig. 2C–G). The genitalia of the *eucharioides* species group are 243–331 (mean 278)  $\mu\text{m}$  long (Fig. 3C–F). The male genitalia have all of the three apical parameral setae situated distinctly apically.

**Species included.** *A. eucharioides* (Dalman, 1818), *A. martiniae* sp.nov., *A. maxima* sp. nov., *A. minima* sp. nov., *A. petiolata* (Zetterstedt, 1838), stat. rev. & *A. typica* Walker, 1835, stat. rev.

**Remarks.** For a discussion of the relationship between the two species groups, see remarks under *immunis* species groups.

The PCA of the *eucharioides* species group (Fig. 7) including all species shows wide overlap, i.e. that it is not possible to discriminate the species on single morphometric ratios alone. It indicates that species are quite variable morphometrically. In addition, the low values of variation explained by PC1 and PC2 indicate that all species are relatively similar morphometrically. In summary, the results shown in Fig. 7 indicate that diagnosing species in the *eucharioides* species group must largely rely on qualitative characters, and an integration of the species delimitation results from analysis of molecular sequence data.

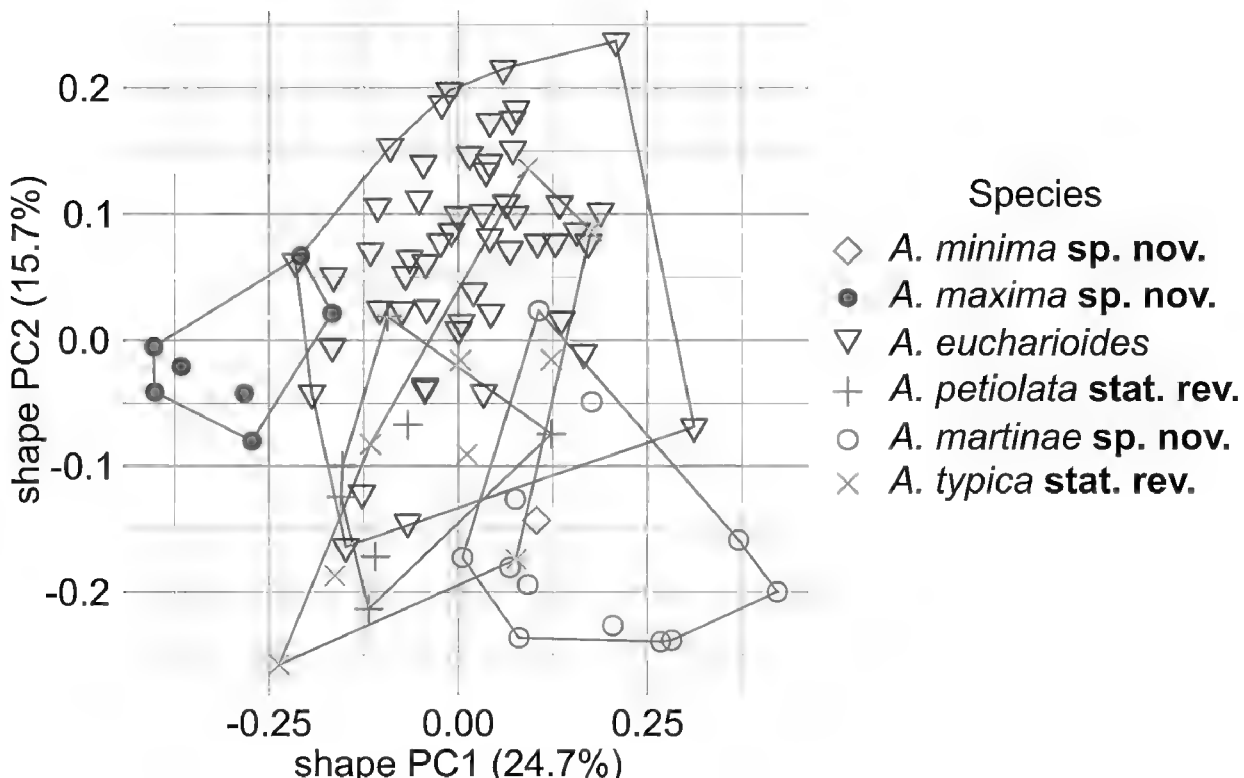


**Figure 7.** PCA of all species of the *eucharioides* species group.

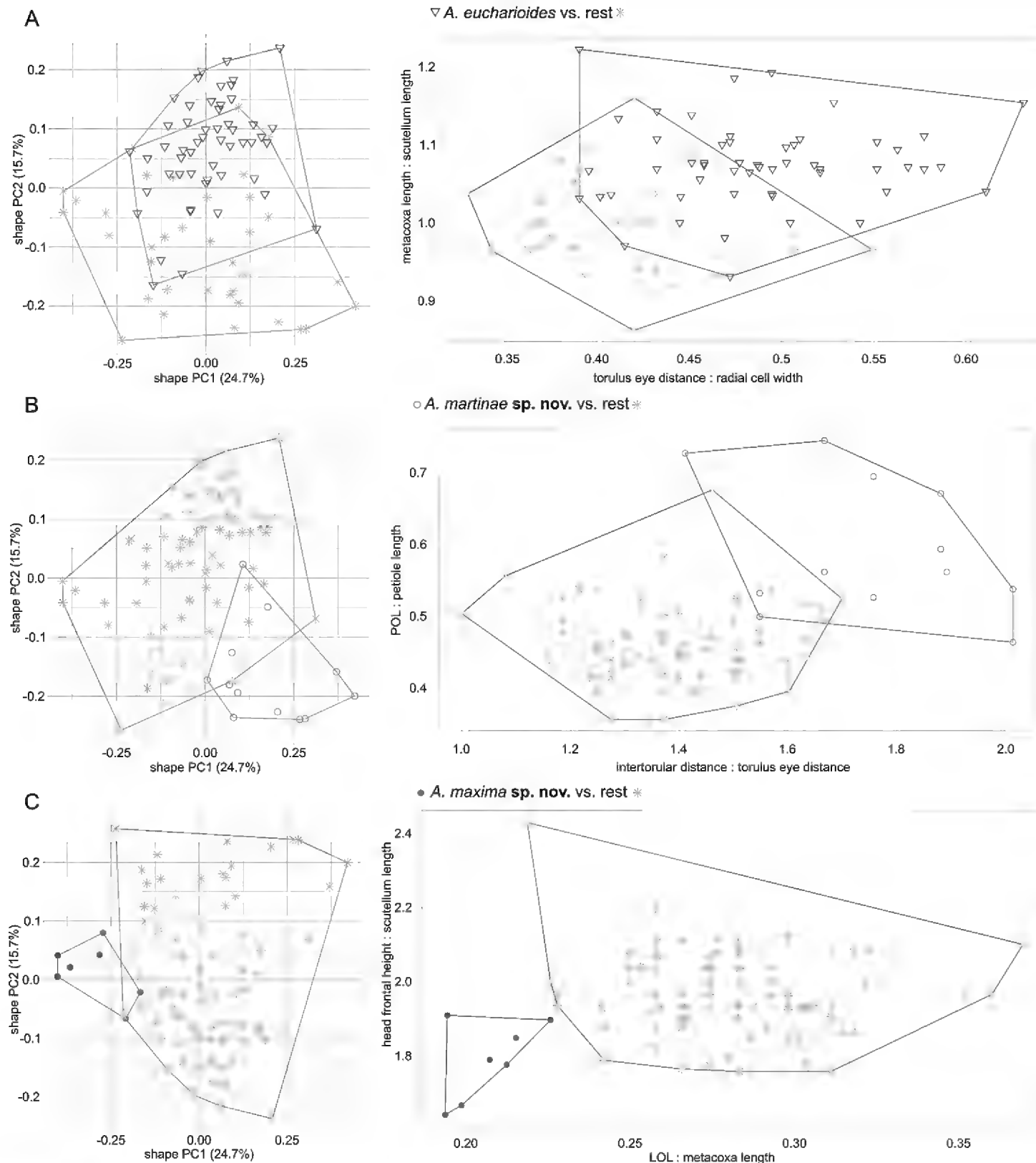


**Figure 8.** The PCA plot (left) and lda extractor plot (right) of **A** *A. eucharioides* against the rest of the *eucharioides* species group **B** *A. martiniae* sp. nov. against the rest of the *eucharioides* species group **C** *A. maxima* sp. nov. against the rest of the *eucharioides* species group.

#### *Anacharis ensifer* Walker, 1835, stat. rev.

Figs 2A, 3A, 9A–E

*Anacharis ensifer* Walker, 1835: 522 - lectotype (NHMUK) ♀, photographs examined.  
*Megapelmus rufiventris* Hartig, 1841: 358 (removed from synonymy with *A. immunis*) - lectotype (ZSM) ♀, photographs examined.

**Diagnosis (n=13).** Belongs to the *immunis* species group. Similar to *A. norvegica* in generally having a largely sculptured mesoscutellum (largely smooth in *A. immunis*) (Fig.

9D). Different from *A. norvegica* by having its mesoscutellum covered with reticulate-foveate sculpture resulting in larger foveae (smaller foveae on mesoscutellum in *A. norvegica*) (Fig. 9D). The circumscutellar carina is distinct and usually flanged upwards and appears in lateral view like a posterodorsal tooth (circumscutellar carina not flanged and less distinct in *A. norvegica*, not appearing like a tooth) (Fig. 9B). The mesopleural line is dorsally well-defined in its anterior half (dorsal margin in anterior half diffused by rugose sculpture of mesopleuron in *A. norvegica*) (Fig. 9B). The mesoscutum lacks, or has just a few, wrinkles and has no distinct anterodorsal median signa (in *A. norvegica*, wrinkles on mesoscutum strong, amplifying the visibility of anterodorsal median signa) (Fig. 9D).

**CO1 barcode.** n=12. Maximum intraspecific distance = 0.5%. Minimum distance to closest species (*A. immunis*) = 7.8%. CO1 barcode consensus sequence:

AATTTTATACTTATTAGGAATCTGGTCAGCAATATTAGGAT-  
CAAGACTTAGTATAATTATTCGAATAGAATTAGGCACCCATCTCAAT-  
TAATCAGAAATGACCAAATTACAATTCAATTGTAACAGCTCATGCATT-  
TATTATAATTTTTTATAGTTACCTATTATAGTCGGAGGATTG-  
GAAATTACCTAATTCCATTAATACTCCTATCCCCAGATATAGCTTCC-  
CACGATTAAATAATATAAGATTGATTCTAATCCCCTTTAATT-  
TAATAGCTTCAAGATTATTGATCAAGGAGCAGGAACCGGATGAA-  
CAGTATATCCCCTTATCTTCATTAACAGGTCACTCAGGGATTGCAGT-  
AGACATAACAATTACTCTTCATTAAAGAGGAATTCTCAATTAG-  
GCTCAATTAAATTATTAGAACAAATTAAATACGAATCAATAAGTAT-  
CAATAGATAAAATTACCCATTACATGATCAATTAACTACAATT-  
TATTACTTTATCATTACCCGTCCTAGCAGGAGGGATCACTATACTT-  
TATTGACCGAAACTTAAATACCTCCTTTGATCCCATTAGGAGGAG-  
GAGACCCAATTATCAACATTATT

**Type material.**

**Lectotype of *Anacharis ensifer* Walker, 1835, designated by Fergusson (1986)**

F Walker Coll. 81–86

LECTO-TYPE

B.M. 1981 . Under *A. ensifer*

LECTOTYPE of *A. ensifer* Walker det. N.D.M.Fergusson, 1981

B.M. TYPE HYM 7. 161

[QR-code] NHMUK010640456

[for images, see <https://data.nhm.ac.uk/dataset/56e711e6-c847-4f99-915a-6894bb5c5dea/resource/05ff2255-c38a-40c9-b657-4ccb55ab2feb/record/10638964>]

**Lectotype of *Anacharis rufiventris* Hartig, 1841, designated by Fergusson (1986)**

LECTO-TYPE

Megapelmus n. sp. ? [handwritten, probably by Hartig himself]

rufiventris. [handwritten, probably by Hartig himself]

LECTOTYPE of *Megapelmus rufiventris* Hartig det. N.D.M.Fergusson 1982

*Anacharis immunis* det. N.D.M.Fergusson 1982

**Other material examined. DNA barcode vouchers.** BELGIUM • 1 ♀; West Flanders, Ypres, De Triangel, Urban park (bushes); 50.8418°N, 2.8838°E; ca 20 m a.s.l.; 2–23 Jul. 2022; Verheyde, Fons leg.; Malaise trap; ZFMK-TIS-2640867.

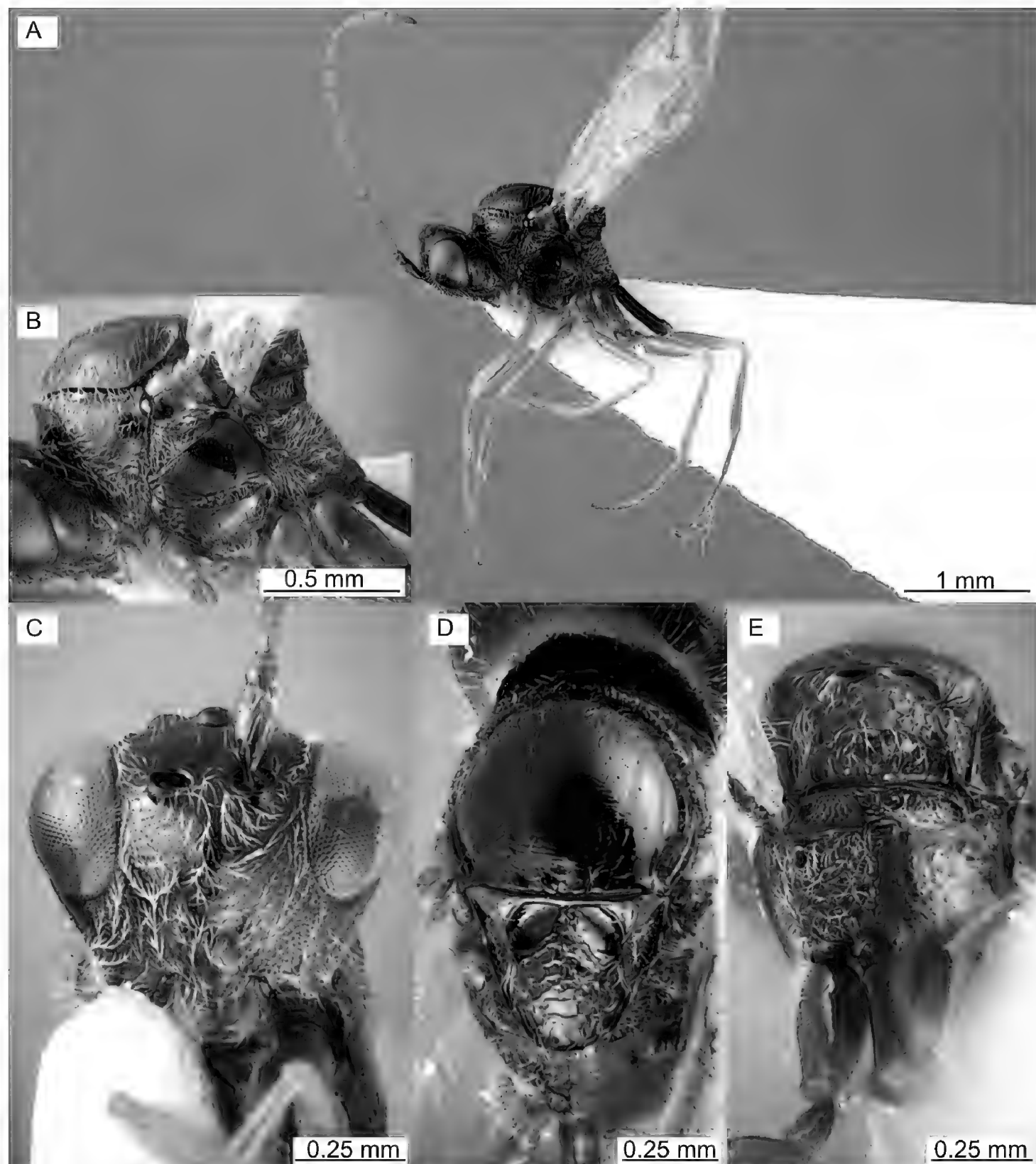


**Figure 9.** *Anacharis ensifer*, male (ZFMK-TIS-2629206) **A** habitus **B** mesosoma lateral **C** face **D** mesosoma dorsal **E** mesosoma posterior view.

NORWAY • 2 ♂♂; Rogaland Ytre, Sola, Indraberget; 58.9124°N, 5.6628°E; ca 20 m a.s.l.; 24 Aug.-6 Sep. 2020; Leendertse, Arjen leg.; Malaise trap; ZFMK-TIS-2629222, ZFMK-TIS-2629223. • 1 ♂; same collection data as for preceding; 20 Sep.-5 Oct. 2020; ZFMK-TIS-2629221. • 1 ♀, 3 ♂♂; Rogaland Ytre, Stavanger, Byhaugen; 58.9731°N, 5.6988°E; ca 50 m a.s.l.; 6–29 Aug. 2020; Birkeland, Jarl leg.; Malaise trap; female - ZFMK-TIS-2629272; males - ZFMK-TIS-2629209, ZFMK-TIS-2629210, ZFMK-TIS-2629211. • 1 ♀; same collection data as for preceding; 25 Sep.-31 Oct. 2020; ZFMK-TIS-2629249. • 3 ♂♂; Rogaland Ytre, Mossige;

58.69°N, 5.7239°E; ca 60 m a.s.l.; 17 Sep.-11 Oct. 2020; Mjøs, Alf Tore leg.; Malaise trap; ZFMK-TIS-2629206, ZFMK-TIS-2629207, ZFMK-TIS-2629208.

**Material without DNA barcode.** BELGIUM • 3 ♂♂; Walloon Brabant, Ottignies; 16–23 Jul. 1983; Paul Dessart leg.; Malaise trap; JV\_Prel\_0047 (RBINS), JV\_Prel\_0048 (RBINS), JV\_Prel\_0049 (RBINS). • 1 ♀; West Flanders, Ypres, De Triangel, Urban park (pool vegetation); 50.8427°N, 2.884°E; ca 20 m a.s.l.; 18 Jun.-2 Jul. 2022; Fons Verheyde leg.; Malaise trap; ZFMK-TIS-2640864.

DENMARK • 1 ♂; Eastern Jutland, Alminde hule, 20 km S of Vejle; 30 May 1982; Torkhild Munk leg.; NHRS-HEVA 000023120 (NHRS). • 1 ♂; Eastern Jutland, Klatstrup, 10 km S of Vejle, Bygade, on compost heap; 28–29 Jul. 1982; Torkhild Munk leg.; NHRS-HEVA 000023118 (NHRS). • 1 ♀; Eastern Jutland, Nørreskov, 10 km E of Kolding; 31 Jul. 1984; Torkhild Munk leg.; NHRS-HEVA 000023119 (NHRS).

GERMANY • 2 ♀♀; Bavaria, near Schwandorf; 49.3042°N, 12.1184°E; ca 360 m a.s.l.; Ernst Klimsa leg.; specimen in coll MF. • 1 ♂; Brandenburg, Potsdam-Mittelmark, Kleinmachnow; 22 Jun. 1925; S. Bollow leg.; JV\_Prel\_0042 (SDEI). • 1 ♀; North Rhine-Westphalia, Rhein-Sieg-Kreis, Schladern near Windeck, Sieg river, right river bank; 50.8°N, 7.585°E; ca 130 m a.s.l.; 4–11 Jul. 2017; ZFMK et al. leg.; Malaise trap; ZFMK-TIS-2629278.

THE NETHERLANDS • 1 ♀; Gelderland, Nijmegen, Gelderse poort; 23 Aug. 2022; R. Lexmond leg.; Malaise trap; JV\_Prel\_0050 (RBINS).

NORWAY • 2 ♀♀; Akershus, Baerum, Ostøya; 10 Jun.-1 Jul. 1984; Fred Midtgård leg.; NHRS-HEVA 000023124 (NHRS), NHRS-HEVA 000023125 (NHRS). • 1 ♀; Norvegia alpina (“Nv alp”); [1832]; Carl Henning Boheman leg.; NHRS-HEVA 000023123 (NHRS). • 2 ♀♀; Rogaland Ytre, Stavanger, Byhaugen; 58.9731°N, 5.6988°E; ca 50 m a.s.l.; 6–29 Aug. 2020; Jarl Birkeland leg.; Malaise trap; ZFMK-TIS-2629273, ZFMK-TIS-2629274. • 1 ♂; same collection data as for preceding 25 Sep.-31 Oct. 2020; ZFMK-TIS-2629205.

SWEDEN • 1 ♀; Gotska sandön, Lilla lövskogen; 6 Aug. 1952; Anton Jansson leg.; NHRS-HEVA 000023126 (NHRS). • 3 ♂♂; Öland, Ås, Ottenbylund, glade in deciduous grove; 56.2194°N, 16.4224°E; ca 10 m a.s.l.; 24 Jul.-1 Aug. 2003; Swedish Malaise Trap Project (Swedish Museum of Natural History) leg.; Malaise trap; NHRS-HEVA 000023139 (NHRS), NHRS-HEVA 000023140 (NHRS), NHRS-HEVA 000023141 (NHRS). • 1 ♂; Öland, Kastlösa; 26 Jun. 1952; Karl-Johan Hedqvist leg.; NHRS-HEVA 000023138 (NHRS). • 1 ♂; Öland, Torslunda, Gamla skogsby, Diversitetsängen, rich transitional meadow with shrubs near nemoral forest; 56.6167°N, 16.5076°E; ca 40 m a.s.l.; 17 Jul.-7 Aug. 2003; Swedish Malaise Trap Project (Swedish Museum of Natural History) leg.; Malaise trap; NHRS-HEVA 000023142 (NHRS). • 2 ♂♂; Östergötland, Omberg, Stocklycke, meadow in Tilia-dominated forest; 58.3075°N, 14.631°E; ca 130 m a.s.l.; 22 Jul.-5 Aug. 2003; Swedish Malaise Trap Project (Swedish Museum of Natural History) leg.; Malaise trap; NHRS-HEVA 000023143 (NHRS), NHRS-HEVA 000023144 (NHRS). • 3 ♀♀, 1 ♂; Småland; [18xx]; Carl Henning Boheman leg.; females - NHRS-HEVA 000023127 (NHRS), NHRS-HEVA 000023128 (NHRS), NHRS-HEVA 000023129 (NHRS);

male - NHRS-HEVA 000023130 (NHRS). • 1 ♀, 1 ♂; Södermanland, Ludgo s:n, Tovetorp fieldstation; 58.9478°N, 17.1485°E; ca 50 m a.s.l.; 6 Aug. 2012; Mattias Forshage leg.; sweep net; female - NHRS-HEVA 000023131 (NHRS); male - NHRS-HEVA 000023132 (NHRS). • 1 ♀; Södermanland, Trosa kommun, Hunga södergård 1, agricultural backyard, heavily eutrophicated, in tall grass near stable manure pile; 58.9207°N, 17.5212°E; ca 20 m a.s.l.; 9–19 Aug. 2004; Swedish Malaise Trap Project (Swedish Museum of Natural History) leg.; Malaise trap; NHRS-HEVA 000023133 (NHRS). • 1 ♀; Uppland, Håbo kommun, Biskops-Arnö, northern beach, elm grove; 59.6721°N, 17.5009°E; ca 10 m a.s.l.; 20 May–20 Jun. 2005; Swedish Malaise Trap Project (Swedish Museum of Natural History) leg.; Malaise trap; NHRS-HEVA 000023136 (NHRS). • 1 ♀; Uppland, Uppsala kommun, Ekdalen, herb-rich open oak forest; 59.9715°N, 18.355°E; ca 40 m a.s.l.; 21 Jul.–4 Aug. 2003; Swedish Malaise Trap Project (Swedish Museum of Natural History) leg.; Malaise trap; NHRS-HEVA 000023135 (NHRS). • 1 ♀; same collection data as for preceding 23 Aug.–6 Sep. 2004; NHRS-HEVA 000023134 (NHRS). • 1 ♂; Uppland, Vallentuna, forest; 19 Jul. 1959; Karl-Johan Hedqvist leg.; sweep net; NHRS-HEVA 000023137 (NHRS).

SWITZERLAND • 1 ♀; Genève, La Louton; 12 Aug. 1960; André Comellini leg.; specimen at MHNG. • 1 ♀; Neuchâtel, Auvernier; 2 Aug. 1960; Jacques de Beaumont leg.; specimen at MHNG. • 1 ♀; same collection data as for preceding 5 Aug. 1959; specimen at MHNG. • 1 ♂; same collection data as for preceding 8 Aug. 1957; specimen at MHNG. • 1 ♂; same collection data as for preceding 18 Aug. 1986; specimen at MHNG. • 1 ♀; same collection data as for preceding 26 Aug. 1956; specimen at MHNG. • 1 ♀; same collection data as for preceding 28 Aug. 1956; specimen at MHNG. • 1 ♂; same collection data as for preceding 31 Aug. 1956; specimen at MHNG. • 1 ♂; Vaud, Bussigny; 26 Jul. 1958; Jacques de Beaumont leg.; specimen at MHNG. • 1 ♂; Vaud, Lutry Aug. 1956; Jacques Aubert leg.; specimen at MHNG. • 1 ♀; Vaud, Pampigny; 19 Jun. 1960; Jacques de Beaumont leg.; specimen at MHNG.

**Biology.** Summer species, flying mainly from May to October, peak in August. Collected mainly in deciduous forest and in open nemoral habitats.

**Distribution.** Verified by morphological examination: Belgium, Denmark, Germany, The Netherlands, Norway, Sweden, Switzerland, United Kingdom (locus typicus: England, near London or Windsor forest).

No DNA barcode matches with publicly available sequences from other countries. Lowland species, occurring in elevations below 400 m a.s.l.

**Remarks.** We remove *A. ensifer* from the synonymy with *A. immunis* that was established by Fergusson (1986).

Walker's original name *Anacharis ensifer* was changed into *A. ensifera* by Reinhard (1860). While Thomson (1862) maintained 'ensifer', most authors from Cameron (1890) on followed Reinhard's emendation. However, 'ensifer' can be a noun as well as an adjective (and Walker's intentions are not clear in the description), but Reinhard's emendation for gender agreement purposes makes sense only if it is an adjective. §31.2.2 in the zoological code (ICZN 1999) clearly states that in such ambiguous

cases it is to be treated as a noun, thus the original spelling is retained and the gender ending remains unchanged.

Almost all specimens of *A. ensifer* show an intermediate stage of sculpturing of the mesoscutellum between *A. immunis* (largely smooth) and *A. norvegica* Mata-Casanova & Pujade-Villar, 2018 (finely foveate on both dorsal and posterior surface of the mesoscutellum), with the exception of ZFMK-TIS-2629272, which has a largely smooth mesoscutellum like in *A. immunis* but clusters within *A. ensifer* by its CO1 barcode sequence.

*Anacharis ensifer* falls within the diagnosis of *A. immunis* in Mata-Casanova et al. (2018) and thus the two host records and all distributional data given therein must be re-evaluated considering the existence of two species behind *A. immunis* sensu Mata-Casanova et al. (2018).

Works prior to Fergusson (1986) describe *A. ensifer* largely based on colouration, but always state a smooth mesoscutellum (e.g. Reinhard 1860 & von Dalla-Torre and Kieffer 1910), which is not in line with our findings. Historical literature records therefore require critical evaluation, too.

### *Anacharis eucharioides* (Dalman, 1818)

Figs 2G, 3F, 10A–E

*Cynips eucharioides* Dalman, 1818: 78 - type lost.

*Anacharis tinctus* Walker, 1835: 520 - lectotype (NHMUK) ♀, synonymised in Fergusson (1968), photographs examined.

*Megapelmus spheciformis* Hartig, 1840: 202 (removed from synonymy with *A. typica*) - lectotype (ZSM) ♂, first synonymised in Reinhard (1860), examined.

*Anacharis fergussoni* Mata-Casanova & Pujade-Villar, 2018: 16 syn. nov. - holotype (CNC) ♀, photographs examined.

*Anacharis eucharioides* auct., common misspelling.

**Diagnosis (n=290).** Most common species within the *eucharioides* species group. Medium sized body (2.7–3.4, mean 3.1 mm, similar to *A. typica*, *A. petiolata* & *A. martiniae*). Differing from *A. typica* and *A. petiolata* by having a mesoscutellum with a median carina present, which is typically interrupted centrally by reticulation (largely smooth and even in *A. petiolata* and *A. typica*) (Fig. 10D). Differing from *A. martiniae* by having the lateromedial area of the pronotum smooth to rugose (Fig. 10B, with longitudinal carinae that are a continuation of the ventral carinae in *A. martiniae*). Unique in usually having the mesoscutum glabrous to more sparsely pubescent than the rest of the mesoscutum (Fig. 10D, more evenly pubescent in all other species). The male genitalia of *A. eucharioides* (Fig. 3F) are unique in not being significantly widened basally or medially, i.e. being more parallel-sided (basally or medially widened in all other species Fig. 3C–E).

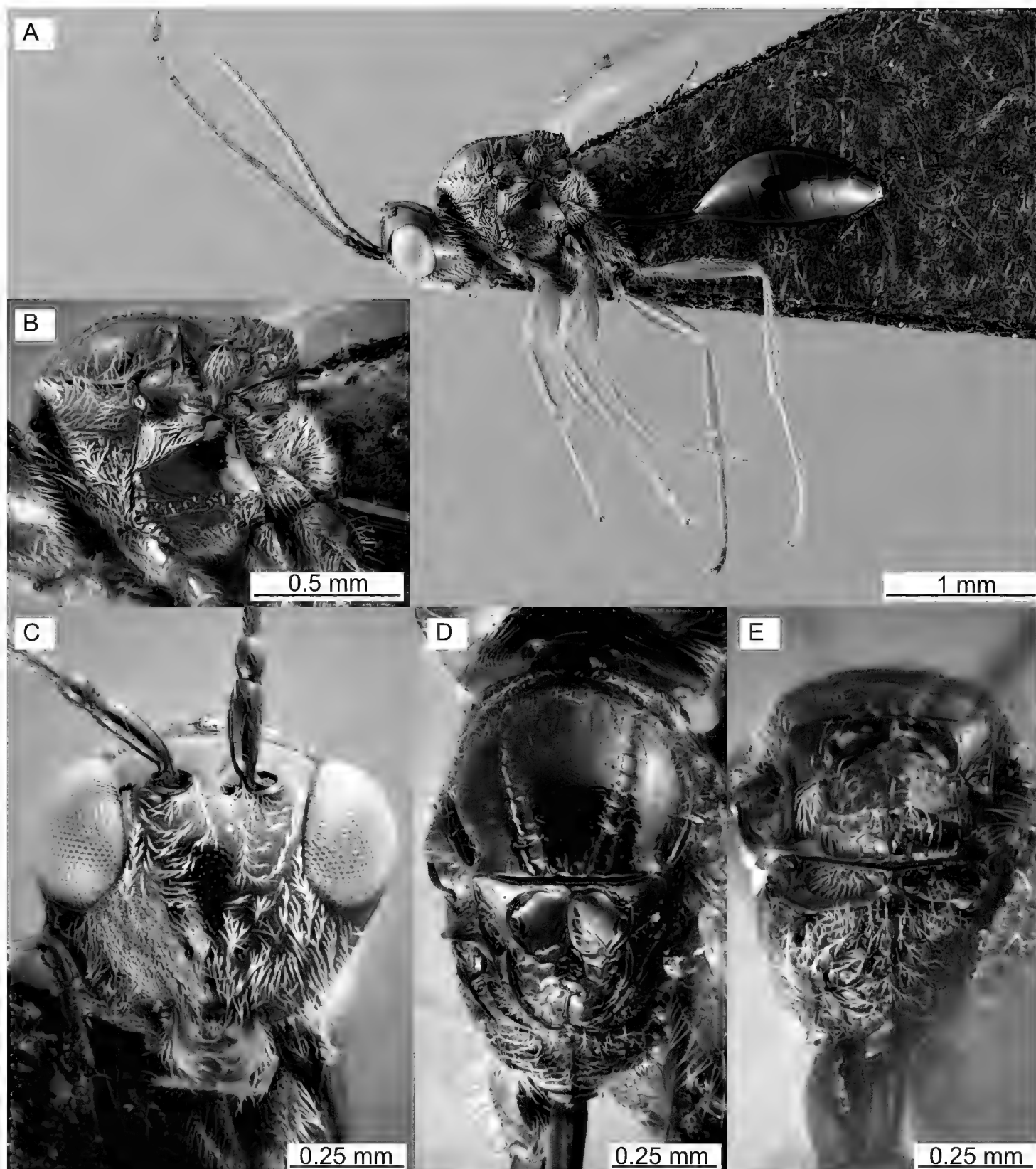


**Figure 10.** *Anacharis eucharioides*, female (ZFMK-TIS-2640762) **A** habitus **B** mesosoma lateral **C** face **D** mesosoma dorsal **E** mesosoma posterior view

**CO1 barcode.** n=289. Maximum intraspecific distance = 2.5%. Minimum distance to closest species (*A. petiolata*) = 2.9%. CO1 barcode consensus sequence:

AATTTTATACTTATTAGGTATTGATCTGGAATAATAGGAT-  
CAAGATTAAGAATAATTATCGAATAGAATTAGGAACCCCCTCAAT-  
TAATCATAAAATGATCAAATTATAATTCAATTGTAACTGCTCATGCATT-  
TATTATAATTCTTATAGTTACCTATTATAGTTGGAGGATTGG-  
GAATTATTTAGTACCTTAATATTAATTATTCCTGATATAGCTTTTC-  
CACGATTAAATAATTAAAGATTTGATTTAATCCCTTCCTTATT

TAATAACAATTAATTATTGATCAAGGAGCAGGAACAGGATGAAC-T  
 GTTACCCCTCCATTATCCTCCCTAACAGGTCATCCATCTATCAGTA-  
 GATTAGTTATTACTCATTACATTAAAGTGGAATTTCATCAATTCTTG-  
 GATCAATTAATTATTGTAACCATTAAATATAACGAATAACTCTA-  
 TATCTATAGACAAAATTTCATTATTGATCTATTCTAACTA-  
 CAATTACTATTATTACCTTACCCGTACTAGCAGGAGGATTAACGA-  
 TACTATTATTGATCGAAATTAAATACATCTTTTGACCCCACAG-  
 GAGGAGGAGACCCTATTCTTATCAACATTATT

**Type material.**

**Lectotype of *Anacharis tinctus* Walker, 1835, designated by Fergusson (1986)**

81 86 [on backside of mounting board]

Type

B.M.1981 . Under tincta

LECTO-TYPE

LECTOTYPE *Anacharis tincta* Walker det. N.D.M.Fergusson, 1981

B.M. TYPE HYM 7.162

[QR code] NHMUK 012858912

[for images, see <https://data.nhm.ac.uk/dataset/56e711e6-c847-4f99-915a-6894bb5c5dea/resource/05ff2255-c38a-40c9-b657-4ccb55ab2feb/record/10470209>]

**Lectotype of *Megapelmus spheciformis* Hartig, 1840, designated by Weld (1952)**

Weld 1931

*Megapelmus spheciformis* [handwritten, probably by Hartig himself]

LECTOTYPE of *MEGAPELMUS spheciformis* det. N.D.M.Fergusson, 1982

*Anacharis eucharoides* Dal. det. N.D.M.Fergusson, 1982

*Anacharis eucharoides* (Dalman, 1818) ♂ Det. Jonathan Vogel 2024

**Holotype of *Anacharis fergussoni* Mata-Casanova & Pujade-Villar, 2018**

GERMANY • 1 ♀; Rhineland Palatinate, Mainz-Bingen, Ingelheim am Rhein, orchard; 1–30 Sep. 1968; I. Sreffan leg.; Malaise trap.

[for images, see <https://www.cnc.agr.gc.ca/taxonomy/Specimen.php?id=3274133>]

**Other material examined. DNA barcode vouchers.** BELGIUM • 1 ♀; East Flanders, Assenede, Isabellepolder, Agricultural land with Partridge mix; 51.266°N, 3.71°E; ca 0 m a.s.l.; 12–19 Jun. 2019; UGent leg.; yellow pan trap; ZFMK-TIS-2640673. • 2 ♂♂; West Flanders, Ypres, De Triangel, Urban park (bushes); 50.8418°N, 2.8838°E; ca 20 m a.s.l.; 30 Apr.–14 May 2022; Verheyde, Fons leg.; Malaise trap; ZFMK-TIS-2640843, ZFMK-TIS-2640844. • 3 ♀♀, 9 ♂♂; same collection data as for preceding 14–28 May 2022; females - ZFMK-TIS-2640845, ZFMK-TIS-2640846, ZFMK-TIS-2640847, ZFMK-TIS-2640859, ZFMK-TIS-2640860, ZFMK-TIS-2640861; males - ZFMK-TIS-2640848, ZFMK-TIS-2640849, ZFMK-TIS-2640850, ZFMK-TIS-2640851, ZFMK-TIS-2640852, ZFMK-TIS-2640853, ZFMK-TIS-2640854, ZFMK-TIS-2640855, ZFMK-TIS-2640856, ZFMK-TIS-2640862, ZFMK-TIS-2640863. • 1 ♂; same collection data as for preceding 2–23 Jul. 2022; ZFMK-TIS-2640868. • 3 ♀♀, 2 ♂♂; West Flanders, Ypres, De Triangel, Urban park (pool vegetation); 50.8427°N, 2.884°E; ca 20 m a.s.l.; 14–28 May 2022; Verheyde, Fons

leg.; Malaise trap; females - ZFMK-TIS-2640859, ZFMK-TIS-2640860, ZFMK-TIS-2640861; males - ZFMK-TIS-2640862, ZFMK-TIS-2640863.

GERMANY • 1 ♂; Baden-Württemberg, Biberach, Altheim; 48.1399°N, 9.4491°E; ca 540 m a.s.l.; 6–19 Aug. 2013; Schmalfuß, H. leg.; Malaise trap; ZFMK-TIS-2629512. • 2 ♀♀, 8 ♂♂; Baden-Württemberg, Karlsruhe, Malsch, Hansjakobstraße, garden; 48.8835°N, 8.3197°E; ca 120 m a.s.l.; 26 Apr.–10 May 2020; Dieter Doczkal leg.; Malaise trap; females - ZFMK-TIS-2640753, ZFMK-TIS-2640754; males - ZFMK-TIS-2640745, ZFMK-TIS-2640746, ZFMK-TIS-2640747, ZFMK-TIS-2640748, ZFMK-TIS-2640749, ZFMK-TIS-2640750, ZFMK-TIS-2640751, ZFMK-TIS-2640752. • 1 ♂; same collection data as for preceding 25 Oct.–8 Nov. 2020; ZFMK-TIS-2640726. • 11 ♀♀, 1 ♂; Baden-Württemberg, Stuttgart, Espan; 49.6167°N, 9.2667°E; ca 280 m a.s.l.; 28 Jul.–28 Aug. 2014; Woog, F. leg.; females - ZFMK-TIS-2640775, ZFMK-TIS-2640776, ZFMK-TIS-2640777, ZFMK-TIS-2640778, ZFMK-TIS-2640779, ZFMK-TIS-2640780, ZFMK-TIS-2640781, ZFMK-TIS-2640782, ZFMK-TIS-2640783, ZFMK-TIS-2640784, ZFMK-TIS-2640785; male - ZFMK-TIS-2640786. • 1 ♀, 10 ♂♂; Baden-Württemberg, Tübingen, Hirschau, Oberes Tal, orchard; 48.505°N, 8.993°E; ca 390 m a.s.l.; 29 Apr.–13 May 2014; Kothe, T., Engelhardt, M., Bartsch, D. leg.; Malaise trap; female - ZFMK-TIS-2629263; males - ZFMK-TIS-2629200, ZFMK-TIS-2629201, ZFMK-TIS-2629202, ZFMK-TIS-2629203, ZFMK-TIS-2629204, ZFMK-TIS-2629218, ZFMK-TIS-2629540, ZFMK-TIS-2629541, ZFMK-TIS-2629542, ZFMK-TIS-2640774. • 1 ♂; Baden-Württemberg, Tübingen, Hirschau, Oberes Tal, orchard; 48.505°N, 8.9935°E; ca 370 m a.s.l.; 23 May–6 Jun. 2014; Kothe, T., Engelhardt, M., Bartsch, D. leg.; Malaise trap; ZFMK-TIS-2628235. • 3 ♀♀; Baden-Württemberg, Tübingen, Hirschau, Wiesenweingärten; 48.5043°N, 8.9956°E; ca 380 m a.s.l.; 17–31 Jul. 2014; Kothe, T., Engeldhardt, M., König, C. leg.; Malaise trap; ZFMK-TIS-2629238, ZFMK-TIS-2629267, ZFMK-TIS-2629268. • 1 ♀; Baden-Württemberg, Tübingen, Steinenberg; 48.5306°N, 9.0312°E; ca 470 m a.s.l.; 31 Jul.–14 Aug. 2014; Kothe, T., Engeldhardt, M., König, C. leg.; Malaise trap; ZFMK-TIS-2629237. • 4 ♀♀; Baden-Württemberg, Tübingen, Steinenberg; 48.5313°N, 9.03°E; ca 490 m a.s.l.; 4–17 Jul. 2014; Kothe, T., Engelhardt, M., König, Ch. leg.; ZFMK-TIS-2629504, ZFMK-TIS-2629505, ZFMK-TIS-2629506, ZFMK-TIS-2629507. • 1 ♀, 1 ♂; Baden-Württemberg, Tübingen, Steinenbergturm; 48.531°N, 9.03°E; ca 490 m a.s.l.; 14–29 Aug. 2014; Kothe, T., Engeldhardt, M., König, C. leg.; Malaise trap; female - ZFMK-TIS-2629236; male - ZFMK-TIS-2629219. • 1 ♂; Baden-Württemberg, Tübingen, Wurmlingen, Gengental, orchard; 48.5131°N, 8.9923°E; ca 370 m a.s.l.; 13–23 May 2014; Kothe, T., Engeldhardt, M., König, C. leg.; Malaise trap; ZFMK-TIS-2640681. • 1 ♀, 1 ♂; Bavaria, Main-Spessart, Lohr, Nat. res. Romberg, pasture woodland; 49.9864°N, 9.5896°E; ca 190 m a.s.l.; 9 Jun.–6 Jul. 2018; Dieter Doczkal leg.; Malaise trap; female - ZFMK-TIS-2640717; male - ZFMK-TIS-2640716. • 1 ♂; Bavaria, Rhön-Grabfeld, Fladungen, Nat. res. Schwarzes Moor, Karpatenbirkenwald; 50.5117°N, 10.071°E; ca 780 m a.s.l.; 26 Jun.–18 Jul. 2017; Dieter Doczkal leg.; Malaise trap; ZFMK-TIS-2629538. • 2 ♀♀; Hesse, Gießen, Nat. res. Holzwäldchen bei

Gleiberg; 50.605°N, 8.6316°E; ca 190 m a.s.l.; 14 Jun. 2021; GBOL III leg.; sweep net; ZFMK-TIS-2629494, ZFMK-TIS-2629495. • 1 ♀; Hesse, Kassel, Nat. res., „Fuldaschleuse Wolfsanger“, meadow along Fulda river with *Salix* and *Phragmites*; 51.329°N, 9.5565°E; ca 130 m a.s.l.; 13–27 Oct. 2020; GBOL III leg.; sweep net; Loc. 1; ZFMK-TIS-2628230. • 3 ♀♀; Hesse, Rheingau-Taunus, Lorch am Rhein, above Nollig castle; 50.0491°N, 7.7978°E; ca 240 m a.s.l.; 27 May–7 Jun. 2013; Niehuis, Oliver leg.; Malaise trap; MF 1; ZFMK-TIS-2629498, ZFMK-TIS-2629499, ZFMK-TIS-2629500. • 1 ♀, 1 ♂; same collection data as for preceding 17–25 Jun. 2015; MF 4; female - ZFMK-TIS-2629248; male - ZFMK-TIS-2629214. • 8 ♂♂; same collection data as for preceding 15–21 Jul. 2013; MF 1; ZFMK-TIS-2629227, ZFMK-TIS-2629240, ZFMK-TIS-2629241, ZFMK-TIS-2629521, ZFMK-TIS-2629522, ZFMK-TIS-2629523, ZFMK-TIS-2629524, ZFMK-TIS-2629525. • 20 ♂♂; same collection data as for preceding 21–27 Jul. 2013; ZFMK-TIS-2629225, ZFMK-TIS-2629226, ZFMK-TIS-2629553, ZFMK-TIS-2629554, ZFMK-TIS-2629555, ZFMK-TIS-2629556, ZFMK-TIS-2629557, ZFMK-TIS-2629558, ZFMK-TIS-2629559, ZFMK-TIS-2629560, ZFMK-TIS-2629576, ZFMK-TIS-2629577, ZFMK-TIS-2640820, ZFMK-TIS-2640821, ZFMK-TIS-2640822, ZFMK-TIS-2640823, ZFMK-TIS-2640824, ZFMK-TIS-2640825, ZFMK-TIS-2640826, ZFMK-TIS-2640827. • 1 ♀; Hesse, Rheingau-Taunus, Lorch am Rhein, above Nollig castle; 50.0495°N, 7.7966°E; ca 250 m a.s.l.; 12–17 Jun. 2015; Niehuis, Oliver leg.; Malaise trap; MF 3; ZFMK-TIS-2629252. • 3 ♂♂; same collection data as for preceding 17–25 Jun. 2015; ZFMK-TIS-2628232, ZFMK-TIS-2629212, ZFMK-TIS-2629213. • 1 ♀; Hesse, Rheingau-Taunus, Lorch am Rhein, above Nollig castle; 50.0498°N, 7.7974°E; ca 260 m a.s.l.; 27 May–7 Jun. 2013; Niehuis, Oliver leg.; Malaise trap; MF 2; ZFMK-TIS-2629266. • 2 ♀♀; same collection data as for preceding 7–15 Jun. 2013; ZFMK-TIS-2628233, ZFMK-TIS-2629250. • 5 ♀♀; same collection data as for preceding 15–23 Jun. 2013; ZFMK-TIS-2629269, ZFMK-TIS-2629270, ZFMK-TIS-2629271, ZFMK-TIS-2629501, ZFMK-TIS-2629502. • 7 ♂♂; same collection data as for preceding 15–21 Jul. 2013; ZFMK-TIS-2629513, ZFMK-TIS-2629515, ZFMK-TIS-2629550, ZFMK-TIS-2629551, ZFMK-TIS-2629552, ZFMK-TIS-2640710, ZFMK-TIS-2640711. • 12 ♂♂; same collection data as for preceding 21–27 Jul. 2013; ZFMK-TIS-2629243, ZFMK-TIS-2629244, ZFMK-TIS-2629245, ZFMK-TIS-2629246, ZFMK-TIS-2629496, ZFMK-TIS-2629497, ZFMK-TIS-2629527, ZFMK-TIS-2629528, ZFMK-TIS-2629529, ZFMK-TIS-2629530, ZFMK-TIS-2629531, ZFMK-TIS-2629532. • 1 ♀, 1 ♂; Hesse, Waldeck-Frankenberg, National park Kellerwald-Edersee, Banfehaus, old floodplain of the Banfe; 51.167°N, 8.9749°E; ca 270 m a.s.l.; 22 Jul.–5 Aug. 2021; GBOL III leg.; Malaise trap (Krefeld version); female - ZFMK-TIS-2640790; male - ZFMK-TIS-2640792. • 2 ♀♀; Hesse, Waldeck-Frankenberg, National park Kellerwald-Edersee, Maierwiesen; 51.1555°N, 9.0015°E; ca 370 m a.s.l.; 22 Jun.–8 Jul. 2021; GBOL III leg.; Malaise trap (Krefeld version); ZFMK-TIS-2640807, ZFMK-TIS-2640808. • 9 ♀♀, 1 ♂; Hesse, Waldeck-Frankenberg, NP Kellerwald-Edersee, „Banfe-Haus“; 51.167°N, 8.9749°E; ca 270 m a.s.l.; 7–21 Jul.

2022; GBOL III leg.; Malaise trap; females - ZFMK-TIS-2640761, ZFMK-TIS-2640762, ZFMK-TIS-2640763, ZFMK-TIS-2640764, ZFMK-TIS-2640765, ZFMK-TIS-2640766, ZFMK-TIS-2640767, ZFMK-TIS-2640768, ZFMK-TIS-2640769; male - ZFMK-TIS-2640755. • 1 ♀; Hesse, Waldeck-Frankenberg, NP Kellerwald-Edersee, „Kleiner Mehlberg“; 51.2105°N, 9.042°E; ca 360 m a.s.l.; 30 Sep.-14 Oct. 2021; GBOL III leg.; Malaise trap; ZFMK-TIS-2640610. • 1 ♂; Hesse, Waldeck-Frankenberg, NP Kellerwald-Edersee, „Maierwiesen“; 51.1555°N, 9.0015°E; ca 370 m a.s.l.; 8–22 Jul. 2021; GBOL III leg.; Malaise trap; ZFMK-TIS-2640732. • 1 ♀; Lower Saxony, Lüchow-Dannenberg, Pevestorf, Deichvorland & Deich; 53.0636°N, 11.4742°E; ca 20 m a.s.l.; 6–10 Aug. 2013; Krogmann, Lars leg.; Malaise trap; ZFMK-TIS-2629251. • 1 ♀, 3 ♂♂; North Rhine-Westphalia, Bonn, Garden of Museum Koenig, Various habitats; 50.7215°N, 7.1137°E; ca 70 m a.s.l.; 4 Jul. 2022; Schwingeler, Josefine, Jonathan Vogel leg.; sweep net; female - ZFMK-TIS-2640738; males - ZFMK-TIS-2640735, ZFMK-TIS-2640736, ZFMK-TIS-2640737. • 2 ♀♀; North Rhine-Westphalia, Bonn, Museum Koenig, garden; 50.7214°N, 7.1139°E; ca 70 m a.s.l.; 4 Oct. 2022; Salden, Tobias leg.; sweep net; ZFMK-TIS-2635303, ZFMK-TIS-2635304. • 1 ♀; North Rhine-Westphalia, Borken, Borken, spinach field with flower strip; 51.8078°N, 6.8324°E; ca 60 m a.s.l.; 2–9 Aug. 2016; Schwarz et al. leg.; Malaise trap; ZFMK-TIS-2629284. • 1 ♂; North Rhine-Westphalia, Delbrück, Delbrück, Nat. res. „Steinhorster Becken“; 51.8217°N, 8.542°E; ca 90 m a.s.l.; 22 Jul.-5 Aug. 2021; GBOL III leg.; Malaise trap; ZFMK-TIS-2640677. • 1 ♀; North Rhine-Westphalia, Paderborn, Delbrück, Nat. res. „Erdgarten-Lauerwiesen“, alder carr surrounded by wet meadows, ponds, muddy, geese; 51.7989°N, 8.6582°E; ca 110 m a.s.l.; 31 Aug.-14 Sep. 2021; GBOL III leg.; Malaise trap; ZFMK-TIS-2640674. • 1 ♀; North Rhine-Westphalia, Paderborn, Delbrück, Nat. res. „Steinhorster Becken“; 51.82°N, 8.5409°E; ca 90 m a.s.l.; 19 Aug.-2 Sep. 2021; GBOL III leg.; Malaise trap; ZFMK-TIS-2640692. • 1 ♀, 1 ♂; same collection data as for preceding 2–16 Sep. 2021; female - ZFMK-TIS-2640715; male - ZFMK-TIS-2640714. • 1 ♀, 4 ♂♂; same collection data as for preceding 16–30 Sep. 2021; female - ZFMK-TIS-2640803; males - ZFMK-TIS-2640799, ZFMK-TIS-2640800, ZFMK-TIS-2640801, ZFMK-TIS-2640802. • 9 ♂♂; same collection data as for preceding 30 Sep.-14 Oct. 2021; ZFMK-TIS-2640810, ZFMK-TIS-2640811, ZFMK-TIS-2640812, ZFMK-TIS-2640813, ZFMK-TIS-2640814, ZFMK-TIS-2640815, ZFMK-TIS-2640816, ZFMK-TIS-2640817, ZFMK-TIS-2640818. • 1 ♀; North Rhine-Westphalia, Paderborn, Delbrück, Nat. res. „Steinhorster Becken“; 51.8252°N, 8.5359°E; ca 90 m a.s.l.; 19 Aug.-2 Sep. 2021; GBOL III leg.; Malaise trap; ZFMK-TIS-2640693. • 6 ♂♂; same collection data as for preceding 2–16 Sep. 2021; ZFMK-TIS-2640793, ZFMK-TIS-2640794, ZFMK-TIS-2640795, ZFMK-TIS-2640796, ZFMK-TIS-2640797, ZFMK-TIS-2640798. • 4 ♂♂; same collection data as for preceding 16–30 Sep. 2021; ZFMK-TIS-2640727, ZFMK-TIS-2640728, ZFMK-TIS-2640729, ZFMK-TIS-2640730. • 1 ♀; North Rhine-Westphalia, Rhein-Sieg-Kreis, Oberdrees, Buschfeld; 50.6371°N, 6.9157°E; ca 160 m a.s.l.; 28 May-6 Jun. 2021; GBOL III leg.; Malaise trap; ZFMK-TIS-2640679. • 1 ♀; North Rhine-Westphalia, Rhein-Sieg-Kre-

is, Schladern near Windeck, Sieg river, right river bank; 50.8°N, 7.585°E; ca 130 m a.s.l.; 30 May-6 Jun. 2017; ZFMK et al. leg.; Malaise trap; ZFMK-TIS-2628234. • 1 ♀; same collection data as for preceding 6–13 Jun. 2017; ZFMK-TIS-2629239. • 1 ♀; same collection data as for preceding 13–20 Jun. 2017; ZFMK-TIS-2629262. • 4 ♀♀; same collection data as for preceding 20–27 Jun. 2017; ZFMK-TIS-2629279, ZFMK-TIS-2629280, ZFMK-TIS-2629281, ZFMK-TIS-2629282. • 2 ♀♀; same collection data as for preceding 27 Jun.-4 Jul. 2017; ZFMK-TIS-2629260, ZFMK-TIS-2629261. • 3 ♀♀; same collection data as for preceding 4–11 Jul. 2017; ZFMK-TIS-2629264, ZFMK-TIS-2629275, ZFMK-TIS-2629277. • 10 ♀♀, 23 ♂♂; same collection data as for preceding 18–25 Jul. 2017; females - ZFMK-TIS-2629290, ZFMK-TIS-2629292, ZFMK-TIS-2629487, ZFMK-TIS-2629488, ZFMK-TIS-2629489, ZFMK-TIS-2629490, ZFMK-TIS-2629508, ZFMK-TIS-2629561, ZFMK-TIS-2629562, ZFMK-TIS-2629563; males - ZFMK-TIS-2629217, ZFMK-TIS-2629247, ZFMK-TIS-2629265, ZFMK-TIS-2629286, ZFMK-TIS-2629287, ZFMK-TIS-2629288, ZFMK-TIS-2629291, ZFMK-TIS-2629293, ZFMK-TIS-2629294, ZFMK-TIS-2629486, ZFMK-TIS-2629492, ZFMK-TIS-2629510, ZFMK-TIS-2629511, ZFMK-TIS-2629518, ZFMK-TIS-2629519, ZFMK-TIS-2629520, ZFMK-TIS-2629564, ZFMK-TIS-2629565, ZFMK-TIS-2629566, ZFMK-TIS-2629567, ZFMK-TIS-2629569, ZFMK-TIS-2629570, ZFMK-TIS-2629571. • 7 ♀♀, 19 ♂♂; same collection data as for preceding 1–8 Aug. 2017; females - ZFMK-TIS-2629253, ZFMK-TIS-2629254, ZFMK-TIS-2629255, ZFMK-TIS-2629256, ZFMK-TIS-2629257, ZFMK-TIS-2629258, ZFMK-TIS-2629259; males - ZFMK-TIS-2629215, ZFMK-TIS-2629224, ZFMK-TIS-2629228, ZFMK-TIS-2629231, ZFMK-TIS-2629232, ZFMK-TIS-2629233, ZFMK-TIS-2629234, ZFMK-TIS-2629235, ZFMK-TIS-2629543, ZFMK-TIS-2629544, ZFMK-TIS-2629545, ZFMK-TIS-2629546, ZFMK-TIS-2629547, ZFMK-TIS-2629548, ZFMK-TIS-2629549, ZFMK-TIS-2629572, ZFMK-TIS-2629573, ZFMK-TIS-2629574, ZFMK-TIS-2629575. • 2 ♂♂; same collection data as for preceding 15–30 Aug. 2017; ZFMK-TIS-2629220, ZFMK-TIS-2640675. • 1 ♂; Rhineland-Palatinate, Ahrweiler, Niederzissen, Bausenberg; 50.4679°N, 7.2223°E; ca 330 m a.s.l.; 12–27 Jul. 2022; Jaume-Schinkel, Santiago leg.; Gressit Malaise trap; ZFMK-TIS-2640672. • 1 ♀, 1 ♂; Rhineland-Palatinate, Ahrweiler, Niederzissen, Bausenberg, dry grassland; 50.4647°N, 7.2222°E; ca 320 m a.s.l.; 14–20 Jul. 2017; ZFMK et al. leg.; Malaise trap; MF 5; female - ZFMK-TIS-2629509; male - ZFMK-TIS-2629516. • 1 ♀; Rhineland-Palatinate, Alzey-Worms, Wine fields north of Monsheim, shrub islands between wine fields, mostly poplars; 49.6406°N, 8.2137°E; ca 150 m a.s.l.; 5–24 Aug. 2021; Gilgenbach, Carolin leg.; Malaise trap; ZFMK-TIS-2640678. • 1 ♂; Rhineland-Palatinate, Cochem, Nat. res. Brauselay; 50.1421°N, 7.1881°E; ca 120 m a.s.l.; 29 May 2020; DINA leg.; Malaise trap; ZFMK-TIS-2629216 (EVK). • 1 ♀; Saarland, Neunkirchen, Schiffweiler, Landsweiler-Reden, Höfertal; 50.0767°N, 7.3283°E; ca 370 m a.s.l.; 18 Jun. 2022; AK Diptera leg.; sweep net; ZFMK-TIS-2640838. • 1 ♂; Saarland, Saarpfalz, Gersheim; 49.31°N, 8.1683°E; ca 140 m a.s.l.; 19 Jun. 2022; AK Diptera leg.; sweep net; ZFMK-TIS-2640839. • 2 ♂♂;

Schleswig-Holstein, Nordfriesland, Nat. res. Luetjenholmer Heidedünen; 54.6963°N, 9.0643°E; ca 0 m a.s.l.; 29 May 2020; DINA leg.; Malaise trap; ZFMK-TIS-2629229 (EVK), ZFMK-TIS-2629230 (EVK).

LITHUANIA • 1 ♀; Silute distr., Sysa, Sysa, control plot; 55.3127°N, 21.4049°E; ca 0 m a.s.l.; 15–25 Jul. 2020; Petrasiuas, Andrius leg.; Malaise trap; ZFMK-TIS-2637713.

THE NETHERLANDS • 1 ♂; Noord-Holland, Amsterdam, Vondelpark; 52.3581°N, 4.8681°E; ca 0 m a.s.l.; 3–12 Jun. 2019; Taxon Expeditions Team leg.; Malaise trap; ZFMK-TIS-2640687. • 2 ♀♀, 1 ♂; same collection data as for preceding 12–15 Jun. 2019; females - ZFMK-TIS-2640718, ZFMK-TIS-2640719; male - ZFMK-TIS-2640720. • 1 ♂; same collection data as for preceding 21–25 Jun. 2019; ZFMK-TIS-2640689. • 1 ♀; same collection data as for preceding 19–27 Jul. 2019. • 2 ♀♀, 1 ♂; same collection data as for preceding 7 Aug. 2019; females - ZFMK-TIS-2640721, ZFMK-TIS-2640722; male - ZFMK-TIS-2640723. • 2 ♂♂; Noord-Holland, Amsterdam, Vondelpark, Urban park; 52.356°N, 4.861°E; ca 0 m a.s.l.; 19–27 Jul. 2019; Taxon Expeditions (M. Schilthuizen) leg.; Malaise trap; ZFMK-TIS-2640841, ZFMK-TIS-2640842. • 1 ♀; same collection data as for preceding 2019; ZFMK-TIS-2640840.

NORWAY • 1 ♂; Rogaland Ytre, Finnøy, Nordre Vignes; 59.1679°N, 5.7883°E; ca 10 m a.s.l.; 22 Sep.–1 Nov. 2020; Tengesdal, Gaute leg.; Malaise trap; ZFMK-TIS-2640680.

**Material without DNA barcode.** BELGIUM • 1 ♂; Walloon Brabant, Ottignies; 3–10 Sep. 1983; Paul Dessart leg.; Malaise trap; JV\_Prel\_0057 (RBINS). • 1 ♀, 1 ♂; Walloon Region, Luik, Wanze, Antheit (Corphalie); 50.5363°N, 5.2515°E; ca 110 m a.s.l.; 14–28 Jul. 1989; R. Detry leg.; Malaise trap; ZFMK-HYM-00039669, JV\_Prel\_0044 (RBINS). • 1 ♂; same collection data as for preceding 28 Jul.–11 Aug. 1989; JV\_Prel\_0054 (RBINS). • 1 ♀, 1 ♂; West Flanders, Oostkamp, Private garden; 51.168°N, 3.276°E; ca 0 m a.s.l.; 16–30 Aug. 2020; Arnout Zwaenepoel leg.; Malaise trap; female - ZFMK-TIS-2640697; male - ZFMK-TIS-2640696. • 1 ♂; West Flanders, Snellegem, Vloethembos; 9 Jun. 1983; P. Grootaert leg.; hand caught; JV\_Prel\_0059 (RBINS). • 1 ♀; West Flanders, Ypres, De Triangel, Urban park (bushes); 50.8418°N, 2.8838°E; ca 20 m a.s.l.; 28 May–18 Jun. 2022; Fons Verheyde leg.; Malaise trap; JV\_Prel\_0058 (RBINS). • 1 ♀; same collection data as for preceding 20 Aug.–3 Sep. 2022; JV\_Prel\_0053 (RBINS). • 1 ♀; same collection data as for preceding 17 Sep.–1 Oct. 2022; JV\_Prel\_0055 (RBINS). • 15 ♀♀, 8 ♂♂; West Flanders, Ypres, De Triangel, Urban park (pool vegetation); 50.8427°N, 2.884°E; ca 20 m a.s.l.; 6–20 Aug. 2022; Fons Verheyde leg.; Malaise trap; females - JV\_Prel\_0111 (RBINS), JV\_Prel\_0112 (RBINS), JV\_Prel\_0113 (RBINS), JV\_Prel\_0114 (RBINS), JV\_Prel\_0115 (RBINS), JV\_Prel\_0116 (RBINS), JV\_Prel\_0117 (RBINS), JV\_Prel\_0118 (RBINS), JV\_Prel\_0119 (RBINS), JV\_Prel\_0120 (RBINS), JV\_Prel\_0121 (RBINS), JV\_Prel\_0122 (RBINS), JV\_Prel\_0123 (RBINS), JV\_Prel\_0124 (RBINS), JV\_Prel\_0125 (RBINS); males - JV\_Prel\_0103 (RBINS), JV\_Prel\_0104 (RBINS), JV\_Prel\_0105 (RBINS), JV\_Prel\_0106 (RBINS), JV\_Prel\_0107 (RBINS), JV\_Prel\_0108 (RBINS), JV\_Prel\_0109 (RBINS), JV\_Prel\_0110 (RBINS). • 8 ♀♀, 10 ♂♂; same collection data as for preceding 20 Aug.–

3 Sep. 2022; females - JV\_Prel\_0095 (RBINS), JV\_Prel\_0096 (RBINS), JV\_Prel\_0097 (RBINS), JV\_Prel\_0098 (RBINS), JV\_Prel\_0099 (RBINS), JV\_Prel\_0100 (RBINS), JV\_Prel\_0101 (RBINS), JV\_Prel\_0102 (RBINS); males - JV\_Prel\_0085 (RBINS), JV\_Prel\_0086 (RBINS), JV\_Prel\_0087 (RBINS), JV\_Prel\_0088 (RBINS), JV\_Prel\_0089 (RBINS), JV\_Prel\_0090 (RBINS), JV\_Prel\_0091 (RBINS), JV\_Prel\_0092 (RBINS), JV\_Prel\_0093 (RBINS), JV\_Prel\_0094 (RBINS). • 5 ♀♀, 9 ♂♂; same collection data as for preceding 3–17 Sep. 2022; females - JV\_Prel\_0068 (RBINS), JV\_Prel\_0069 (RBINS), JV\_Prel\_0070 (RBINS), JV\_Prel\_0071 (RBINS), JV\_Prel\_0072 (RBINS); males - JV\_Prel\_0061 (RBINS), JV\_Prel\_0062 (RBINS), JV\_Prel\_0063 (RBINS), JV\_Prel\_0064 (RBINS), JV\_Prel\_0065 (RBINS), JV\_Prel\_0066 (RBINS), JV\_Prel\_0067 (RBINS), ZFMK-HYM-00039673, ZFMK-HYM-00039672.

DENMARK • 4 ♂♂; Southern Jutland, Rømø; 24 Sep. 2000; Torkhild Munk leg.; NHRS-HEVA 000023146 (NHRS), NHRS-HEVA 000023147 (NHRS), NHRS-HEVA 000023148 (NHRS), NHRS-HEVA 000023149 (NHRS). • 1 ♀; Western Jutland, Baldersbaek, plantation; 12 Jul. 1993; Torkhild Munk leg.; NHRS-HEVA 000023150 (NHRS).

GERMANY • 1 ♀; Baden-Württemberg, Karlsruhe, Malsch, Luderbusch, south faced slope; 48.9131°N, 8.3325°E; ca 120 m a.s.l.; 26 Jul.–2 Aug. 2020; Dieter Doczkal | K. Grabow leg.; Malaise trap; ZFMK-TIS-2640695. • 1 ♂; Bavaria, Allgäu, Balderschwang, Leiterberg; 47.4858°N, 10.0899°E; ca 1290 m a.s.l.; 4–21 Sep. 2017; Dieter Doczkal | Johannes Voith leg.; Malaise trap; ZFMK-TIS-2640708. • 1 ♀; Berlin, Berlin, Chausseestraße 109, ruderal area; 29 Jun.–5 Jul. 2009; A. Wiesener | V. Richter | F. Koch leg.; MfN URI: 57384a (ZHMB). • 1 ♀; Hesse, Gießen, Botanical garden; 50.5859°N, 8.678°E; ca 170 m a.s.l.; 18 Jun. 2021; GBOL III leg.; sweep net; ZFMK-TIS-2629491. • 1 ♂; Hesse, Rheingau-Taunus, Lorch am Rhein, oberhalb der Burg Nollig; 50.0491°N, 7.7978°E; ca 240 m a.s.l.; 21–27 Jul. 2013; Oliver Niehuis leg.; Malaise trap; ZFMK-TIS-2629579. • 1 ♂; Hesse, Rheingau-Taunus, Lorch am Rhein, oberhalb der Burg Nollig; 50.0498°N, 7.7974°E; ca 260 m a.s.l.; 15–21 Jul. 2013; Oliver Niehuis leg.; Malaise trap; ZFMK-TIS-2629514. • 2 ♂♂; same collection data as for preceding 21–27 Jul. 2013; ZFMK-TIS-2629242, ZFMK-TIS-2629526. • 5 ♂♂; Hesse, Werra-Meißner-Kreis, Großalmerode, Private garden, Siedlerweg, semi-abandoned garden with wet spot, ivy hedge and salix; 51.2591°N, 9.7871°E; ca 380 m a.s.l.; 12–20 Jul. 2022; Jonathan Vogel leg.; Malaise trap; ZFMK-TIS-2640700, ZFMK-TIS-2640701, ZFMK-TIS-2640702, ZFMK-TIS-2640703, ZFMK-TIS-2640705. • 2 ♀♀; North Rhine-Westphalia, Bonn, ZFMK garden, lawn and bushes; 50.7218°N, 7.1132°E; ca 70 m a.s.l.; 30 Aug. 2022; AG Hymenoptera leg.; sweep net; ZFMK-TIS-2640698, ZFMK-TIS-2640699. • 1 ♀; same collection data as for preceding 1 Sep. 2022; ZFMK-HYM-00039670. • 1 ♀; North Rhine-Westphalia, Rhein-Sieg-Kreis, Alfter, Mirbachstrasse; 50.7307°N, 7.0142°E; ca 90 m a.s.l.; 22 Jul. 2021; GBOL III leg.; sweep net; ZFMK-TIS-2629298. • 1 ♀; North Rhine-Westphalia, Rhein-Sieg-Kreis, Schladern near Windeck, Sieg river, right river bank; 50.8°N, 7.585°E; ca 130 m a.s.l.; 20–27 Jun. 2017; ZFMK et al. leg.; Malaise trap; ZFMK-TIS-2629283. • 1 ♀, 2 ♂♂; same collection data as for preceding 20–27 Jun. 2017; ZFMK-TIS-2629283.

ing 18–25 Jul. 2017; female - ZFMK-TIS-2629289; males - ZFMK-TIS-2629485, ZFMK-TIS-2629568. • 2 ♂♂; Rhineland-Palatinate, Ahrweiler, Niederzissen, Bausenbergslope of volcanic mountain, mixed broad-leaved forest; 50.4679°N, 7.2223°E; ca 330 m a.s.l.; 12–27 Jul. 2022; Santiago Jaume Schinkel leg.; Gressitt Malaise trap; ZFMK-HYM-00039687, ZFMK-HYM-00039688. • 1 ♂; Rhineland-Palatinate, Ahrweiler, Niederzissen, Bausenbergslope of volcanic mountain, next to oak tree; 50.4672°N, 7.2212°E; ca 310 m a.s.l.; 12–27 Jul. 2022; Santiago Jaume Schinkel leg.; Gressitt Malaise trap; ZFMK-HYM-00039671. • 1 ♂; Saxony, Leipzig, surroundings of Naunhof; 28 Jul. 1957; Michalk leg.; JV\_Prel\_0046 (SDEI).

THE NETHERLANDS • 1 ♀; Gelderland, Beek-Ubbergen, Goudenregenstraat, garden; 51.8268°N, 5.9332°E; ca 10 m a.s.l.; 1 Oct. 2023; Jochem Kühnen leg.; hand caught; ZFMK-HYM-00039657. • 1 ♂; Gelderland, Nijmegen, Gelderse poort; 10 May 2022; R. Lexmond leg.; Malaise trap; JV\_Prel\_0043 (RBINS). • 1 ♀, 7 ♂♂; same collection data as for preceding 20 Jul. 2022; female - JV\_Prel\_0077 (RBINS); males - JV\_Prel\_0078 (RBINS), JV\_Prel\_0079 (RBINS), JV\_Prel\_0080 (RBINS), JV\_Prel\_0081 (RBINS), JV\_Prel\_0082 (RBINS), JV\_Prel\_0083 (RBINS), JV\_Prel\_0084 (RBINS). • 1 ♀; same collection data as for preceding 23 Aug. 2022; JV\_Prel\_0060 (RBINS).

PORTUGAL • 1 ♂; Madeira, Funchal, Curral das Romeiros; ca 550 m a.s.l.; 8 Feb. 1991; Martti Koponen leg.; specimen in coll. Koponen.

SWEDEN • 1 ♂; Dalarna, Rättvik, Glostjärn; 20 May-30 Jun. 1977; Tord Tjeder leg.; NHRS-HEVA 000023151 (NHRS). • 1 ♀; Hälsingland, Älgesjön; 62.16°N, 16.212°E; ca 300 m a.s.l.; 17 May-15 Jun. 2002; Erik Sahlin leg.; window trap; Tömn 1, specimen in coll. MF. • 1 ♂; Närke; 10 Aug. 1953; Anton Jansson leg.; NHRS-HEVA 000023153 (NHRS). • 1 ♂; Närke, Oset; 8 Aug. 1941; Anton Jansson leg.; NHRS-HEVA 000023152 (NHRS). • 1 ♂; Öland, Kastlösa; 26 Jun. 1962; Karl-Johan Hedqvist leg.; NHRS-HEVA 000023175 (NHRS). • 1 ♀; Öland, Mörbylånga kommun, Skogsby, Ecological research station, lawn in garden with sandy soil; 56.6283°N, 16.4918°E; ca 30 m a.s.l.; 29 Aug.-11 Sep. 2008; Swedish Malaise Trap Project (Swedish Museum of Natural History) leg.; Malaise trap; NHRS-HEVA 000023174 (NHRS). • 1 ♂; Östergötland, S:t Anna, Svensmarö, Sanningholmen; 7 Aug. 1976; Gustaf Wängsjö leg.; NHRS-HEVA 000023176 (NHRS). • 1 ♂; Scania, Kristianstads kommun, Trunelän, Degeberga, Grazed meadow at alder stand along stream; 55.7746°N, 14.2156°E; ca 80 m a.s.l.; 1–13 Aug. 2019; Swedish Insect Inventory Programme (SIIP), Station Linné leg.; Malaise trap; NHRS-HEVA 000023155 (NHRS). • 1 ♂; Scania, Malmö kommun, Klagshamn, Limhamns kalkbrott, Limestone quarry; 55.5694°N, 12.9267°E; ca -50 m a.s.l.; 4–12 Jun. 2018; Swedish Insect Inventory Programme (SIIP), Station Linné leg.; Malaise trap; NHRS-HEVA 000023154 (NHRS). • 2 ♂♂; Södermanland, Trosa kommun, Hunga södergård 1, agricultural backyard, heavily eutrophicated, in tall grass near stable manure pile; 58.9207°N, 17.5212°E; ca 20 m a.s.l.; 16 May-13 Jun. 2004; Swedish Malaise Trap Project (Swedish Museum of Natural History) leg.; Malaise trap; NHRS-HEVA 000023156 (NHRS), NHRS-HEVA 000023157 (NHRS). • 4 ♀♀, 3 ♂♂; same collection data as for preceding 9–19 Aug. 2004; females - NHRS-HEVA 000023158 (NHRS), NHRS-HEVA 000023160

(NHRS), NHRS-HEVA 000023161 (NHRS), NHRS-HEVA 000023164 (NHRS); males - NHRS-HEVA 000023159 (NHRS), NHRS-HEVA 000023162 (NHRS), NHRS-HEVA 000023163 (NHRS). • 1 ♂; Södermanland, Väsbyön; 11 Aug. 1950; Anton Jansson leg.; NHRS-HEVA 000023165 (NHRS). • 1 ♀; Uppland, Almunge, Harparbol; 20 Jun. 1948; Olov Lundblad leg.; NHRS-HEVA 000023169 (NHRS). • 1 ♀, 1 ♂; Uppland, Älvkarleby, Båtfors, flood-regiment oldgrowth birch edge of pine forest; 60.4607°N, 17.3178°E; ca 40 m a.s.l.; 14 Jun.-4 Jul. 2005; Swedish Malaise Trap Project (Swedish Museum of Natural History) leg.; Malaise trap; female - NHRS-HEVA 000023167 (NHRS); male - NHRS-HEVA 000023166 (NHRS). • 1 ♂; Uppland, Håbo kommun, Biskops-Arnö, elm grove; 59.6721°N, 17.5009°E; ca 10 m a.s.l.; 27 Aug.-10 Sep. 2004; Swedish Malaise Trap Project (Swedish Museum of Natural History) leg.; Malaise trap; NHRS-HEVA 000023168 (NHRS). • 1 ♀; Uppland, Uppsala, Vårdsätra skog, forest; 7-28 Oct. 2002; Fredrik Ronquist leg.; Malaise trap; specimen in coll MF. • 2 ♂♂; Västerbotten, Hällnäs; 22 Aug. 1961; Karl-Johan Hedqvist leg.; NHRS-HEVA 000023170 (NHRS), NHRS-HEVA 000023171 (NHRS). • 1 ♀; Västergötland, South of Alingsås; 29 Jul. 1998; Torkhild Munk leg.; NHRS-HEVA 000023172 (NHRS). • 1 ♀; Västmanland, Sala kommun, Västerfärnebo, Nötmyran (Östermyran), birch stand in moist haymaking meadow; 59.942°N, 16.3095°E; ca 70 m a.s.l.; 18 Aug.-1 Sep. 2003; Swedish Malaise Trap Project (Swedish Museum of Natural History) leg.; Malaise trap; NHRS-HEVA 000023173 (NHRS).

SWITZERLAND • 1 ♀; Neuchâtel, Montmollin; 1 Aug. 1966; Jacques de Beaumont leg.; specimen at MHNG. • 2 ♂♂; same collection data as for preceding 3 Aug. 1957; specimens at MHNG. • 1 ♂; same collection data as for preceding 17 Aug. 1962; specimen at MHNG. • 1 ♂; same collection data as for preceding 19 Aug. 1957; specimen at MHNG. • 2 ♂♂; same collection data as for preceding 31 Aug. 1956; specimens at MHNG. • 1 ♂; same collection data as for preceding 29 Sep. 1956; specimen at MHNG. • 1 ♀; St. Gallen, Pfäfers; 9 Sep. 1992; F. Amiet leg.; specimen at NMBE. • 1 ♀; Valais, Visperterminen; ca 1550 m a.s.l.; 4 Aug. 1996; Gerhard Bächli | Bernhard Merz leg.; specimen at NMBE. • 1 ♂; Vaud, Ferreyres; 8 Sep. 1964; Jacques de Beaumont leg.; specimens at MHNG. • 1 ♀; Vaud, Lausanne, Vidy; 9 Sep. 1948; Jacques Aubert leg.; specimens at MHNG. • 1 ♀; Vaud, Lutry; 18 Jun. 1954; Jacques Aubert leg.; specimens at MHNG. • 1 ♂; Vaud, Rougemont; ca 1000 m a.s.l.; 14 Jun. 1963; Claude Besuchet leg.; specimens at MHNG.

**Biology.** Summer species, flying mainly from May to October, peak in July. Collected in all kinds of habitats: deciduous and coniferous forests, gardens, parks and orchards, agricultural fields, pastures and meadows, ruderal land, ponds and marshes

**Distribution.** Verified by morphological examination: Belgium, Denmark, Germany (locus typicus of *A. spheciformis*; locus typicus of *A. fergussoni*: Ingelheim am Rhein), Lithuania, The Netherlands, Norway, Portugal, Sweden (locus typicus of *A. eucharoides*: Västergötland), Switzerland, United Kingdom (locus typicus of *A. tincta*: unclear, either near London, Isle of Wight or Machynlleth (North Wales)).

CO1 barcode sequence matches: Belarus (e.g. GMBMQ746-17) and Canada (e.g. BBHYJ932-10).

Lowland species, usually occurring in elevations below 500 m a.s.l., rarely collected in higher altitudes, most specimens between 0–100 m a.s.l.

**Remarks.** *A. eucharioides* is both the most commonly collected and the most morphologically heterogeneous species within the genus *Anacharis*. Specimens often exhibit slight metallic sheen on their mesoscutum and head that is more notable in ethanol-stored specimens but sometimes retains on dried specimens.

The type of *A. eucharioides* is reportedly lost (Fergusson 1986, Mata-Casanova et al. 2018), which we confirm herein by having searched the collection of the NHRS in addition to previous efforts at other possible depositories (NHMUK, MZLU). In the current situation with several new species, we disagree with Fergusson's statement, that "...there is no confusion about the identity of this species" and that "a neotype is not required" (Fergusson 1986) and rather stress the necessity to designate a neotype from the broader type locality at Västergötland. However, as we were not able to acquire a fresh specimen suitable for DNA sequencing from the type locality, we withhold taking action until a more suitable occasion.

The lectotype of *A. tincta* is glued to its ventral side on cardboard, face down, the wings also glued to the board. It is overall intact, except the terminal four segments of the left antenna, which are detached from the rest of the specimen but still present on the cardboard. Also, the left fore tarsomeres are detached, the second tarsomere is missing, the rest is glued on the card. Both wings and legs obscure the lateral mesosoma on both sides. We here confirm the synonymy with *A. eucharioides*.

The lectotype of *A. spheciformis* (Hartig, 1840) was designated by Weld (1952), who reported the syntype series to consist of 12 specimens. Interestingly, Fergusson (1986) reports only one specimen under the name *A. spheciformis* from the Hartig collection, meaning that 11 syntypes might be lost. Fergusson additionally states the sex of the lectotype to be female, while the specimen is clearly a male. The species was treated as a synonym of *A. typica* by Dalla-Torre and Kieffer (1910) and Weld (1952), as established by Reinhard (1860), but the lectotype has a clearly sculptured mesoscutellum, which makes it distinct from *A. typica*. We agree with the latest treatments of *A. spheciformis* as synonym of *A. eucharioides* (Fergusson 1986; Mata-Casanova et al. 2018) but as we consider *A. typica* a valid species, we formally move it from synonymy with *A. typica* to *A. eucharioides*.

*A. fergussoni* is diagnosed against *A. parapsidalis* and *A. melanoneura* in Mata-Casanova et al. (2018). The reason why it is not considered similar to *A. eucharioides* by the authors is likely due to the distinction they make based on the parascutal sulcus (present in *A. fergussoni*, absent in *A. eucharioides*), as used in their key (couplet 3). As we found this character to be very variable within *A. eucharioides*, this is not sufficient for discrimination. The character states used to diagnose *A. fergussoni* against *A. parapsidalis* and *A. melanoneura* given by Mata-Casanova et al. (2018) match with the re-description of *A. eucharioides* by Mata-Casanova et al. (2018) and our observations. The morphometric values given for *A. fergussoni* fall into the range of *A. eucharioides* as diagnosed herein (Table 2), except the head width:length and the petiole length:metacoxa length which exhibit unusual high values in the description of *A. fergussoni*. However, the former is only 0.1 off of the range of *A. eucharioides*, and might well fall into the error range, and

the latter (relative petiole length) seems erroneous in the description (“about 2.0 times as long as metacoxa” Mata-Casanova et al. 2018), as we measure a value of 1.4 on the images of the holotype, which falls well into the range of what we measured for *A. eucharioides* and is even close to the mean (1.0–1.7, mean 1.5). In terms of qualitative characters, the centrally sparsely pubescent to glabrous median lobe of the mesoscutum, the well-foveated notauli, the median carina of the mesoscutellum that is medially morphing into reticulate sculpture and the smooth to rugose lateromedial area of pronotum are typical for *A. eucharioides*. Based on this re-evaluation of possible morphometric differences and the similarity in qualitative characters between the specimens examined herein and the holotype of *A. fergussoni* we synonymise *A. fergussoni* with *A. eucharioides*.

We want to note that images of the holotype, kindly provided to kindly provided to us by the team at CNC, do not correspond to all the SEM images in Mata-Casanova et al. (2018, Fig. 4A–C). Fig. 4A clearly shows the holotype before the right wings were removed, as does fig. 4B though the image is vertically flipped, but fig. 4C shows a different antennal position and must be a different specimen.

Here, we demonstrate that, given the morphometric variability within *A. eucharioides* and the whole *eucharioides* species group, morphometric characters/analyses cannot reliably separate this species from the others (Fig. 8A). Our diagnosis rather relies on qualitative characters and species delimitation has been crucially informed by the results from analysis of molecular sequence data, which show a distinct cluster/putative species with small intraspecific variability based on almost 300 specimens from various localities. Without this reverse taxonomy approach included, finding and defining species limits within the *eucharioides* species group, and especially of *A. eucharioides* would have been difficult if not impossible.

Additional distribution records are listed in Mata-Casanova et al. (2018) for Andorra, France, Romania, Spain, Slovakia and Hungary. Since our circumscription of *A. eucharioides* is narrower than that of Mata-Casanova et al. (2018), we cannot confirm the presence of the species in these countries (specimens listed as *A. eucharioides* could also belong to *A. typica* or *A. petiolata*) but it is likely present in these regions, too.

**Table 2.** Comparison of morphometric values between **A** *A. fergussoni* in the description of Mata-Casanova et al. (2018), **B** measurements taken from images of the holotype of *A. fergussoni*, **C** *A. eucharioides* in the redescription of Mata-Casanova et al. (2018), and **D** our measured values for *A. eucharioides* (n = 58).

Entities measured	Head dorsal width: length	Head frontal width: height	Malar sulcus length: eye height	Eye-to-eye dist.: eye height	mesoscutum width:length	mesoscutellum_1 width:length	Radial cell length: width	Petiole length: metacoxa length
<b>A</b> <i>A. fergussoni</i> in description (Mata-Casanova et al. 2018)	2.4	1.3	0.7	1.1	1.2	0.6	2.7	2
<b>B</b> <i>A. fergussoni</i> holotype, measured herein		1.2	0.6	1.0	1.2	0.8		1.4
<b>C</b> <i>A. eucharioides</i> in redescription (Mata-Casanova et al. 2018)	2	1.3	0.6	1	1.2	0.8	2.6	>1
<b>D</b> <i>A. eucharioides</i> range, measured herein	1.8–2.3	1.0–1.3	0.6–0.8	1.0–1.1	1.0–1.2	0.6–0.8	2.4–3.3	1.0–1.7

***Anacharis immunis* Walker, 1835**

Figs 2B, 3B, 11A–E

*Anacharis immunis* Walker, 1835: 521 - lectotype (NHMUK) ♂, syn. by Fergusson (1968), photographs examined.

*Anacharis staegeri* Dahlbom, 1842: 4 - lectotype (MZLU) ♀, syn. by Dalla Torre (1893), photographs examined.

*Synapsis aquisgranensis* Förster, 1869: 361 - Holotype (ZMHB) ♂, syn. by Kierych (1984), not examined.

**Diagnosis (n = 14).** Belongs to the *immunis* species group. *Anacharis immunis* can be distinguished from *A. ensifer* and *A. norvegica* by having a largely smooth and even dorsal surface of the mesoscutellum, especially centrally (reticulate-foveate in *A. ensifer* and *A. norvegica*) (Fig. 11D). The fore and mid coxae are usually as dark as the hind coxa (usually distinctly paler than the hind coxa in *A. ensifer*).

**CO1 barcode.** n = 14. Maximum intraspecific distance = 0.2%. Minimum distance to closest species (*A. ensifer*) = 7.8%. CO1 barcode consensus sequence:

AATTTTATACTTTATTATAGGAATCTGATCAGCAATATTAG-GATCAAGACTTAGTATAATTATCCGAATAGAATTAGGGACTCCAT-CACAATTAAATTAGAAATGAACAAATTACAATTCAATTGTAACCGCA-CATGCATTATCATAATTTTTTATAGTTATACCTATTATAGTAG-GAGGATTGGAAATTACCTAATCCCATTAAATACTTTATCTCCAGA-TATAGCTTTCCACGATTAAATAATATAAGATTGATTTAATTCC-CTCTTAGCTTAATATCTTCTAGTTATTGATCAAGGGGCAG-GAACAGGATGAACAATTACCCCTTATCTTCATTAAACAG-GACACTCAGGAATTGCAGTAGATATAACAATCTACTCCCTCATTAA-GAGGAATTCTCAATTAGGATCAATTAAATTATCAGAACAAATT-TAAACATACGAATTAAAGTATCAATAGATAAAATTACTCTATTAGATGATCAATCTTTAACTACAATTATTACTTCTATCATTACCT-GTGCTTGCAGGAGGAATTACTATACTTTATTGACCGAAACTAAACACCTCCTTTGACCCATAGGGGGAGGAGACCCAATCTTATAT-CAACATTATT

**Type material.****Lectotype of *A. immunis* Walker, 1835:**

Type

immunis, Walk. [handwritten, probably by Walker himself]

In coll under immunis

LECTOTYPE

B.M. TYPE HYM 7. 160

LECTOTYPE of *A. immunis* Walker det. N.D.M.Fergusson, 1981

[QR code] NHMUK010640455

[for images, see <https://data.nhm.ac.uk/dataset/56e711e6-c847-4f99-915a-6894bb5c5dea/resource/05ff2255-c38a-40c9-b657-4ccb55ab2feb/record/10638963>]

**Lectotype of *A. staegeri* Dahlbom, 1842:**

♀

LECTOTYPE

LECTOTYPE of *Anacharis staegeri* Dahlm det. N.D.M.Fergusson, 1983

1983 366

MZLU 00215544

MZLU Type no. 6511:1

[for images, see <https://www.flickr.com/photos/tags/mzlutype06511>]

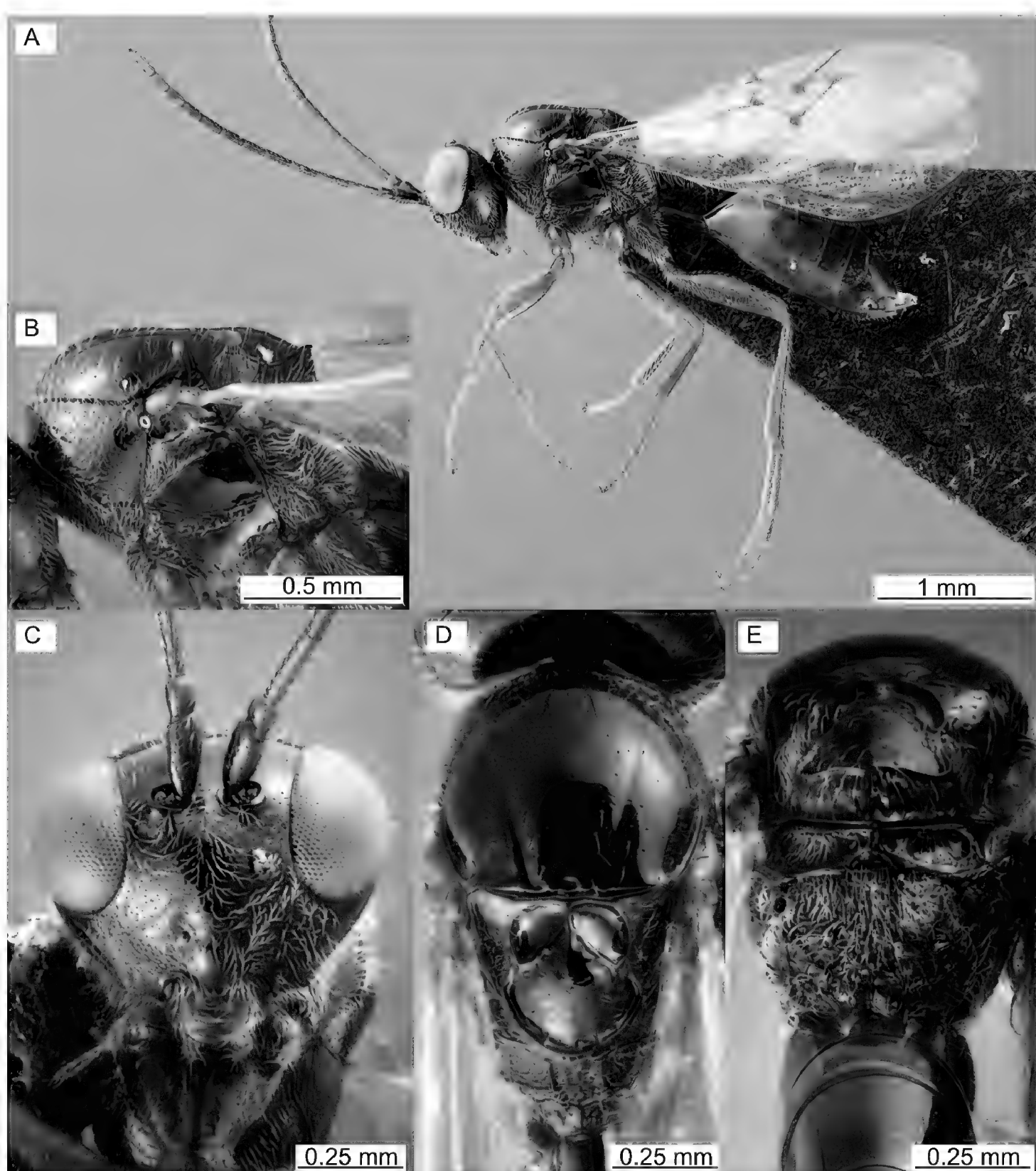


**Figure 11.** *Anacharis immunis*, female (ZFMK-TIS-2640709) **A** habitus **B** mesosoma lateral **C** face **D** mesosoma dorsal **E** mesosoma posterior view.

**Other material examined. DNA barcode vouchers.** GERMANY • 1 ♀; Baden-Württemberg, Karlsruhe, Malsch, Hansjakobstraße, garden; 48.8835°N, 8.3197°E; ca 120 m a.s.l.; 25 Oct.-8 Nov. 2020; Dieter Doczkal leg.; Malaise trap; ZFMK-TIS-2640725. • 1 ♀; Bavaria, Allgäu, Balderschwang, Leiterberg; 47.4858°N, 10.0899°E; ca 1290 m a.s.l.; 4–21 Sep. 2017; Doczkal, Dieter, Voith, J. leg.; Malaise trap; ZFMK-TIS-2640709. • 1 ♀; Bavaria, Garmisch-Partenkirchen, Zugspitze, mountain; 47.4068°N, 11.008°E; ca 2010 m a.s.l.; 20 Jun.-5 Jul. 2018; Doczkal, D., Voith, J. leg.; Malaise trap; ZFMK-TIS-2628218. • 6 ♂♂; Bavaria, Rhön-Grabfeld, Fladungen, Nat. res. Schwarzes Moor, Karpatenbirkenwald; 50.5117°N, 10.071°E; ca 780 m a.s.l.; 26 Jun.-18 Jul. 2017; Dieter Doczkal leg.; Malaise trap; ZFMK-TIS-2629533, ZFMK-TIS-2629534, ZFMK-TIS-2629535, ZFMK-TIS-2629536, ZFMK-TIS-2629537, ZFMK-TIS-2629539. • 2 ♂♂; Hesse, Waldeck-Frankenberg, NP Kellerwald-Edersee, „Banfe-Haus“; 51.167°N, 8.9749°E; ca 270 m a.s.l.; 7–21 Jul. 2022; GBOL III leg.; Malaise trap; ZFMK-TIS-2640756, ZFMK-TIS-2640759. • 3 ♂♂; Rhineland-Palatinate, Ahrweiler, Niederzissen, Bausenberge, upper part of volcanic mountain, next to oak tree; 50.4672°N, 7.2212°E; ca 310 m a.s.l.; 12–27 Jul. 2022; Jaume-Schinkel, Santiago leg.; Gressit Malaise trap; ZFMK-TIS-2640771, ZFMK-TIS-2640772, ZFMK-TIS-2640773.

**Material without DNA barcode.** BELGIUM • 1 ♂; Walloon Brabant, Ottignies; 9–16 Jul. 1983; Paul Dessart leg.; Malaise trap; JV\_Prel\_0073 (RBINS). • 1 ♀; same collection data as for preceding 24 Sep.-1 Oct. 1983; JV\_Prel\_0051 (RBINS). • 1 ♀; Walloon Region, Luik, Wanze, Antheit (Corphalie); 50.5363°N, 5.2515°E; ca 110 m a.s.l.; 16–30 May 1989; R. Detry leg.; Blue pan trap; JV\_Prel\_0056 (RBINS).

DENMARK • 1 ♂; Eastern Jutland, Fugslev; 56.2667°N, 10.7167°E; ca 20 m a.s.l.; 1999; Torkhild Munk leg.; NHRS-HEVA 000023102 (NHRS). • 4 ♂♂; Eastern Jutland, Hjelm; 3–5 Aug. 1992; Torkhild Munk leg.; NHRS-HEVA 000023104 (NHRS), NHRS-HEVA 000023104 (NHRS), NHRS-HEVA 000023104 (NHRS), NHRS-HEVA 000023105 (NHRS). • 1 ♂; Eastern Jutland, Rugård, Sønderskov; 56.2667°N, 10.8167°E; ca 30 m a.s.l.; 20 Jul. 1996; Torkhild Munk leg.; NHRS-HEVA 000023103 (NHRS). • 1 ♀, 1 ♂; Northwestern Jutland, Torup, klitplantage; 56.9667°N, 8.4°E; ca 20 m a.s.l.; 27 Jul. 1989; Torkhild Munk leg.; female - NHRS-HEVA 000023106 (NHRS); male - NHRS-HEVA 000023101 (NHRS).

GERMANY • 1 ♀; Bavaria, Garmisch-Partenkirchen, Zugspitze, mountain; 47.4053°N, 11.0091°E; ca 1980 m a.s.l.; 2–13 Aug. 2018; Dieter Doczkal | Johannes Voith leg.; Malaise trap; ZFMK-HYM-00039683. • 3 ♂♂; Rhineland-Palatinate, Ahrweiler, Niederzissen, Bausenberge, slope of volcanic mountain, mixed broad-leaved forest; 50.4679°N, 7.2223°E; ca 330 m a.s.l.; 12–27 Jul. 2022; Santiago Jaume Schinkel leg.; Gressitt Malaise trap; ZFMK-HYM-00039684, ZFMK-HYM-00039685, ZFMK-HYM-00039686. • 18 ♂♂; Rhineland-Palatinate, Ahrweiler, Niederzissen, Bausenberge, upper part of volcanic mountain, next to oak tree; 50.4672°N, 7.2212°E; ca 310 m a.s.l.; 12–27 Jul. 2022; Santiago Jaume Schinkel leg.; Gressitt Malaise trap; ZFMK-HYM-00039689, ZFMK-HYM-00039690, ZFMK-HYM-00039691, ZFMK-HYM-00039692, ZFMK-HYM-00039693, ZFMK-HYM-00039694,

ZFMK-HYM-00039695, ZFMK-HYM-00039696, ZFMK-HYM-00039697,  
 ZFMK-HYM-00039698, ZFMK-HYM-00039699, ZFMK-HYM-00039700,  
 ZFMK-HYM-00039701, ZFMK-HYM-00039702, ZFMK-HYM-00039703,  
 ZFMK-HYM-00039704, ZFMK-HYM-00039705.

**SWEDEN** • 1 ♀; Närke, Örebro, Adolfsberg; 19 Sep. 1953; Anton Jansson leg.; NHRS-HEVA 000023107 (NHRS). • 1 ♀; Öland, Ekerums strand, dry meadow with mixed trees; 31 Jul. 1977; Sven Johansson leg.; NHRS-HEVA 000023115 (NHRS). • 1 ♂; Östergötland, S:t Anna, Svensmarö, Sanningsholmen; 11 Aug. 1976; Gustav Wängsjö leg.; NHRS-HEVA 000023117 (NHRS). • 1 ♂; Östergötland, Tjärholm; 5 Jul. 1976; Gustav Wängsjö leg.; NHRS-HEVA 000023116 (NHRS). • 1 ♂; Scania, Kristianstads kommun, Trunelän, Degeberga, Grazed meadow at alder stand along stream; 55.7746°N, 14.2156°E; ca 80 m a.s.l.; 16–26 Sep. 2018; Swedish Insect Inventory Programme (SIIP), Station Linné leg.; Malaise trap; NHRS-HEVA 000023109 (NHRS). • 1 ♂; Scania, Kristianstads kommun, Trunelän, Degeberga, Grazed meadow at alder stand along stream; 55.7746°N, 14.2156°E; ca 80 m a.s.l.; 31 May–9 Jun. 2019; Swedish Insect Inventory Programme (SIIP), Station Linné leg.; Malaise trap; NHRS-HEVA 000023108 (NHRS). • 1 ♂; Scania, Kvistofta; 1 Aug. 1949; Anton Jansson leg.; NHRS-HEVA 000023110 (NHRS). • 1 ♀; Småland, Bäckebo, Grytsjön, moist haymaking meadow at birch-spruce forest edge; 56.9314°N, 16.0855°E; ca 80 m a.s.l.; 12 Jul.–18 Aug. 2005; Swedish Malaise Trap Project (Swedish Museum of Natural History) leg.; NHRS-HEVA 000023113 (NHRS). • 2 ♀♀; Småland; [19<sup>th</sup> cent.]; Carl Henning Boheman leg.; NHRS-HEVA 000023111 (NHRS), NHRS-HEVA 000023112 (NHRS). • 1 ♀; Södermanland, Åva; 20 Sep. 1953; Tor-Erik Leiler leg.; NHRS-HEVA 000023114 (NHRS).

**SWITZERLAND** • 1 ♂; Neuchâtel, Auvernier; 1 Aug. 1953; Jacques de Beaumont leg.; specimen at MHNG. • 1 ♂; same collection data as for preceding 10 Aug. 1957; specimen at MHNG. • 1 ♀; same collection data as for preceding 15 Aug. 1956; specimen at MHNG. • 1 ♀; same collection data as for preceding 25 Aug. 1966; specimen at MHNG. • 1 ♂; Neuchâtel, La Tourne; 26 Aug. 1960; Jacques de Beaumont leg.; specimen at MHNG. • 1 ♂; Neuchâtel, Montmollin; 14 Aug. 1957; Jacques de Beaumont leg.; specimen at MHNG. • 1 ♀; Valais, Mayens de Sion Aug. 1957; Jean-Louis Nicod leg.; specimen at MHNG. • 1 ♀; Vaud, Jorat; 29 Jun. 1960; Jacques de Beaumont leg.; specimen at MHNG. • 1 ♀; Vaud, Vidy; 28 Sep. 1953; Jacques de Beaumont leg.; specimen at MHNG.

**Biology.** Summer species, flying mainly from July to September, peak in July. No clear habitat preference but in Sweden and Denmark often collected in open sandy pine forest.

**Distribution.** Verified by morphological examination: Belgium, Denmark, Germany (locus typicus of *A. aquisgranensis*: Aachen and *Megapelmus rufiventris* Hartig, 1841), Sweden (locus typicus of *A. staegeri*), Switzerland, United Kingdom (locus typicus of *A. immunis*: near London).

No DNA barcode matches with publicly available sequences from other countries.

Mainly collected in lowlands below 400 m a.s.l., occasionally found in higher altitudes at 700–900 m a.s.l. and rarely even higher.

**Remarks.** *Anacharis aquisgranensis* was described by Förster (1869) because of its holotype having the mesoscutum fused with the mesoscutellum. He even erected the monotypic genus *Synapsis* (later replaced by *Prosynapsis* Dalla Torre & Kieffer, 1910, due to homonymy) based on that state. Kierych (1984) considered the fusion as an aberrant state and synonymised *Prosynapsis* under *Anacharis* and *A. aquisgranensis* under *A. immunis*. We have not seen such a character state, but it seems rather aberrant if real, and we see no reason to question Kierych's judgment until further.

The distribution records of *A. immunis* reported by Mata-Casanova et al. (2018) require re-evaluation as *A. immunis* sensu Mata-Casanova et al. (2018) also includes *A. ensifer* (see remarks there).

### *Anacharis martinae* Vogel, Forshage & Peters, sp. nov.

<https://zoobank.org/D30ADE83-C297-4381-AEA7-FAA4AB2376C5>

Figs 2F, 3C, 12A–E

**Diagnosis (n = 18).** Belongs to the *eucharioides* species group. Medium sized species (2.6–3.3, mean 2.9 mm, similar to *A. eucharioides*, *A. petiolata* and *A. typica*). Different from *A. petiolata* and *A. typica* in having a centrally carinate mesoscutellum (Fig. 12D, centrally smooth in *A. petiolata* and *A. typica*). Different from *A. eucharioides* by having oblique carinae on the lateromedial area of the pronotum (Fig. 12B). This character is shared with *A. belizini*, which is an Indomalayan species described from Thailand. *Anacharis martinae* differs from *A. belizini* by having a larger glabrous area on the clypeus medioventrally (largely pubescent in *A. belizini*) (Fig. 12C) and a brown to dark-brown metasoma (black in *A. belizini*) (Fig. 12A). WIPs: The band pattern of the fore wings reaching along about half the length of the non-sclerotised vein M (Fig. 2C, reaching along at least 2/3 the length of the non-sclerotised vein M in all other species, including those of the *immunis* species group). The apical spot of the hind wing fills almost the entire apical area (Fig. 2C, filling about half the apical area in other species of the *eucharioides* species group).

**Description. Both sexes. Size.** Body: ♀ 2.6–3.2 (3.2) mm, ♂ 2.3–2.9 mm. Antennae: ♀ 1.7–2.3 (2.1) mm, ♂ 2–2.3 mm. Fore wing: 2.1–2.8 (2.5) mm

**Colour.** Body black to reddish-brown (Fig. 12A); base of scape usually (Fig. 12A, C), head always (Fig. 12A, C), base of mandibles usually (Fig. 12C), mesosoma usually (Fig. 12A, B, D, E), coxa to a varying degree (Fig. 12A), hind-trochanter usually basally, and petiole usually black (Fig. 12A); scape usually apically (Fig. 12C), rest of antennae (Fig. 12A), tegulae (Fig. 12B, D) and metasoma brown (Fig. 12A); mandibles & palps (Fig. 12C) and rest of legs (Fig. 12A) testaceous.

**Head.** Roundish-trapezoid in frontal view, genae gently kinked, in an angle <90° to the vertical axis of the face (Fig. 12C); lower face with thick silvery hairs, densely punctured (Fig. 12C); clypeal margin bilobed, somewhat flanged upwards, clypeus otherwise convex, medioventrally smooth, otherwise punctate (Fig. 12C); malar area with coriaceous texture, reaching from ventral eye margin along entire stretch of mandibular

base (Fig. 18B), anteroventral corner of mandibular base sometimes smooth; genae smooth around eye, with increasingly dense punctuation and regular setae towards the hind margin; upper face with somewhat thinner setae, punctured, with usually shallow median dent; space between toruli sometimes transversally striolate, intertorular distance:torulus to eye distance 1.4–2.0(1.9); eyes with scattered setae, extent varying (Fig. 12C); POL:OOL:LOL:OD 2.4–2.8(2.6):1.2–2.1(1.3):1–1.4(1.2):1, POL:petiole length 0.45–0.75(0.59); vertex pubescent between lateral ocellus and compound eye, small glabrous area anterior of median ocellus reaching until median dent of upper face; head in dorsal view 1.9–2.5 (2.3) times wider than long, laterally longer than medially; vertex and occiput sometimes with shallow and smooth median furrow, occiput with transverse striae (Fig. 12D), interrupted medially by furrow if present.

**Antennae.** ♀ formula:

1.9–2.3(2.1):1:2.1–2.8(2.5):1.6–2.1(2.0):1.4–2(1.8):1.3–1.9(1.8):1.3–1.7(1.6):1.3–1.6(1.6):1.3–1.7(1.5):1.3–1.6(1.4):1.1–1.5(1.4):1.1–1.5(1.4):2.1–2.5(2.3)

♂ formula:

1.6–2.7:1:2–2.9:1.6–2.5:1.4–2.3:1.3–2:1.3–1.9:1.3–2.1:1.3–2:1.3–2:1.1–2:1.1–2:1.3–2

**Mesosoma.** Mesosoma 1.3–1.4(1.4) times longer than high (Fig. 12B); pronotal plate variable in sculpture, usually smooth with some few radial carinae; pronotum laterally setose, with longitudinal carinae along entire stretch reaching the posterior margin (Fig. 12B), sometimes somewhat branching; mesopleuron without coriaceous texture, rugulose anteroventrally, setose anteroventrally and along ventral margin, otherwise glabrous (Fig. 12B); mesopleural line merging with posteroventral hypoco-xal furrow, ventral margin somewhat continuous, dorsally marked by influent striae (Fig. 12B); mesopleural triangle separated from mesopleuron by carina that fades before reaching the posterior subalar pit, posterodorsally smooth and shiny; axillulae well delimited (Fig. 12B), inside setose and longitudinally striate; mesoscutum 1.0–1.2 (1.1) times wider than long and 1.3–1.5(1.4) times longer than the mesoscutellum (Fig. 12D); notauli distinct, sometimes deep, with weak or strong transversal carination inside that is less dense than in *A. eucharioides*, usually surrounded by weak to strong wrinkles (Fig. 12D); median lobe of mesoscutum setose, gradually weakening towards posterior end (Fig. 12D), lateral lobes denser setose along outer margins than along inner margins; mesoscutellar foveae sometimes each delimited by a circumfoveal carina (Fig. 12D), which is sometimes not fusing with median carina; median carina sometimes extending over entire dorsal surface of mesoscutellum (Fig. 12D), sometimes interrupted, rarely completely absent, usually accompanied by lateral carinae that are less distinct but are not prone to disappear among general reticulate inside (as in *A. eucharioides*); posterior surface of mesoscutellum medially broadly raised (Fig. 12E), evenly setose, with one, two or more (sub-)median longitudinal carinae (Fig.

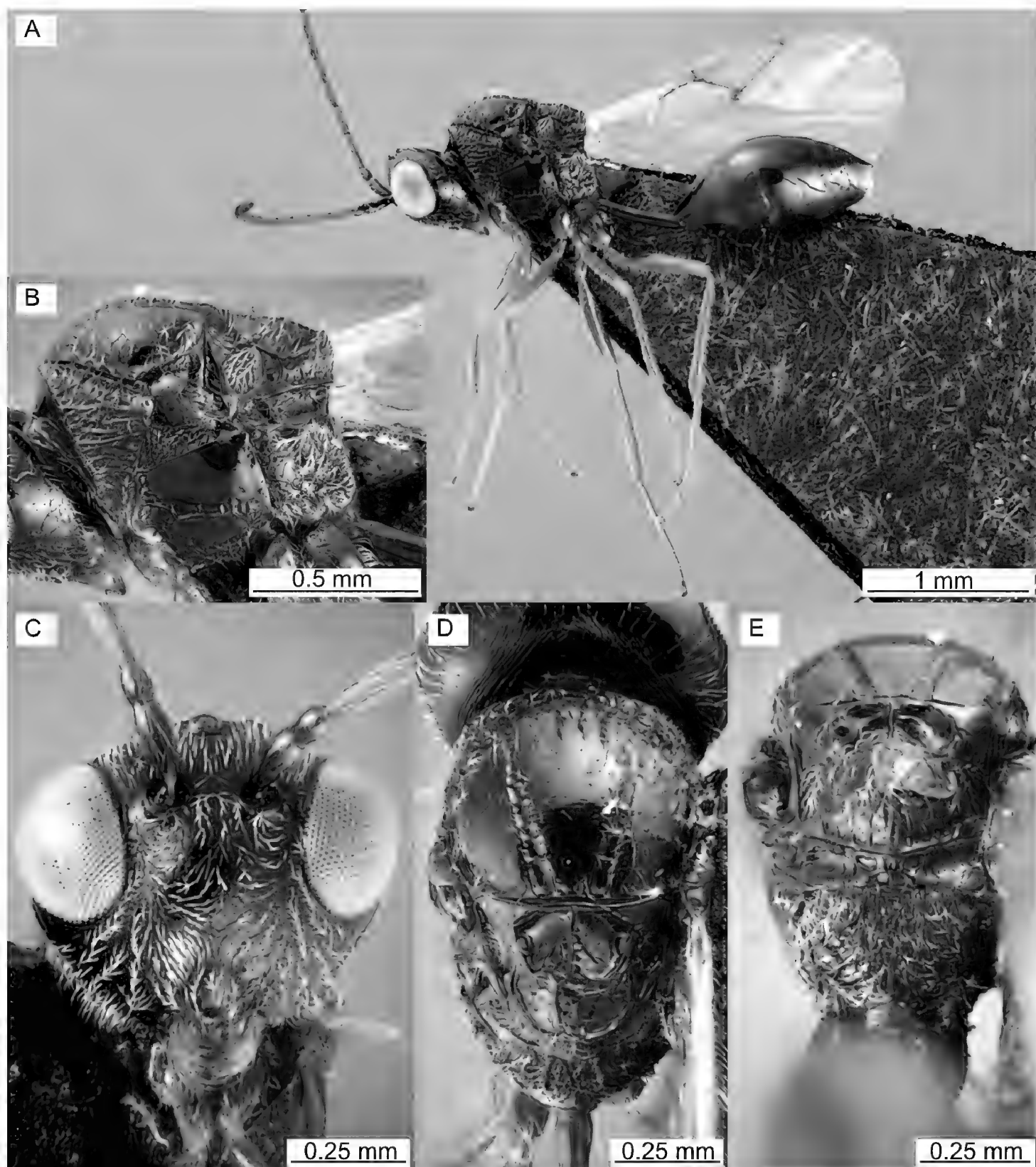


**Figure 12.** *Anacharis martinae* sp. nov., holotype, female (ZFMK-TIS-2640787) **A** lateral habitus **B** mesosoma lateral **C** face frontal **D** mesoscutum and mesoscutellum dorsal **E** mesosoma posterior view.

12E), rarely branching, laterally smooth to reticulate; dorsal axillular area laterally rugose to striate (Fig. 12D–E); sculpture of propodeum variable; nuchal collar usually with a narrow tooth dorsomedially (Figs 6C, 12E).

**Wings.** Marginal cell of fore wing 2.5–2.8 (2.6) times longer than wide (Fig. 2C). WIPs (Fig. 2C): Purple band pattern of fore wing reaching along about half the length of vein M. Apical spot of hind wing large, filling almost entire apical area.

**Metasoma.** 0.9–1.2 (1.2) times longer than rest of body (Fig. 12A); gaster 2.1–2.4 (2.4) times longer than petiole (Fig. 12A); petiole 1.0–1.6 (1.4) times longer than

hind coxa (Fig. 12A); metasomal tergite 2 (T2) with 0–4 (2) lateral setae on each side, with irregular punctures, T3-4 with narrow bands of punctures, dorsally usually interrupted, T5 with broad band of punctures, decreasing in width on T6-7, T7 with few setae along the band and more setae in posterior half than in the anterior half.

**Male genitalia.** Parameral plate submedially widened, basoventral margin rounded, without tooth.

**Males.** Flagellomeres dorsoventrally bicoloured yellow-dark brown, gaster shorter than in females. T7 in males almost entirely punctured except medially, long setae across surface, except on smooth area.

**Variation.** The specimens from the Bavarian Forest National Park (BC-ZSM-HYM-27596-F10 & BC-ZSM-HYM-27596-F09) are in colouration similar to the holotype (Fig. 12), but more distinct, i.e. the head is distinctly darker than the rest of the body. They are also smaller than the average. ZFMK-TIS-2640713 has a strong sculpture on its pronotal plate, whilst other specimens are rather smooth and of weaker sculpture. ZFMK-TIS-2640791 has a completely smooth dorsal surface of the mesoscutellum but fits otherwise well within the species morphologically.

**CO1 barcode.** n=18. Maximum intraspecific distance = 2.3%. Minimum distance to closest species (*A. eucharioides*) = 7.9%. CO1 barcode consensus sequence:

AATTTTATACTTATTAGGTATTGATCAGGAATAATAGGAT-CAAGATTAAGAATAATTATCGAATAGAATTAGGAACCCATCTCAAT-TAACATAAAATGATCAAATTATAACTCAATTGTAACTGCTCATGCATT-TATTATAATTTTTTATAGTAATACCAATTATAGTAGGAGGATTG-GAAATTATCTGGTTCCTCTAATACTAATTCTCCTGATATAGCCTTCC-CACGATTAAATAATTAAAGATTGATTTAATCCCATCCCTATTAAATAACAATAAAATTATTGATCAAGGAGCTGGTACAGGATGAAC-GTATAACCCTCCACTATCCTCCTAACGGGTACATCCATCAATATCAGTAGTTAGTTATTATTCTCTTCATTAAAGAGGAATTCTTCAATTCTGGTCAATTAAATTATTATTGTAACAATTAAATACGAATAAAACT-CAATAACAATAGATAAAATTCTATTATTGATCTATTCTTAAACAACTATTACTATTATTACATTACCTGTATTAGCTGGAGGTT-TAACAAATATTACTTTGATCGAAACTAAATACATCATTGATCCT-ACAGGAGGAGGAGACCAATTATCAACATTATT

**Type material. Holotype.** GERMANY • ♀; Hesse, Waldeck-Frankenberg, National park Kellerwald-Edersee, Banfehaus, old floodplain of the Banfe; 51.167°N, 8.9749°E; ca 270 m a.s.l.; 22 Jul.-5 Aug. 2021; GBOL III leg.; Malaise trap (Krefeld version); ZFMK-TIS-2640787.

**Paratypes.** GERMANY • 2 ♂♂; same collection data as for holotype; ZFMK-TIS-2640788, ZFMK-TIS-2640791. • 1 ♂; Bavaria, Bavarian Forest National Park; 48.937°N, 13.42°E; ca 830 m a.s.l.; 1 Jun. 2013; BC-ZSM-HYM-27764-H01 (ZSM). • 1 ♀, 1 ♂; Bavaria, Bavarian Forest National Park; 49.099°N, 13.233°E; ca 710 m a.s.l.; 1 Jun. 2013; female - BC-ZSM-HYM-27596-F10 (ZSM); male - BC-ZSM-HYM-27596-F09 (ZSM). • 1 ♂; Bavaria, Garmisch-Partenkirchen, Zugspitze, mountain; 47.4062°N, 11.0095°E; ca 1970 m a.s.l.; 20 Jun.-5 Jul. 2018; Doczkal, D., Voith,

J. leg.; Malaise trap; ZFMK-TIS-2637892 (NHMUK). • 1 ♂; Hesse, Gießen, Hohberg, Groß-Buseck; 50.6196°N, 8.7844°E; ca 300 m a.s.l.; 17 Jun. 2021; GBOL III leg.; sweep net; ZFMK-TIS-2629493. • 1 ♂; Hesse, Rheingau-Taunus, Lorch am Rhein, above Nollig castle; 50.0495°N, 7.7966°E; ca 250 m a.s.l.; 17–25 Jun. 2015; Niehuis, Oliver leg.; Malaise trap; MF 3; ZFMK-TIS-2628231. • 1 ♀, 2 ♂♂; Hesse, Waldeck-Frankenberg, National park Kellerwald-Edersee, Maierwiesen; 51.1555°N, 9.0015°E; ca 370 m a.s.l.; 22 Jun.-8 Jul. 2021; GBOL III leg.; Malaise trap (Krefeld version); female - ZFMK-TIS-2640809 (NHRS); males - ZFMK-TIS-2640804, ZFMK-TIS-2640805 (NHRS). • 1 ♀; Hesse, Waldeck-Frankenberg, NP Kellerwald-Edersee, „Banfe-Haus“; 51.167°N, 8.9749°E; ca 270 m a.s.l.; 7–21 Jul. 2022; GBOL III leg.; Malaise trap; ZFMK-TIS-2640770. • 1 ♀; Hesse, Waldeck-Frankenberg, NP Kellerwald-Edersee, „Große Küche“; 51.1564°N, 8.9879°E; ca 320 m a.s.l.; 19 Aug.-2 Sep. 2021; GBOL III leg.; Malaise trap; ZFMK-TIS-2640690 (NHMUK). • 1 ♀, 2 ♂♂; Hesse, Waldeck-Frankenberg, NP Kellerwald-Edersee, „Maierwiesen“; 51.1555°N, 9.0015°E; ca 370 m a.s.l.; 8–22 Jul. 2021; GBOL III leg.; Malaise trap; female - ZFMK-TIS-2640734 (SMNS); males - ZFMK-TIS-2640731, ZFMK-TIS-2640733 (SMNS). • 1 ♀; Rhineland-Palatinate, Ahrweiler, Niederzissen, Bausen-berg, upper part of volcanic mountain, next to oak tree; 50.4672°N, 7.2212°E; ca 310 m a.s.l.; 26 May-12 Jun. 2022; Jaume-Schinkel, Santiago leg.; Gressit Malaise trap; ZFMK-TIS-2640713.

**Other material examined. Without DNA barcode.** BELGIUM • 1 ♀; Walloon Region, Namur, Nismes; 50.0744°N, 4.5556°E; ca 220 m a.s.l.; 10 Jul. 2022; W. Declercq leg.; Light trap; ZFMK-HYM-00039668 (RBINS). • 1 ♀; Walloon Region, Tellin, Ri d'Howisse; 50.1113°N, 5.2531°E; ca 260 m a.s.l.; 18 Jul. 2022; W. Declercq leg.; Light trap; ZFMK-HYM-00039667 (RBINS).

FRANCE • 1 ♂; Bitche; 7 Aug. 1979; Henk J. Vlug leg.; sweep net; specimen in coll ME.

SWEDEN • 1 ♂; Hälsingland, Skog sn, Noran; 5 Aug. 1949; Olov Lundblad leg.; NHRS-HEVA 000023178 (NHRS). • 1 ♂; Scania, Ystad kommun, Sandhammaren, Järahusen, oak shrub forest on coastal sand dunes; 55.4038°N, 14.1999°E; ca 10 m a.s.l.; 22 May-15 Jul. 2005; Swedish Malaise Trap Project (Swedish Museum of Natural History) leg.; Malaise trap; NHRS-HEVA 000023179 (NHRS).

SWITZERLAND • 1 ♂; Neuchâtel, Auvernier; 8 Aug. 1957; Jacques de Beaumont leg.; specimen at MHNG. • 1 ♀; same collection data as for preceding 15 Aug. 1956; specimen at MHNG.

**Biology.** Summer species, flying mainly from June to September, peak in July. No clear preferences in terms of habitat.

**Distribution.** Belgium, France, Germany (locus typicus: Kellerwald-Edersee National Park, Banfehaus), Sweden, Switzerland.

No DNA barcode matches with publicly available sequences from other countries.

Mainly collected in lowlands below 400 m a.s.l., occasionally found in higher altitudes at 700–900 m a.s.l. and rarely even higher.

**Etymology.** Named after the first author's wife, Martina Vogel.

**Remarks.** In the molecular analysis, *A. martinae* is split into two clades by ASAP. The gap between the two clusters is 2.3% and cannot be attributed to poor quality sequences. As ASAP is the only analysis to split this cluster by that gap and we cannot find morphological evidence for a split into two species, we regard this result as an oversplit.

The diagnosis against *A. belizini* is based on the description and the accompanying SEM images of the holotype in Mata-Casanova et al. (2018). There, *A. belizini* is described as having a smooth occiput. In the SEM images, however, we can see occipital striolation or striation, which would match with the diagnosis of the *eucharioides* species group. In Mata-Casanova et al. (2018), *A. belizini* is said to be most similar to *A. antennata*, while we think that *A. antennata* is much closer morphologically to *A. petiolata typica* based on the SEM images provided, showing the interrupted mesopleural line, the smooth mesoscutellum and the smooth to rugose lateromedial area of the pronotum.

On the SEM images of *A. belizini*, the pronotal plate is significantly laterally projecting in dorsal view (Fig. 3. C. in Mata-Casanova et al. (2018) vs. Fig. 12D). This is not the case in *A. martinae*, and shape of the pronotal plate could be another diagnostic feature to separate *A. belizini* and *A. martinae*. Additionally, the parascutal sulcus seems very strongly impressed and carinate in *A. belizini*, much more so than in any of our specimens of *A. martinae* (Fig. 12B). As we discussed in the treatment of *A. eucharioides*, the parascutal sulcus is very variable and cannot be used as a diagnostic character. If such extremes as present in *A. belizini* are consistent or not is currently impossible to evaluate because there is only a single specimen (the holotype) known for *A. belizini*.

The morphometric analysis (Fig. 8B) revealed overlap with the remaining species of the *eucharioides* species group. However, the morphospace overlaps only partially, which allows us to make statements of inclusive and exclusive ranges in the two ratios extracted as separating species best. The intertorular distance:torulus to eye distance (Fig. 8B, right) ranges from 1.4 to 2.0, but no other species than *A. martinae* has a ratio of higher than 1.7, making >1.7 to 2.0 the exclusive *A. martinae* range. For POL:petiole length, a ratio of >0.7 is exclusive for *A. martinae*, but any ratio below could be other species. While we included the ratios in the description of the species, we refrained from including them in the diagnosis. This partial separation between *A. martinae* and the remaining species in the morphometric analyses again highlights the morphometric variability of the species in *Anacharis* (see also remarks on *A. eucharioides*) but also points towards the potential power of morphometric analyses which will prove helpful in delimitation of another species (*A. maxima*, see below).

#### *Anacharis maxima* Vogel, Forshage & Peters, sp. nov.

<https://zoobank.org/94B47FEC-2AE0-42C4-92E9-0B82C143488C>

Figs 2G, 3F, 13A–E

**Diagnosis (n = 6, all males).** Belongs to the *eucharioides* species group. Large species (3.5–4.0, mean 3.8 mm, unique in Northwestern European fauna). Similar to

*A. euchariooides* by having the lateromedial area of the pronotum smooth to rugose (Fig. 13B, smooth in *A. minima*, *A. petiolata* and *A. typica*, longitudinal carinae in *A. martinae*). Differing from all other Northwestern European species by its large size (other species usually not larger than 3.5 mm), its mesoscutellar sculpture having oblique to transversal carinae only in the anterior half between the mesoscutellar foveae (Fig. 13D, smooth to entirely carinate or differently oriented carinae in other Northwestern European species) and having a LOL:metacoxa ratio of  $< 0.225$  combined with a head frontal height:mesoscutellum length ratio of  $\leq 1.9$  (Fig. 8C right, LOL:metacoxa ratio usually  $> 0.225$ , if around 0.225, then head frontal height:mesoscutellum length ratio  $> 1.9$  in other Northwestern European species). In the Western Palaearctic fauna, *A. maxima* is most similar to *A. parapsidalis*, mainly due to its size. *Anacharis parapsidalis* was not reported from Northwestern Europe but from Japan and Romania (Mata-Casanova et al. 2018). *Anacharis maxima* differs from *A. parapsidalis* in its mesoscutellar sculpture (Fig. 13D, mesoscutellum reticulate-carinate all over mesoscutellum in *A. parapsidalis*), the lateromedial area of the pronotum is smooth to rugose (Fig. 13B, reticulate-carinate in *A. parapsidalis*), the mesopleural line not reaching the poster-oventral hypocoxal furrow (Fig. 13B) (reaching it in *A. parapsidalis*) and the presence of punctures on the metasomal tergites (absent in *A. parapsidalis*).

**Description. Male. Size.** Large; body: 3.5–4.0 (3.9) mm; antennae: 2.7–3.4 (3.1) mm; fore wing: 2.5–3.3 (3.3) mm

**Colour.** Body black (Fig. 13A); scape, head, mesosoma, and metasoma entirely black (Fig. 13); pedicel largely black (Fig. 13C), flagellomeres bicoloured dorsoventrally (Fig. 13A); mid and hind coxa, as well as hind femur largely (Fig. 13A), fore coxa partially black (Fig. 13A, B) and hind tarsomeres darkened (Fig. 13A), otherwise yellow (Fig. 13A); mandibles basally and apically darkened, otherwise yellow (Fig. 13C); palps pale yellow (Fig. 13C).

**Head.** Trapezoid in frontal view, genae abruptly kinked, meeting mandibular base in an angle  $< 90^\circ$  (Fig. 13C); lower face with thick silvery hairs (Fig. 13C), punctate; clypeal margin usually slightly bilobed, clypeus with central convex area, medially to medioventrally smooth (Fig. 13C), otherwise punctate-rugulose; malar area coriaceous, reaching from ventral eye margin along entire stretch of mandibular base (Fig. 18B), anteroventral corner of mandibular base sometimes smooth; genae smooth around eye, with increasingly dense punctuation and regular setae towards the hind margin (Fig. 13B); upper face setose, punctured, with usually noticeable, sometimes shallow median dent; space between toruli smooth (Fig. 13C); eyes with few scattered setae (Fig. 13C); vertex setose; POL:OOL:OL:OD 2.2:1.3:0.8:1 (2.3:1.3:0.8:1), glabrous along OOL and anterior to median ocellus; head in dorsal view 2.0 times wider than long, laterally longer than medially; vertex and occiput usually with shallow median furrow, occiput broadly yet finely striate to striolate (Fig. 13D), not interrupted by median furrow.

**Antennae.** ♂ formula:

2.1-2.4(2.2):1:2.6-2.7(2.7):2.3-2.4(2.4):2.2-2.3(2.2):2-2.1(2.1):2-2.1(2):1.9-2.1(1.9):1.9-2(1.9):1.8-2(1.9):1.8-1.9(1.8):1.7-1.9(1.8):1.7-1.8(1.7):2-2.6(2.5)

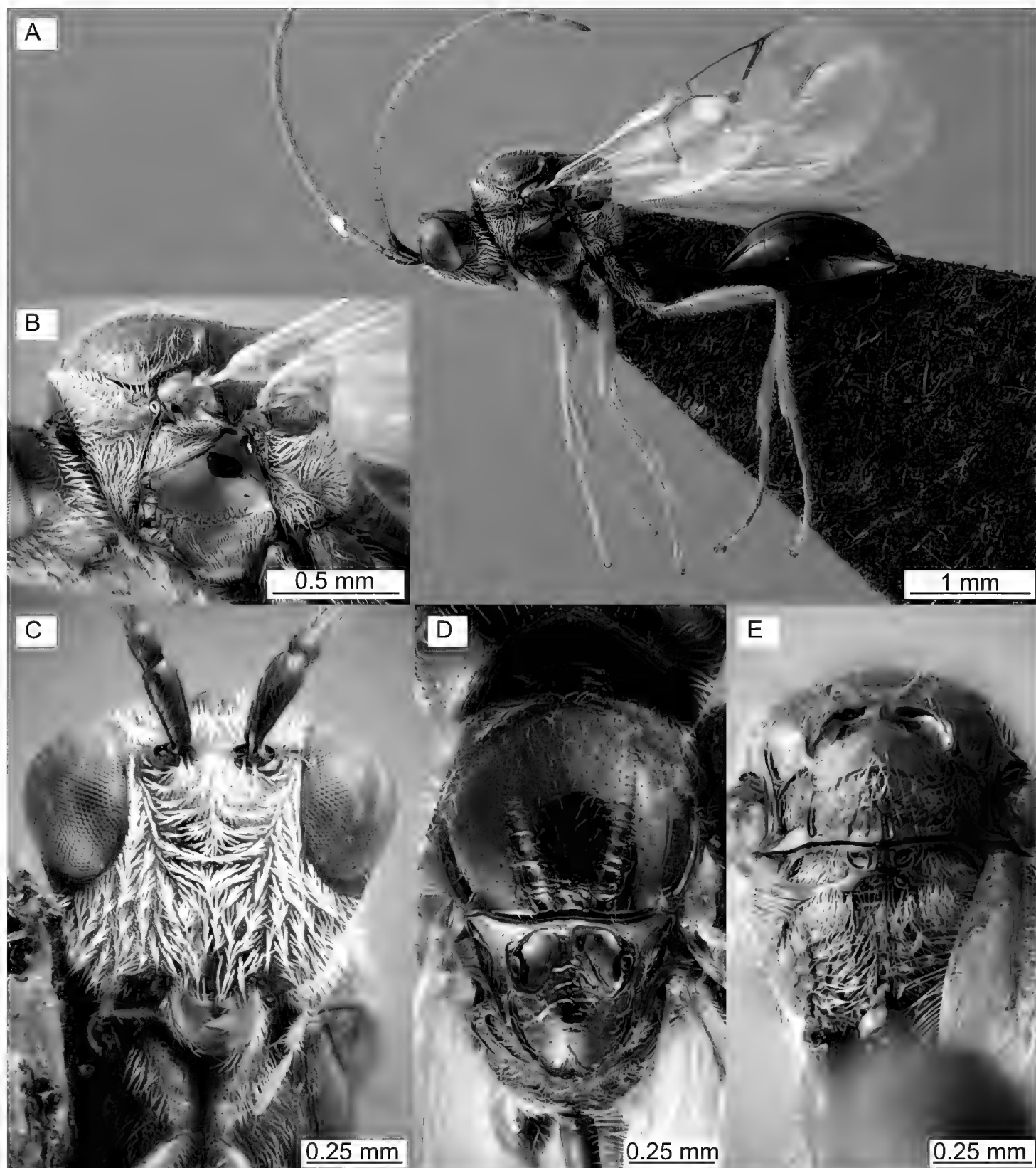


**Figure 13.** *Anacharis maxima* sp. nov., holotype, male (ZFMK-TIS-2640744) **A** lateral habitus **B** mesosoma lateral **C** face frontal **D** mesosoma dorsal **E** mesosoma posterior view.

**Mesosoma.** Mesosoma 1.3 times longer than high (Fig. 13B); pronotal plate centrally smooth, laterally coriaceous with a few carinae radiating from the centre, setose centrally and laterally, otherwise glabrous; pronotum laterally with dense silvery setae (Fig. 13B), with longitudinal carinae along anterior margin, reaching hind margin in ventral region, lateromedial area slightly rugose, without regular carinae (Fig. 13B); mesopleuron sometimes coriaceous dorsally and ventrally of mesopleural line, otherwise smooth (Fig. 13B), scrobiculate along anteroventral margin (Fig. 13B), reaching into venter; mesopleuron setose along ventral margin,

otherwise glabrous (Fig. 13B); mesopleural line separated from posteroventral hypocoaxal furrow (Fig. 13B), ventral margin somewhat continuous, dorsally marked by few to some influent striae (Fig. 13B); mesopleural triangle separated from mesopleuron by carina that fades before reaching the posterior subalar pit (Fig. 13B), posterodorsally smooth and shiny (Fig. 13B); axillulae well delimited (Fig. 13E), inside setose and longitudinally striolate; mesoscutum 1.1 times wider than long and 1.3–1.4 (1.3) times longer than the mesoscutellum (Fig. 13D); notauli deep and distinct, with strong transversal carinae inside (Fig. 13D), without (Fig. 13D) or with fine wrinkles along them; median lobe of mesoscutum setose (Fig. 13D), sometimes somewhat coriaceous, then lateral lobes also coriaceous, but less than median lobe; mesoscutellar foveae usually well delimited posteriorly by circumfoveal carinae (Fig. 13D), fusing with median carina or not (Fig. 13D); median carina starting to branch obliquely to transversally before reaching posterior end of foveae (Fig. 13D), circumscutellar carina raised posteriorly (Fig. 13D, E), appearing like a posterodorsal tooth on the mesoscutellum in lateral view; posterior surface of mesoscutellum medially broadly raised, evenly setose, ventrally scrobiculate, surface reticulate-striate (Fig. 13E); dorsal axillular area striate on posterolateral margin, otherwise smooth (Fig. 13D, E); nuchal collar broadly projecting dorsally, point rounded (Figs 6F, 13E); fore trochanter, mid coxa and hind coxa with conspicuously long setae (Fig. 13A).

**Wings.** Marginal cell of fore wing 2.6–2.9 (2.6) times longer than wide (Fig. 2E); WIPs (Fig. 2E): apical spot of hind wing narrow, covering less than half of the apical area.

**Metasoma.** 1.3 times longer than rest of body (Fig. 13A); gaster twice as long as petiole (Fig. 13A); petiole 1.3–1.5 (1.5) times longer than hind coxa (Fig. 13A); metasomal tergite 2 (T2) with two setae dorsolaterally on each side along weak band of punctures; T3 and T4 with narrow bands of punctures, T5 and T6 with broad bands of punctures; T7 medially without punctures, otherwise filled with punctures with long setae dorsally.

**Male genitalia.** Parameral plate basally widened, ventrally with basal tooth-like projections pointing inwards (Fig. 3E).

**Female.** Unknown.

**CO1 barcode.** n=7. Maximum intraspecific distance: 0%. Minimum distance to closest species (*A. euchariooides*): 3.9%. CO1 barcode consensus sequence:

TATTTTATACTTATTAGGTATTGATCTGGAATAATAGGAT-  
CAAGATTAAGAATAATTATTCGAATAGAATTAGGGACCCATCC-  
CAATTAATTATAAAATGATCAAATTATAATTCAATTGTAAGTGCAC-  
CATGCATTATTATAATTCTTATAGTTACCTATCATAGTAG-  
GAGGATTGGAAATTATTAGTACCTTAATATTAATTCTCCTGA-  
TATAGCTTCCCTCGATTAAATAATTAAAGATTGATTAAATC-  
CCTTCCTTATTAAATAACAATTAAATTATTGATCAAGGGA-  
CAGGAACAGGATGAACTGTTATCCCCCATTATCATCCATCACAG-  
GTCATCCATCTATCAGTAGTTAGTTACTCATTACATTAA-

GTGGAATTCTTCAATTCTGGATCAATTAAATTATTGTAACCATT-TAAATATAACGAATAATCTCCATATCTATAGACAAAGTCTCATTATT-TATTGATCTATTTTAACTACAATTACTATTATTCTTACCGTACTAGCAGGAGGATTAACACTATACTATTATTGATCGAAATTAAA-TACATCTTTTGACCCTACAGGAGGGAGACCCTATTCTTAT-CAACACTTATT

**Type material.** *Holotype*. GERMANY • ♂; Bavaria, Rhön-Grabfeld, Hausen, Eisgraben, basalt depot at forest margin; 50.5026°N, 10.0895°E; ca 740 m a.s.l.; 12–23 Jul. 2018; Dieter Doczkal leg.; Malaise trap; ZFMK-TIS-2640744.

**Paratypes.** GERMANY • 5 ♂♂; Same collection data as for holotype; ZFMK-TIS-2640739, ZFMK-TIS-2640740 (ZSM), ZFMK-TIS-2640741 (SMNS), ZFMK-TIS-2640742 (NHMUK), ZFMK-TIS-2640743 (NHRS). • 1 ♂; Rhineland-Palatinate, Vulkaneifel, Jünkerath, private garden, wet meadow, right next to ditch; 50.3343°N, 6.595°E; ca 450 m a.s.l.; 6–8 Aug. 2021; Jonathan Vogel leg.; Malaise trap; ZFMK-TIS-2640676.

**Other material examined. Without DNA barcode.** SWEDEN • 1 ♂; Uppland, Norrtälje, Singö; 15 Jul. 1962; Karl-Johan Hedqvist leg.; NHRS-HEVA 000023177 (NHRS).

SWITZERLAND • 1 ♂; Vaud, Aigle, Solalex; 4 Aug. 1954; Jacques Aubert leg.; specimen at MHNG.

**Biology.** Summer species, flying from July to August, peak in July. No clear preferences in terms of habitat.

**Distribution.** Germany (locus typicus: Bavaria, Rhön-Grabfeld, Hausen, Eisgraben), Sweden, Switzerland.

No DNA barcode matches with publicly available sequences from other countries.

Probably preferring higher altitudes, as all specimens were collected at 400 to 800 m a.s.l.

**Etymology.** From the latin word “maximus”, meaning the greatest, referring to the tall size of the species.

**Remarks.** *A. maxima* is not frequently collected, though with six specimens caught from one collection event at one site, it seems like it can be locally relatively abundant. The diagnosis against *A. parapsidalis* is based on comparisons with the SEM images and the redescription (Mata-Casanova et al. 2018) as no specimen of *A. parapsidalis* was available to us.

The morphometric analysis revealed only little overlap of *A. maxima* with the other species within the *eucharrioides* species group (Fig. 8C left). The lda extractor provided two ratios, which – separately – can almost and – in combination – fully separate *A. maxima* from the remaining species (Fig. 7, Fig. 8C right). We included these ratios into the diagnosis of *A. maxima*. For this species, the morphometric analyses proved helpful in finding diagnostic characters. Note that this was not the case in *A. eucharrioides*, and only partially in *A. martiniae* (see above), highlighting both the morphometric variability and overall similarity of the *Anacharis* species and the power and applicability of multivariate morphometrics.

***Anacharis minima* Vogel, Forshage & Peters, sp. nov.**

<https://zoobank.org/22711BED-98BF-4795-A81E-B709E12667E1>

Fig. 14A–E

**Diagnosis (n = 1).** Belongs to the *eucharioides* species group. Small species (2.4 mm). Similar to *A. petiolata* and *A. typica* by having a centrally smooth mesoscutellum (centrally carinate in *A. eucharioides*, *A. martiniae* and *A. maxima*). The small body size and the narrow coriaceous texture of the malar space that extends only around the dorsal corner of the mandibular base (Fig. 19A) is unique in the Palaearctic fauna (coriaceous texture of malar space extending along entire length of mandibular base in all other species).

**Description. Female. Size.** Small; body: ♀ 2.4 mm. Antennae: ♀ 1.6 mm. Fore wing: 1.9 mm

**Colour.** Body black (Fig. 14A); scape, head, mesosoma, coxa, petiole black (Fig. 14); mandibles (Fig. 14C), palps (Fig. 14B), rest of legs (hind tarsi darker) (Fig. 14A) yellow; pedicel and flagellomeres (Fig. 14A), tegulae (Fig. 14B, D), and gaster (Fig. 14A) dark brown.

**Head.** Roundish triangular in frontal view, genae not abruptly kinked (Fig. 14C); lower face setose (Fig. 14C), with punctures; clypeal margin margin bilobed and flanged, clypeus smooth; coriaceous texture of malar area narrow, coriaceous texture of the malar space narrow, extending only around the dorsal corner of the mandibular base (Fig. 19A); genae smooth around eye, with increasingly dense punctuation and regular setae towards the hind margin (Fig. 14A); upper face sparsely setose and very few punctures, centrally with shallow dent (Fig. 14C); space between toruli smooth; eyes with scattered setal stubs (Fig. 14C); ocellar triangle with wide base, ocelli small, POL:OOL:LOL:OD = 3.1:1.7:1.4:1.0; setose between lateral ocellus and eye, small glabrous area in front of median ocellus not reaching median dent of upper face; head in dorsal view 1.8 times wider than long, laterally longer than medially; vertex and occiput with smooth shallow median furrow, occiput with medially interrupted striation (Fig. 14D).

**Antennae.** ♀ formula:

1.9:1.0:2.1:1.4:1.4:1.4:1.4:1.3:1.2:1.2:1.2:1.1:2.1

**Mesosoma.** Mesosoma 1.3 times longer than high (Fig. 14B); pronotal plate coriaceous, with some few radial carinae; pronotum laterally setose (Fig. 14B), with only few carinae ventrally and along anterior margin (Fig. 14B), posterodorsal area smooth and even (Fig. 14B); mesopleuron without distinct coriaceous sculpture, scrobiculate along anterior margin (Fig. 14B), setose along ventral margin, otherwise glabrous (Fig. 14B); mesopleural line meeting posteroventral hypocoxal furrow with its ventral margin only, ventral margin somewhat continuous, dorsally marked by influent striae (Fig. 14B); mesopleural triangle separated from mesopleuron by carina that fades before reaching the posterior subalar pit, setae mostly in anterior two-thirds; axillulae well delimited, inside setose and longitudinally rugose-carinate; mesoscutum 1.1 times

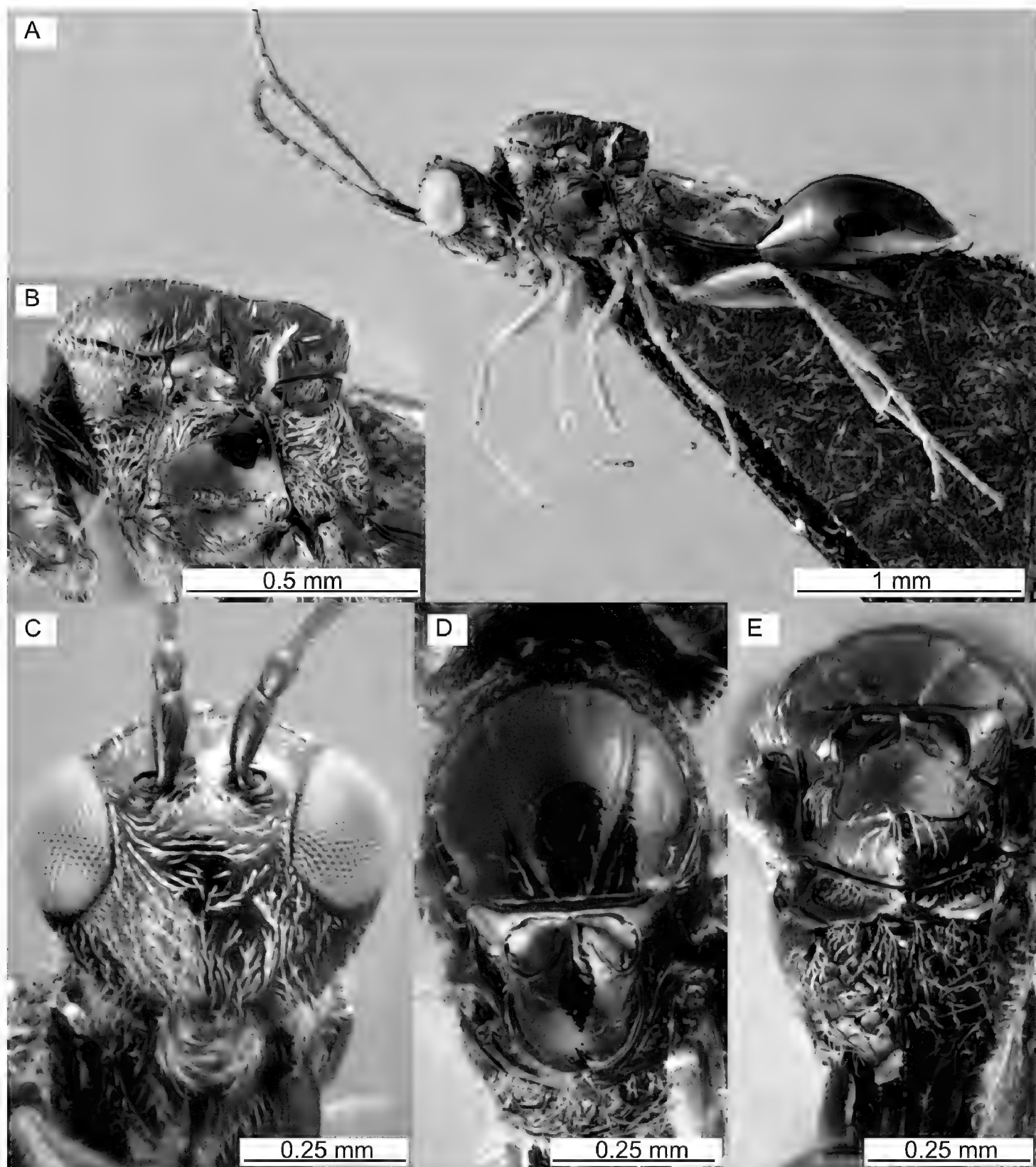


**Figure 14.** *Anacharis minima* sp. nov., holotype, female (ZFMK-TIS-2640724) **A** lateral habitus **B** mesosoma lateral **C** face frontal **D** mesosoma dorsal **E** mesosoma posterior view.

wider than long and 1.4 times longer than the mesoscutellum (Fig. 14D); notauli complete, inside not carinate, wrinkles weak to absent (Fig. 14D); lateral and median lobes of mesoscutum centrally glabrous, otherwise setose, increasingly so towards margins (Fig. 14D); mesoscutellar foveae closed, with circumfoveal carina delimiting each fovea (Fig. 14D), not touching the median carina (Fig. 14D); mesoscutellum smooth on dorsal and posterior surface (Fig. 14D), posterior surface medially distinctly raised (Fig. 14D), laterally smooth (Fig. 14D); ventral half of dorsal axillular area rugose (Fig. 14E); propodeal area defined by carinae (Fig. 14E), inside carinate-rugose, median

carina present ventrally (Fig. 14E); nuchal collar broadly extending posteriorly, tip rounded (Figs 6D, 14E).

**Wings.** Marginal cell of fore wing 2.6 times longer than wide.

**Metasoma.** 1.2 times longer than rest of body (Fig. 14A); gaster 2.3 times longer than petiole (Fig. 14A); petiole 1.5 times longer than hind coxa (Fig. 14A); metasomal tergite 2 (T2) and T3 with weak line of punctures dorsally, T4 with scattered band of punctures, T5-6 with narrow band, T7 with medially weaker band, laterally with few setae.

**Male.** Unknown

**CO1 barcode.** n=1. Maximum intraspecific distance = not applicable. Minimum distance to closest species (*A. euchariooides*) = 5.6%. CO1 barcode consensus sequence:

AATTTTATACTTTAGGTATTGATCCGGAATAATAGGTTCAA-GATTAAGAATAATTATTCGAATAGAACTAGGAACCCATCTCAAT-TAATCATAAAATGATCAAATTATAATTCAATTGTAACCGCACATGCCTT-TATTATAATTTTTTATAGTTACCCATTATAAGTAGGAGGATTG-GAAATTATTAGTGCCTTAATATTAATCTCTCCTGATATAGCTTCC-CACGATTAAATAATTAAAGATTGATTAAATCCCTCCATTAA-TAATAACAATTAACTTATTGATCAAGGGAGCAGGGACAGGATGAAC-GTATAACCCACCATTATCATCCCTCACAGGTACATCTATATCAGTA-GATTAGTTATTCACTACATTAAAGAGGTATCTCATCAATTCTG-GATCAATTAAATTATTGTAACCATTAAATACGAATAACTCTG-TATCTATAGACAAAATTCTATTGATCTATCTTTAACTACAATTAACTATTATTATTGATCGAAATTAAATACATCTTTTGACCCCTACAG-GAGGGGGAGACCCAATTCTTATCAACACTTATT

**Type material. Holotype.** GERMANY • ♀; Baden-Württemberg, Karlsruhe, Malsch, Hansjakobstraße, garden; 48.8835°N, 8.3197°E; ca 120 m a.s.l.; 25 Oct.-8 Nov. 2020; Dieter Doczkal leg.; Malaise trap; ZFMK-TIS-2640724.

**Biology.** The holotype was collected in autumn (between October and November) in a garden.

**Distribution.** Germany (locus typicus: Karlsruhe, Malsch).

No DNA barcode matches with publicly available sequences from other countries.

Holotype collected from ca. 120 m a.s.l.

**Etymology.** From the latin word for “the smallest”, referring to its distinct small body size.

**Remarks.** While *A. minima* is molecularly clearly distinct from other species, the morphology overlaps in many aspects with other species that show a smooth mesoscutellum. It is the name-giving small size that seems to hold the most diagnostic value but there is no way to say for sure which characters are morphologically diagnostic for *A. minima* based on a single specimen. Some specimens, which we currently classify as *A. typica* (NHRS-HEVA 000023181 and a specimen from MHNG) show similarities to the holotype of *A. minima*, but they deviate in size and sculpture to regard them as not conspecific. The morphological diagnosis is in need of extension by studying further material of which the barcode matches that of *A. minima*.

***Anacharis norvegica* Mata-Casanova & Pujade-Villar, 2018**

**Diagnosis (n = 1).** Belongs to the *A. immunis* species group. Similar to *A. ensifer* in generally having a largely sculptured mesoscutellum (largely smooth in *A. immunis*). Different to *A. ensifer* by having its mesoscutellum covered with reticulate-foveate sculpture resulting in smaller foveae (larger foveae in *A. ensifer*). The circumscutellar carina is less distinct and not flanged upwards posteriorly (usually distinctly flanged upwards, appearing in lateral view like a posterodorsal tooth in *A. ensifer* and *A. immunis*). The dorsal margin of the mesopleural line is diffused by rugose sculpture of mesopleuron in its anterior half (dorsally well-defined mesopleural line in its anterior half in *A. ensifer* and *A. immunis*). Wrinkles on mesoscutum, especially in anteromedian area, strong, making the anteromedian signa distinct (less to no wrinkles and thereby less notable anteromedian signa in *A. ensifer* and *A. immunis*).

**Other material examined. Material without DNA barcode.** SWEDEN • 1 ♀; Torne lappmark, Kiruna, Abisko Nationalpark, dry sparse alpine downy birch forest; 68.3539°N, 18.7822°E; ca 410 m a.s.l.; 21 Jul.-7 Aug. 2003; Swedish Malaise Trap Project (Swedish Museum of Natural History) leg.; Malaise trap; NHRS-HEVA 000023145 (NHRS).

**Biology.** Summer species, type series collected in July and August, as was the specimen studied here. Probably preferring boreal habitats.

**Distribution.** Norway (locus typicus: Oppdal), Sweden.

Collected in higher elevations from 400 (specimen studied here) to 900 m a.s.l. (type series).

**Remarks.** Despite not having had a fresh specimen at hand for sequencing, we regard this species as different from *A. ensifer* due to the clear differences in sculpture of the mesoscutum, mesoscutellum and mesopleuron.

The species was described from one locality in central Norway (Oppdal) (Mata-Casanova et al. 2018) and we found only one additional specimen from Abisko national park (Sweden) within the older dry-mounted specimens originating from all over Sweden (coll. NHRS) and Switzerland (coll. MHNG & NMBE). Our diagnosis was made as an amendment to the diagnosis by Mata-Casanova et al. (2018), considering the single specimen we had at hand as well as the data and illustrations given in Mata-Casanova et al. (2018). The fresh samples that we had access to were mainly collected in Germany and Belgium, with a few additions from Southern Norway. As we did not find more specimens of that species, we deem it possible that its distribution is limited to boreal habitats in the scandinic mountains.

***Anacharis petiolata* (Zetterstedt, 1838), stat. rev.**

Figs 2C, 15A–E

*Cynips petiolata* Zetterstedt, 1838:409 - lectotype (MZLU) ♀, photographs examined.

*Anacharis gracilipes* Ionescu, 1969:75 syn. nov. (removed from synonymy with *A. eu-charioides*) - holotype (MGAB) ♀, examined.

**Diagnosis (n = 9).** Belongs to the *eucharioides* species group. Medium sized species (3.0–3.4, mean 3.2 mm, similar to *A. eucharioides*, *A. martiniae* and *A. typica*). Differing from *A. eucharioides* and *A. martiniae* by having a centrally smooth mesoscutellum (Fig. 15D, E, centrally carinate in *A. eucharioides* and *A. martiniae*) and a smooth lateromedial area of the pronotum (Fig. 15B, rugose to obliquely carinate in *A. eucharioides* and *A. martiniae*). Differs from *A. typica* mainly by having the hind coxa less distinctly bicoloured, weak paling is notable apically (Fig. 15A, distinctly bicoloured with distinct paling in hind coxa in *A. typica*). The hind trochanter in *A. petiolata* is similarly dark as the hind coxa (similar pattern of paling as hind coxa or pale as hind femur in *A. typica*). Additional to morphological differences, based on the limited material at hand, *A. petiolata* seems to be exclusively collected in boreal or montane environments from above 1,000 meters above sea level (whilst *A. typica* is collected from temperate environments below 700 meters above sea level).

**CO1 barcode.** n=9. Maximum intraspecific distance: 2.2%. Minimum distance to closest species (*A. eucharioides*): 3.2%. CO1 barcode consensus sequence:

AATTTTATACTTTATTAGGTATTGATCAGGAATAATAGGAT-  
CAAGATTAAGAATAATTATTCGAATAGAGTTAGGTACCCATCTCAAT-  
TAATTATAAATGATCAAATTATAATTCAATTGTAACTGCACATGCATT-  
TATCATAATTCTTCTTATAGTTACCTATCATACTAGTAGGAGGATTG-  
GAAATTATTAGTACCTTAATATTAAATCTCTCCTGATATAGCTTCC-  
CACGATTAAATAATTAAAGATTGATTGCAATCCCTCCTTATTAA-  
TAATAACAATTAAATTATTCGACCAAGGAGCAGGAACAGGATGAAC-  
GTTTATCCTCCATTATCCTCTCTAACAGGTACCCATCTATATCAGTA-  
GATTTAGTTATTATTGATTACATTAAAGTGGAAATCTCTCAATTCTG-  
GATCAATTAAATTATTGTTACCATTAAATACGAATAAATTCTA-  
TATTATAGACAAAATTCAATTATTGATCTATTCTAACTA-  
CAATTAACTATTATTACCTTACCCGTACTAGCAGGAGGATTAAC-  
TAACTATTATTGATCGAAATTAAATACATCTTTTTGACCCCACAG-  
GAGGGGGAGACCCAATCCTTATCAACATTATT

**Type material.**

**Lectotype of *Cynips petiolata* Zetterstedt, 1838**

LECTO-TYPE

*C. petiola* ta ♀.

1982 855

LECTOTYPE *Cynips petiolata* Zett det. N.D.M.Fergusson, 1982

*Anacharis eucharioides* (Dal.) det. N.D.M.Fergusson, 1982

MZLU 00207341

MZLU Type no. 7814:1

[for images, see <https://www.flickr.com/photos/tags/mzlutype07814>]

**Holotype of *Anacharis gracilipes* Ionescu 1969**

*Anacharis gracilipes* n. sp. ♀ Holotip

26.7.956 Rarău,

GAL 0340/9

*Anacharis eucharoides* ♀ (Dalman, 1823) JP-V 2012 det  
HOLOTYPE, *Anacharis gracilipes* Ionescu, 1969, MGAB  
[Fig. 16E]

**Other material examined. DNA barcode vouchers.** GERMANY • 1 ♀; Bavaria, Allgäu, Oberstdorf, Oytal, Schochen, alpine meadow; 47.392°N, 10.37°E; ca 1930 m a.s.l.; 6 Aug. 2014; BC-ZSM-HYM-24109-D01 (ZSM). • 1 ♀; same collection data as for preceding; 4 Sep. 2014; BC-ZSM-HYM-24073-F03 (ZSM). • 1 ♀; Bavaria, Allgäu, Oberstdorf, Schochen, south faced ridge; 47.394°N, 10.369°E; ca

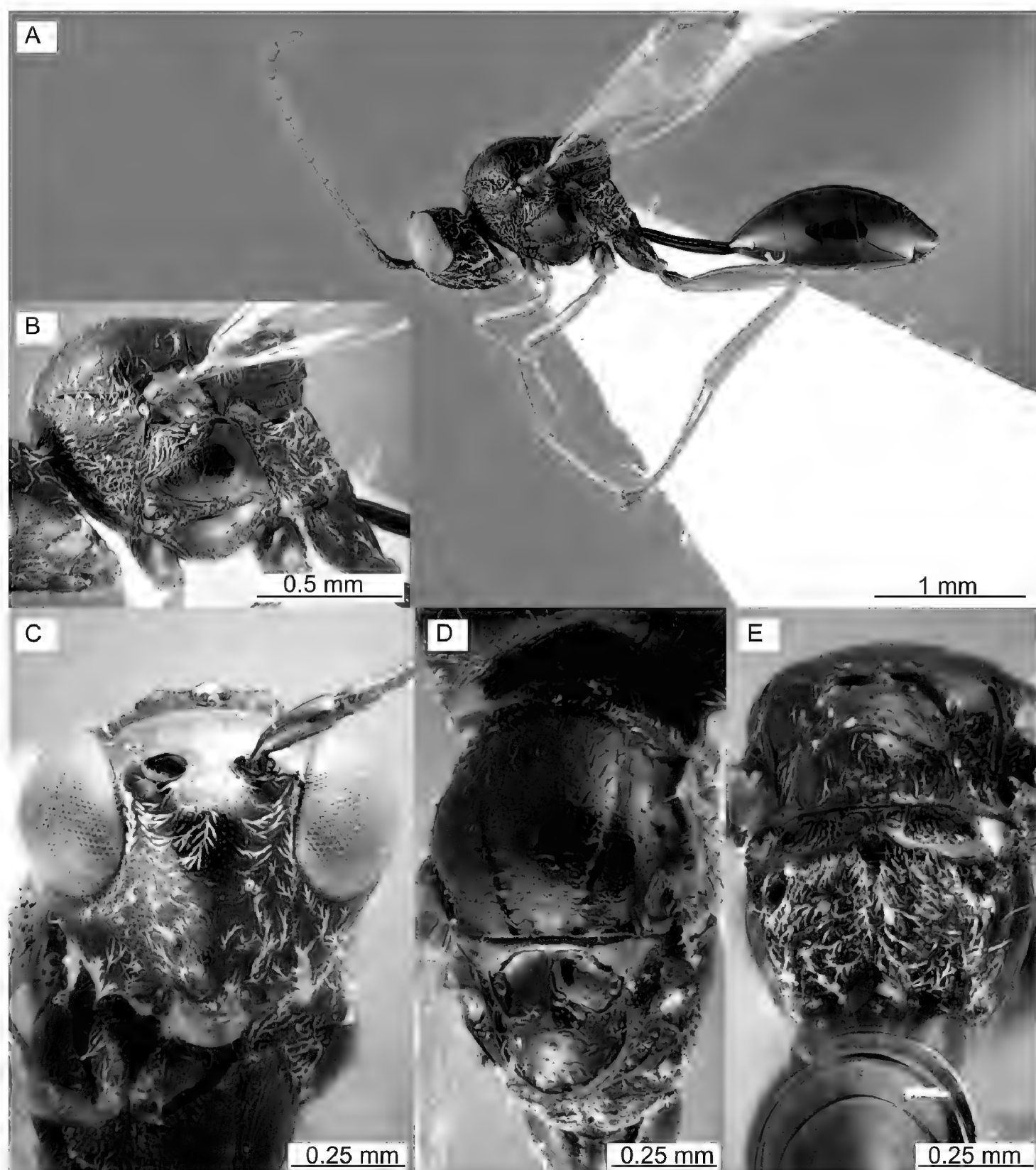


**Figure 15.** *Anacharis petiolata*, female (ZFMK-TIS-2629285) **A** habitus **B** mesosoma lateral **C** face **D** mesosoma dorsal **E** mesosoma posterior view.

2030 m a.s.l.; 6 Aug. 2014; BC-ZSM-HYM-24066-H09 (ZSM). • 1 ♀, 1 ♂; Bavaria, Garmisch-Partenkirchen, Zugspitze, mountain; 47.4062°N, 11.0095°E; ca 1970 m a.s.l.; 20 Jun.-5 Jul. 2018; Doczkal, D., Voith, J. leg.; Malaise trap; female - ZFMK-TIS-2637891; male - ZFMK-TIS-2637890. • 2 ♀♀, 1 ♂; Bavaria, Garmisch-Partenkirchen, Zugspitze, mountain; 47.4068°N, 11.008°E; ca 2010 m a.s.l.; 20 Jun.-5 Jul. 2018; Doczkal, D., Voith, J. leg.; Malaise trap; females - ZFMK-TIS-2628236, ZFMK-TIS-2629285; male - ZFMK-TIS-2628237. • 1 ♀; same collection data as for preceding; 2–13 Aug. 2018; ZFMK-TIS-2637893.

GREENLAND • 1 ♀, 2 ♂♂; SouthWest Greenland, Evighedsfjord, Kangiussaq; 65.8667°N, -52.2°E; ca 30 m a.s.l.; 19 Jul.-20 July 2003; Kissavik Exp., ZMUC leg.; female - zmuc00023359 (ZMUC); males - zmuc00023357 (ZMUC), zmuc00023358 (ZMUC).

**Material without DNA barcode.** GERMANY • 1 ♂; Bavaria, Garmisch-Partenkirchen, Zugspitze, mountain; 47.4053°N, 11.0091°E; ca 1980 m a.s.l.; 18 Jul.-2 Aug. 2018; Dieter Doczkal | Johannes Voith leg.; Malaise trap; ZFMK-HYM-00039678. • 4 ♀♀; Bavaria, Garmisch-Partenkirchen, Zugspitze, mountain; 47.4062°N, 11.0095°E; ca 1970 m a.s.l.; 20 Jun.-5 Jul. 2018; Dieter Doczkal | Johannes Voith leg.; Malaise trap; ZFMK-HYM-00039679, ZFMK-HYM-00039680, ZFMK-HYM-00039681, ZFMK-HYM-00039682. • 1 ♂; same collection data as for preceding 5–18 Jul. 2018; ZFMK-TIS-2642567. • 2 ♀♀; same collection data as for preceding 18 Jul.-2 Aug. 2018; ZFMK-TIS-2642535, ZFMK-TIS-2642547. • 1 ♂; Bavaria, Garmisch-Partenkirchen, Zugspitze, mountain; 47.4068°N, 11.008°E; ca 2010 m a.s.l.; 5–18 Jul. 2018; Dieter Doczkal | Johannes Voith leg.; Malaise trap; ZFMK-TIS-2642544. • 2 ♂♂; Bavaria, Garmisch-Partenkirchen, Zugspitze, Platt, mountain; 47.4053°N, 11.0091°E; ca 1980 m a.s.l.; 5–18 Jul. 2018; Dieter Doczkal | Johannes Voith leg.; Malaise trap; ZFMK-TIS-2640706, ZFMK-TIS-2640707. • 1 ♂; same collection data as for preceding 18 Jul.-2 Aug. 2018; ZFMK-HYM-00039678.

GREENLAND • 1 ♀; Narssarssuaq; 61.1°N, -45.25°E; ca 0 m a.s.l.; 5 Jul. 1983; Peter Nielsen leg.; NHMD918327 (ZMUC). • 2 ♂♂; same collection data as for preceding 1 Aug. 1983; NHMD918299 (ZMUC), NHMD918313 (ZMUC). • 1 ♀; same collection data as for preceding 13 Aug. 1983; NHMD918341 (ZMUC). • 1 ♀, 3 ♂♂; SouthWest Greenland, Evighedsfjord, Kangiussaq; 65.8667°N, -52.2°E; ca 30 m a.s.l.; 19–20 Jul. 2003; Kissavik Exp., ZMUC leg.; female - zmuc00023359 (ZMUC); males - NHMD918215 (ZMUC), zmuc00023357 (ZMUC), zmuc00023358 (ZMUC). • 1 ♂; same collection data as for preceding 24–25 Jul. 2003; NHMD918229 (ZMUC). • 1 ♀; SouthWest Greenland, Itivleq, eastern end; 66.55°N, -52.4333°E; ca 0 m a.s.l.; 22–23 Jul. 2003; Kissavik Exp., ZMUC leg.; NHMD918285 (ZMUC). • 1 ♀; South-West Greenland, Kangerdluarssuk east; 66.9833°N, -53.2°E; ca 20 m a.s.l.; 24–25 Jul. 2003; Kissavik Exp., ZMUC leg.; NHMD918271 (ZMUC). • 1 ♀, 1 ♂; West Greenland, Qarássap munatâ; 70.75°N, -53.62°E; ca 710 m a.s.l.; 18–19 Jul. 1969; Jens Böcher leg.; female - NHMD918243 (ZMUC); male - NHMD918257 (ZMUC).

SWITZERLAND • 1 ♀; Neuchâtel, Auvernier; 16 Aug. 1956; Jacques de Beaumont leg.; specimen at MHNG. • 2 ♂♂; same collection data as for preceding 26 Aug. 1956; specimens at MHNG. • 1 ♂; Vaud, Ferreyres; 22 Aug. 1952; Jacques de Beaumont



**Figure 16.** Lectotype of *A. typica* (**A-C**) and holotype of *A. gracilipes* (**D, E**) **A** labels, frontal **B** lectotype ventral **C** lectotype dorsal **D** holotype dorsal **E** holotype labels frontal, above and the back, below.

leg.; specimen at MHNG. • 1 ♂; Vaud, La Sauge; 10 Aug. 1959; Jacques de Beaumont leg.; specimen at MHNG. • 2 ♂♂; same collection data as for preceding 29 Aug. 1956; specimens at MHNG. • 1 ♀; Vaud, Lioson Sep. 1956; Jacques de Beaumont leg.; specimen at MHNG. • 1 ♀; Vaud, Marchairuz; 21 Jul. 1960; Jacques de Beaumont leg.; specimen at MHNG. • 1 ♀; Vaud, Sta Catharina; 17 Sep. 1955; Jacques de Beaumont leg.; specimen at MHNG.

**Biology.** Summer species, flying from July to September, peak in July. Seems confined to alpine, arctic or boreal habitats.

**Distribution.** Finland (locus typicus of *A. petiolata*: Lapland, Muonio, likely on Finnish side of Muonio River, see remarks), Germany (Alps), Greenland, Romania (locus typicus of *A. gracilipes*: Rarău massif (Eastern Romanian Carpathians) at “1,950 m” altitude according to Ionescu (1969) [highest peak according to Wikipedia is at 1651 m]), Switzerland.

DNA barcode matches with publicly available sequences from Canada (e.g. ABI-NP3207-21) and Norway (e.g. GWNWG2160-14).

In Central Europe restricted to elevations above 1900 m a.s.l. but occurring at lower altitudes in arctic and subarctic, boreal landscapes.

**Remarks.** *A. petiolata* (Zetterstedt, 1838, often erroneously cited as Zetterstedt, 1840) was synonymised with *A. eucharoides* by Fergusson (1986) and was erroneously listed as synonym of *A. immunis* in Mata-Casanova et al. (2018). The type locality of *A. petiolata* is Muonio, Lapland (in the description: “Pinetis Lapponiae ad Muonioniska” (Zetterstedt 1838)). Muonio is a municipality in present-day Finland (belonging to Russia at the time of Zetterstedt’s visit), where Zetterstedt visited local entomologist Kolström during his 1821 Lapland journey. The Muoniojoki river, which flows indirectly downstream into the Torne river, marks the border between Finland and Sweden near the municipality of Muonio and it is unclear whether Zetterstedt crossed it to collect insects from both sides of the river, though he mentions how scary it is to cross the river, making it unlikely that he frequently did so (Zetterstedt 1822). In conclusion, whether the lectotype was collected in modern day Finland or Sweden is probably impossible to tell and the question itself of minor significance.

There are no descriptive labels on the lectotype. Fergusson (1986) stated that the lectotype was held at NHRS, but it is actually deposited at the MZLU. The sex of the lectotype is difficult to discern, due to the missing antennae and only images available to us. We consider it a male, as the original label shows, though that is in contrast to what Fergusson (1986) wrote. Apparently, the specimen was already in a poor condition when Fergusson studied it and he could not reliably identify the sex either.

On the primary type of *A. gracilipes*: Mata-Casanova et al. (2018) cites a lectotype of *A. gracilipes* as primary type. However, Ionescu specifically mentions a holotype in his publication, though without giving unambiguous details about the actual specimen (Ionescu 1969). The ICZN states in 73.1.2., that “If the taxon was established before 2000 evidence derived from outside the work itself may be taken into account [Art. 72.4.1.1] to help identify the specimen.” The loaned specimen from MGAB with the Museum ID “GAL 340/9” bears the word “holotip” on its label, along with informa-

tion on locality and time that match the description of the type series. The specimen thereby constitutes the holotype.

The holotype was kept in a vial with ethanol, already damaged, lacking head and wings, legs incomplete. We mounted the specimen on a white pointed card with Shell-lac Gel glue on the right side of its mesosoma after asking permission from MGAB. All coxae are present, fore trochanters and femora present, trochanter and femora of right hind leg mounted separately along with a tibia. The specimen was about 2.8 mm in body length (measurements on holotype combined with proportions from photograph in Ionescu, 1969) and that falls into the average body size of most *Anacharis* species.

*A. petiolata* is morphologically very similar to *A. typica*. The morphological differences are rather subtle differences in colouration and morphological diagnoses for both species are rather weak. Still, we differentiate between the two species based on the distinct difference in CO1 barcode sequences as well as a difference in habitat type/distribution. All known specimens of *A. petiolata* were collected in alpine or boreal environments, specimens of *A. typica* were collected in temperate environments below 700 meters above sea level.

***Anacharis typica* Walker, 1835, stat. rev.**

Figs 2D, 3D, 17A–E

*Anacharis typicus* Walker, 1835:520 - lectotype (NHMUK) ♀, photographs examined (Fig. 16A–C).

**Diagnosis (n = 10).** Belongs to the *eucharioides* species group. Medium sized species (2.9–3.5, mean 3.2 mm, similar to *A. eucharioides*, *A. martinae* and *A. petiolata*). Differing from *A. eucharioides* and *A. martinae* by having a centrally smooth mesoscutellum (Fig. 17D, E, centrally carinate in *A. eucharioides* and *A. martinae*) and a smooth lateromedial area of the pronotum (Fig. 17B, rugose to obliquely carinate in *A. eucharioides* and *A. martinae*). Differs from *A. petiolata* mainly by having the hind coxa often distinctly bicoloured, with noticeable paling apically (Fig. 17A, hind coxa less distinctly bicoloured, though weak paling is notable apically in *A. petiolata*). The hind trochanter in *A. typica* has a similar pattern of paling as hind coxa or is as pale as in hind femur (hind trochanter similarly dark as the hind coxa in *A. petiolata*). Additional to morphological differences, *A. typica* is exclusively collected in temperate environments below 700 meters above sea level (whilst *A. petiolata* is collected from boreal environments above 1,000 meters above sea level).

**CO1 barcode.** n=10. Maximum intraspecific distance: 0.5%. Minimum distance to closest species (*A. eucharioides*): 5.7%. CO1 barcode consensus sequence:

AATTTTATACTTATTAGGAATTGATCAGGAATAATAGGAT-  
CAAGATTAAGAATAATTATTCGAATAGAATTAGGGACCCCTCTCAAT-  
TAATTATAATGATCAAATTATAACTCAATTGTAAGTGCTCATGCATT-  
TATTATAATTCTTATAGTCATACCTATTATAGTAGGAGGATTG-  
GAAATTATTAGTGCCTTAATATTAATCTCTGATATAGCTTCC-

CCCGATTAAATAATTAGATTGATTTAATCCCCTCTTATTAAATAACAATTAAATTATTGACCAAGGAGCAGGAACAGGGTGAACGTATAACCCCCCATTATCATCACTCACAGGTACATCCATCTATATCGGTA-GATTAGTTATTATTACATTACATTAAAGTCCAATTTCCTCAATTCTGGTTCTATTAATTATTGTAACCATTAAATATACTGAATAACTGTTATCTATAGACAAAATTTCATTATTGATCTATTAAACTACAATTAAATTATTATTATCTTACCAAGTAGCAGGAGGTTAACTATTACTATTGATCGAAATTAAATACATCTTTTGACCCTACAGGAGGAGGGATCCAATCCTTATCAACACTATT

**Type material.**

**Lectotype of *Anacharis typicus* Walker, 1835**

81 61 [on backside of mounting board]

2.

Type

In Coll under typical

B.M.1981 . Under typica

LECTOTYPE

LECTOTYPE *Anacharis typica* Walker det. N.D.M.Fergusson, 1981

B.M. TYPE HYM 7. 163

[QR code] NHMUK 012858913

[for images, see Fig. 16A–C and <https://data.nhm.ac.uk/dataset/56e711e6-c847-4f99-915a-6894bb5c5dea/resource/05ff2255-c38a-40c9-b657-4ccb55ab2feb/record/10470199>]

**Other material examined. DNA barcode vouchers.** AUSTRIA • 1 ♂; Styria, NP Gesäuse, Gsengquelle; 47.5683°N, 14.5902°E; ca 680 m a.s.l.; 2 Sep. 2015; Haseke leg.; ZFMK-TIS-2640691.

BELGIUM • 1 ♀; West Flanders, Beernem, Centrum; 51.1259°N, 3.3202°E; ca 10 m a.s.l.; 8 May 2022; De Ketelaere, Augustijn leg.; hand picked; ZFMK-TIS-2640858. • 1 ♀; West Flanders, Beernem, Gevaerts; 51.1411°N, 3.3215°E; ca 10 m a.s.l.; 24 Apr. 2022; De Ketelaere, Augustijn leg.; hand picked; ZFMK-TIS-2640857.

GERMANY • 1 ♀; Hesse, Waldeck-Frankenberg, National park Kellerwald-Edersee, Maierwiesen; 51.1555°N, 9.0015°E; ca 370 m a.s.l.; 22 Jun.-8 Jul. 2021; GBOL III leg.; Malaise trap (Krefeld version); ZFMK-TIS-2640806. • 3 ♂♂; Hesse, Waldeck-Frankenberg, NP Kellerwald-Edersee, „Banfe-Haus“; 51.167°N, 8.9749°E; ca 270 m a.s.l.; 7–21 Jul. 2022; GBOL III leg.; Malaise trap; ZFMK-TIS-2640757, ZFMK-TIS-2640758, ZFMK-TIS-2640760. • 1 ♀; Mecklenburg-Vorpommern, Vorpommern-Rügen, Großer Vilm, Biosphärenreservat; 54.325°N, 13.539°E; ca 30 m a.s.l.; 24 May-3 Jun. 2016; Rulik, Björn et al. leg.; Malaise trap; ZFMK-TIS-2629503. • 1 ♀; North Rhine-Westphalia, Rhein-Sieg-Kreis, Schladern near Windeck, Sieg river, right river bank; 50.8°N, 7.585°E; ca 130 m a.s.l.; 4–11 Jul. 2017; ZFMK et al. leg.; Malaise trap; ZFMK-TIS-2629276.

LITHUANIA • 1 ♀; Silute distr., Sysa, Sysa, control plot; 55.3127°N, 21.4049°E; ca 0 m a.s.l.; 14–25 Jun. 2020; Petrasius, Andrius leg.; Malaise trap; ZFMK-TIS-2637717.

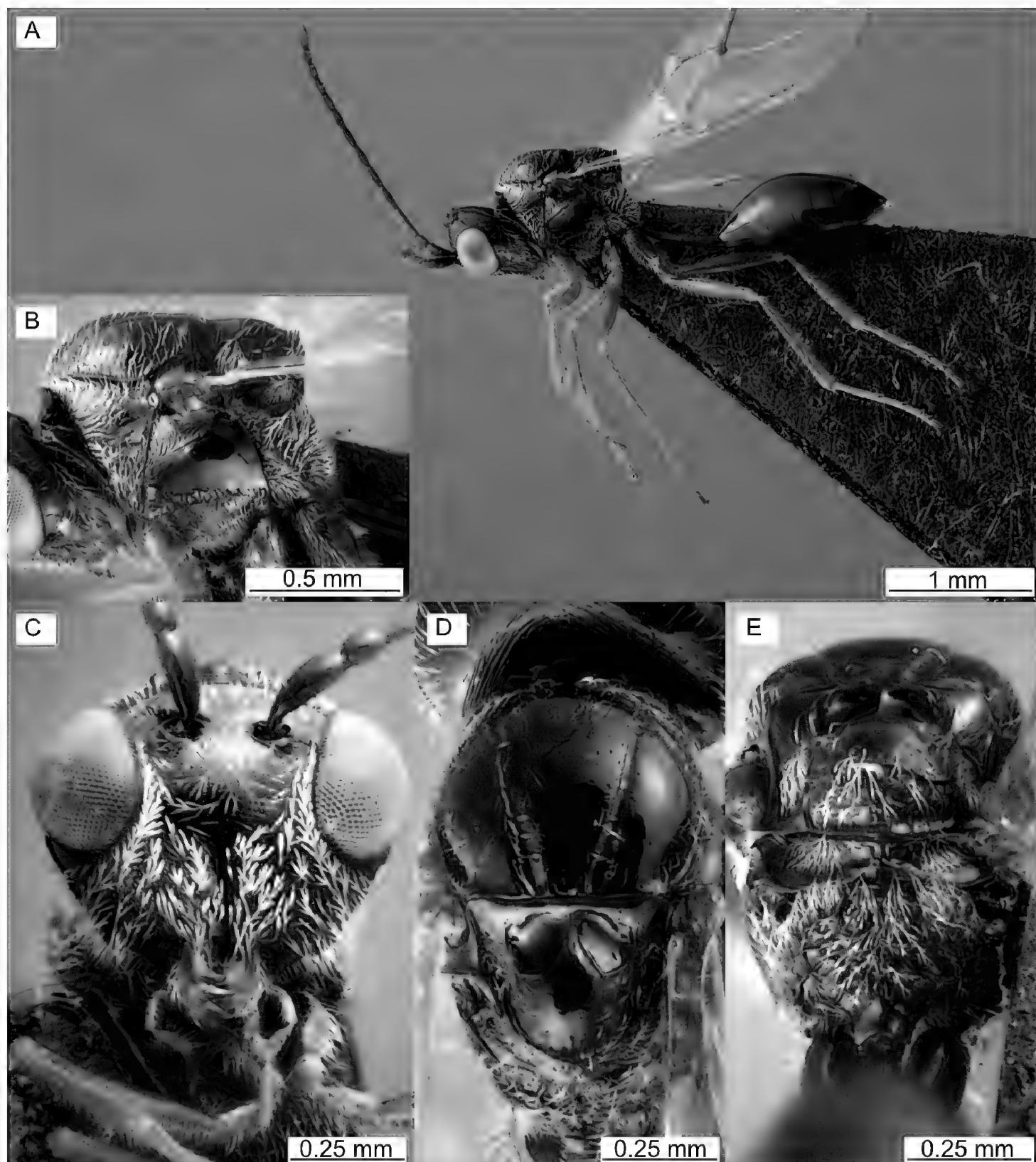


**Figure 17.** *Anacharis typica*, female (ZFMK-TIS-2640806) **A** habitus **B** mesosoma lateral **C** face **D** mesosoma dorsal **E** mesosoma posterior view.

**Material without DNA barcode.** BELGIUM • 2 ♂♂; Walloon Brabant, Ottignies; 9–16 Jul. 1983; Paul Dessart leg.; Malaise trap; JV\_Prel\_0074 (RBINS), JV\_Prel\_0045 (RBINS). • 2 ♂♂; same collection data as for preceding 28 May–4 Jun. 1983; JV\_Prel\_0075 (RBINS), JV\_Prel\_0076 (RBINS). • 1 ♂; West Flanders, Harelbeke, Gavers, Wetland with pools; 50.8379°N, 3.3215°E; ca 10 m a.s.l.; 11 Jun. 2022; Bart Lemey leg.; hand caught; JV\_Prel\_0052 (RBINS).

GERMANY • 1 ♂; Hesse, Werra-Meißner-Kreis, Großalmerode, Private garden, Siedlerweg, semi-abandoned garden with wet spot, ivy hedge and salix; 51.2591°N, 9.7871°E; ca 380 m a.s.l.; 12–20 Jul. 2022; Jonathan Vogel leg.; Malaise trap; ZFMK-

TIS-2640704. • 1 ♂; North Rhine-Westphalia, Rhein-Sieg-Kreis, Schladern near Winddeck, Sieg river, right river bank; 50.8°N, 7.585°E; ca 130 m a.s.l.; 18–25 Jul. 2017; ZFMK et al. leg.; Malaise trap; ZFMK-HYM-00039677. • 2 ♂♂; same collection data as for preceding 1–8 Aug. 2017; ZFMK-HYM-00039674, ZFMK-HYM-00039675.

ITALY • 1 ♂; Val d'Aoste, Boertolaz, (Villeneuve); ca 800 m a.s.l.; 15 Sep. 1978; L. Martile leg.; Malaise trap; NHRS-HEVA 000023180 (NHRS).

SWEDEN • 1 ♂; Gotland, Eksta sn, Stora Karlsö, calcarous low herb pasture; 57.2873°N, 17.9775°E; ca 40 m a.s.l.; 26–29 Aug. 2014; Hymenoptera Inventory 2014 leg.; Malaise trap; MT Loc#2; NHRS-HEVA 000023181 (NHRS). • 1 ♂; Gotska sandön, Kapellängen; 7 Jul. 1964; Bror Hanson leg.; NHRS-HEVA 000023182 (NHRS). • 1 ♂; Öland, Glömminge, Gillsättra; 4 Aug. 2004; Mattias Forshage leg.; specimen in coll MF. • 1 ♀; Öland, Kastlösa; 26 Jun. 1962; Karl-Johan Hedqvist leg.; NHRS-HEVA 000023198 (NHRS). • 1 ♂; Öland, Kastlösa; 28 Jun. 1962; Tor-Erik Leiler leg.; NHRS-HEVA 000023197 (NHRS). • 2 ♂♂; Scania, Kristianstads kommun, Trunelän, Degeberga, Grazed meadow at alder stand along stream; 55.7746°N, 14.2156°E; ca 80 m a.s.l.; 1–13 Aug. 2019; Swedish Insect Inventory Programme (SIIP), Station Linné leg.; Malaise trap; NHRS-HEVA 000023184 (NHRS), NHRS-HEVA 000023185 (NHRS). • 1 ♂; Scania, Lomma; 10 Jul. 1963; Hans von Rosen leg.; NHRS-HEVA 000023188 (NHRS). • 1 ♂; same collection data as for preceding 13 Aug. 1963; NHRS-HEVA 000023189 (NHRS). • 2 ♀♀; same collection data as for preceding 14 Aug. 1963; NHRS-HEVA 000023186 (NHRS), NHRS-HEVA 000023187 (NHRS). • 1 ♂; Scania, Saxtorp; 5 Jun. 1961; Karl-Johan Hedqvist leg.; NHRS-HEVA 000023183 (NHRS). • 1 ♂; Scania, Stenshuvuds NP, lush mixed oak forest; 55.6603°N, 14.2755°E; ca 30 m a.s.l.; 22 Sep.–1 Nov. 2004; Swedish Malaise Trap Project (Swedish Museum of Natural History) leg.; Malaise trap; NHRS-HEVA 000023190 (NHRS). • 1 ♀, 1 ♂; Småland; [18xx]; Carl Henning Boheman leg.; female - NHRS-HEVA 000023191 (NHRS); male - NHRS-HEVA 000023192 (NHRS). • 1 ♂; Södermanland, Tockenön Jul. 1950; Anton Jansson leg.; NHRS-HEVA 000023193 (NHRS). • 1 ♂; Uppland, Vallentuna; 7 Jun. 1959; Karl-Johan Hedqvist leg.; NHRS-HEVA 000023195 (NHRS). • 1 ♀; same collection data as for preceding 15 Sep. 1962; NHRS-HEVA 000023194 (NHRS). • 1 ♂; Västmanland, Köping; 18 May 1975; Walter Siering leg.; NHRS-HEVA 000023196 (NHRS).

SWITZERLAND • 1 ♀; Grisons, Pontresina; unknown leg.; specimen at NMBe.

**Biology.** Summer species, flying mainly from April to September, peak in July. No clear preferences in terms of habitat.

**Distribution.** Austria, Belgium, Germany, Italy, Lithuania, Sweden, Switzerland, United Kingdom (locus typicus of *A. typica*: southern England, near London or Isle of Wight).

Found in elevations up to 400 m a.s.l., rarely up to 800 m a.s.l.

**Remarks.** The specimen labelled as lectotype is clearly a female, not a male as stated by Fergusson (1986). Despite this incongruence we acknowledge the specimen labelled as lectotype by Fergusson as such.

The lectotype is glued to its ventral side on cardboard, face down, wings also glued to the board. It is overall intact, though the 13<sup>th</sup> antennal segment is either broken in half and the fragment is lost, or the segment is malformed. The tarsomeres of the right

fore leg are missing from second tarsomere onwards. Both wings and legs obscure the lateral mesosoma on both sides.

With 2.6 mm body length, the lectotype is a comparably small specimen of this species (average body length 3.2 mm). Additionally, the lectotype is unusual by its overall reddish colouration, which may have been caused by ageing. Otherwise, it is morphologically well-fitting with the specimens we examined.

For a comparison of the similar *A. typica* and *A. petiolata*, see the remarks section of *A. petiolata*.

One specimen from Belgium (JV\_Prel\_0076) was similarly coloured as the Bavarian specimens (BC-ZSM-HYM-27596-F10 & BC-ZSM-HYM-27596-F09, see variation section in description of *A. martiniae*) of *A. martiniae*, having the head distinctly darker than the otherwise pale body.

In the distribution section we only list those records that we can verify by having seen actual specimens. Additional distribution records can be inferred from sequences from BOLD, if they match with our species cluster of *A. typica*. They were obtained from specimens originating from Canada (e.g. SMTPI9646-14). The identities of these sequences as *A. typica* need to be confirmed by examination of the physical specimens before reliably citing *A. typica* for Canada.

### Key to the Northwestern European species of *Anacharis* (females and males)

The characters used in this key are, in part, based on the comparison of a small number of specimens (most notably *A. minima*, *A. petiolata* and *A. typica*). Note especially our concern that the colouration of specimens may be sensitive to the method of killing and the state of the specimen's preservation. Due to the high degree of inter- and intraspecific variability, we stress that the most reliable way to identify the species of *Anacharis* is via comparison of DNA barcode data.

- 1      Occiput smooth (Fig. 18A); notauli weak, fading in anterior region, inside not carinate (Fig. 11D); placodeal sensilla in females starting at fourth flagellomere; inner side of hind coxa with equally distributed pubescence on entire length; petiole relatively short (Fig. 11A) (*immunis* species group) ..... 2
- Occiput with at least some noticeable transversal striolation to striation laterally to medially (Fig. 18B); notauli usually strong, not fading in anterior region and often inside carinate (Fig. 10D); placodeal sensillae in females starting at first flagellomere; inner side of the hind coxa with no continuous pubescence along its entire length; petiole relatively long (Fig. 10A) (*eucharoides* species group) ..... 4
- 2      Dorsal surface of mesoscutellum largely smooth and even, especially centrally (Fig. 11D). Fore and mid coxa often noticeably darker than rest of legs and generally appearing darker (difficult to see in old/paled specimens, Fig. 11A) ..... *A. immunis* Walker, 1835
- Dorsal surface of mesoscutellum with an uneven to reticulate-foveate sculpture centrally (Fig. 9D). Fore and mid coxa usually as pale as rest of legs and

generally appearing paler (difficult to see in old/paled specimens, Fig. 9A). ..... 3

3 Dorsal and posterior surface of mesoscutellum heavily foveate, usually with small foveae that continue on posterior surface of mesoscutellum (Fig. 4E in Mata-Casanova et al. 2018). Circumscutellar carina not distinctly flanged upwards, apically not appearing like a tooth in lateral view (Fig. 4E in Mata-Casanova et al. 2018). Mesopleural sculpture rugose, diffusing the mesopleural line dorsally in its anterior half. Strong wrinkles on mesoscutum, especially in anteromedian area, making the anteroadmedian signa distinct (Fig. 4D in Mata-Casanova et al. 2018) ..... *A. norvegica* Mata-Casanova & Pujade-Villar, 2018

— Dorsal surface of mesoscutellum reticulate-foveate (Fig. 9D), never with small foveae that continue on the posterior surface of mesoscutellum. Circumscutellar carina usually distinctly flanged upwards, apically appearing like a tooth in lateral view (Fig. 9B). Mesopleural sculpture smooth to rugose, not diffusing the mesopleural line in most of its anterior half (Fig. 9B). Less to no wrinkles on mesoscutum and thereby less distinct anteroadmedian signa (Fig. 9D) ..... *A. ensifer* Walker, 1835, stat. rev.

4 Dorsal surface of mesoscutellum centrally with sculpture (Fig. 10D). Lateromedial area of pronotum variable (Fig. 12B). Nuchal collar variable ..... 5

— Dorsal surface of mesoscutellum largely smooth and even (Fig. 17D). Lateromedial area of pronotum smooth (Fig. 14B). Nuchal collar dorsally broadly projecting into a point (Fig. 6D–F) ..... 7

5 Dorsal surface of mesoscutellum with well-defined reticulate carinae in the anterior half between the mesoscutellar foveae, in other areas largely smooth or variable (Fig. 13D); large species, 3.5 mm or larger ..... *A. maxima* Vogel, Forshage & Peters, sp. nov.

— Sculpture of mesoscutellum different; medium sized species, 2.6–3.4 mm body size ..... 6

6 Lateromedial area of pronotum smooth to rugose (Fig. 10B); mesoscutum centrally more sparsely pubescent than in other areas of the mesoscutum; space between toruli often without striolation; mesoscutellar sculpture usually with median carina centrally interrupted, lateral carinae dissolved into general reticulation (Fig. 10D); nuchal collar usually broadly forming a dorsal tooth (Fig. 6D–F); metasoma usually black ..... *A. euchariooides* Dalman, 1818

— Lateromedial area of pronotum sculptured with parallel longitudinal carinae like ventrally (Fig. 12B); mesoscutum more evenly pubescent; space between toruli often with transversal striolation; mesoscutellar sculpture often with median carina reaching posterior margin and two lateral carinae or low crests that delineate a longitudinal median field (Fig. 12D); nuchal collar usually forming a narrow dorsal tooth (Fig. 6C); metasoma brown to dark-brown ... ..... *A. martiniae* Vogel, Forshage & Peters, sp. nov.

7 Small sized species, around 2.4 mm body size; carination of notauli absent; with narrow coriaceous texture of the malar space that extends only around the dorsal corner of the mandibular base (Fig. 19A); mesopleural line usually reaching posteroventral hypocoxal furrow (Fig. 14B). Rare species.....  
 ..... ***A. minima* Vogel, Forshage & Peters, sp. nov.**

— Medium sized species, around 3 mm body size; carination of notauli variable; band of coriaceous texture of malar space extending along entire length of mandibular base (Fig. 19B); mesopleural line usually not reaching posteroventral hypocoxal furrow (Fig. 15B)..... 8

8 Collected in boreal environments or above 1,000 meters above sea level; hind coxa less distinctly bicoloured, though weak paling is notable apically, hind trochanter usually as dark as hind coxa (Fig. 15A).....  
 ..... ***A. petiolata* Zetterstedt, 1838, stat. rev.**

— Collected in nemoral environments, below 700 meters above sea level; hind coxa often distinctly bicoloured, with noticeable paling apically, hind trochanter in has a similar pattern of paling as hind coxa or is as pale as in hind femur (Fig. 17A)..... ***A. typica* Walker, 1835, stat. rev.**

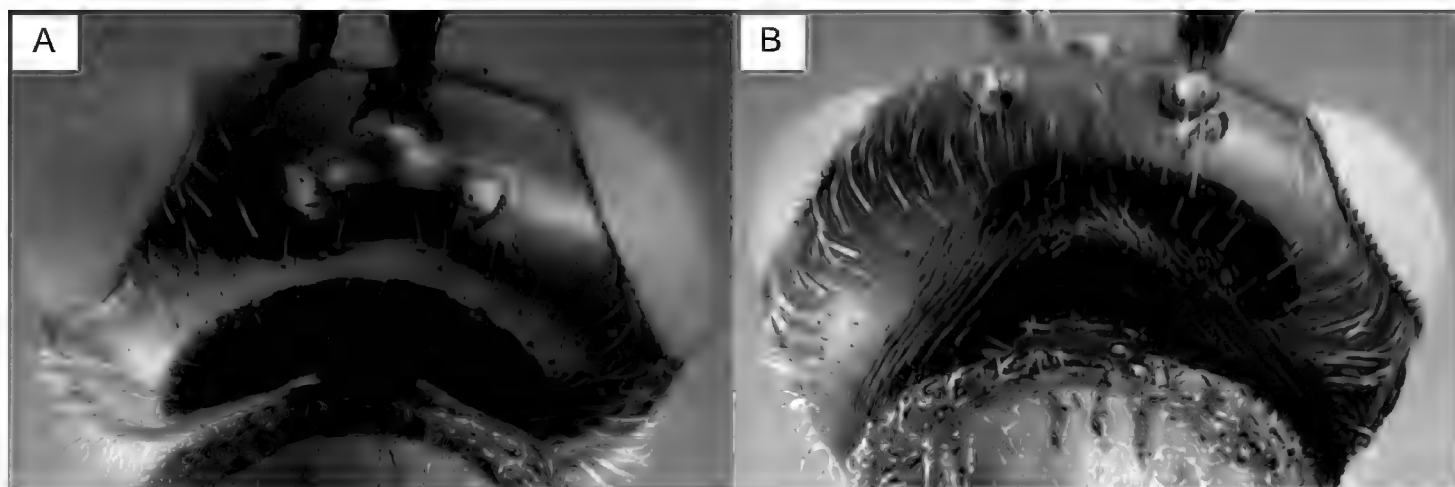


**Figure 18.** (postero-)dorsal view of the head **A** occiput smooth (*A. immunis*, ♀, ZFMK-TIS-2640709) **B** occiput striate (*A. martinae* sp. nov., holotype (ZFMK-TIS-2640787), ♀).

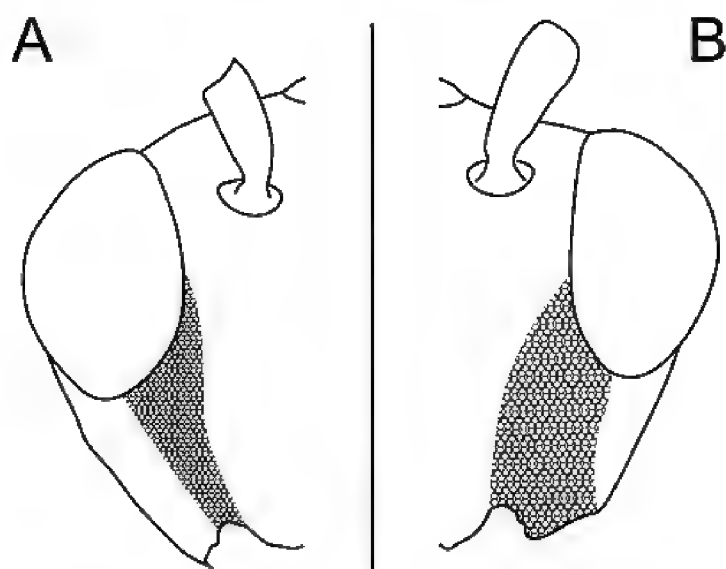


**Figure 19.** Frontal view of head, showing the extent of the coriaceous texture of the malar area in **A** *A. minima* sp. nov. **B** *A. maxima* sp. nov.

## Discussion

By integrating analyses of CO1 barcode data, morphological examination, multivariate morphometrics, WIPs and male genitalia dissections, we were able to detect and delimit nine species of *Anacharis* in Northwestern Europe, belonging to two species groups. The presence of more than two species is in line with the findings of Mata-Casanova et al. (2018) and in contrast to the broad species circumscriptions for *A. eucharioides* and *A. immunis* of Fergusson (1986).

Delimiting species based on morphology proved comparatively difficult due to overall similarity of the species, and strong intraspecific variation. We acknowledge that previous studies which did not include analyses of molecular sequence data, and thereby not having a chance of being informed by a reverse taxonomy approach, were not able to fully delimit the Northwestern European species. Specifically, we found the following previously used characters to vary considerably intraspecifically: The setosity of the eyes, the parascutal sulcus, the depth and carination of the notauli, the mesoscutellar sculpture, the propodeal sculpture, and the petiole length:hind coxa length ratio. We briefly discuss the states of each of these characters as well as their diagnostic value.

Regarding the setosity of the eyes, all species treated in Mata-Casanova et al. (2018) were described as having glabrous eyes. In contrast to that, we found all species to have setose eyes, the setae being either merely stubs, or considerably long (e.g. Fig. 4E, F). It is likely that they fall off during preservation and preparation or are overlooked. Especially with a light background, they are very difficult to see.

Regarding the parascutal sulcus, it was used in couplet three of the key, in the (re-) descriptions of the species, but not in the diagnoses in Mata-Casanova et al. (2018). We found it varying in both presence and extent in all of the species within the *eucharioides* species group (except *A. minima* where  $n=1$ ). It is sometimes clearly present, with anterior transversal carination, and sometimes it lacks this carination and varies in extent, either reaching the notauli or only being impressed in the posterior half. We did not observe a clear allometric effect. As a result, we conclude that this character is not suitable as a diagnostic character.

The notauli can be shallow and weak with no carination inside, as well as distinct and deep, with strong carination in the same species. The expression of the notauli may serve to exemplarily describe intraspecific variability of characters that we observed in *Anacharis*: Most specimens share what can be called a “typical pattern” but others contribute to the strong variation, either being more or less pronounced in the expression of the character. This makes it seemingly easy when studying a limited number of specimens but adds to an increasingly blurry picture when studying a large number of specimens before being finally able to correctly evaluate and describe a character. Again, note that this would have been tremendously difficult if not impossible without the reciprocal information from analyses of sequence data.

Regarding the mesoscutellar sculpture – on both dorsal and posterior face – we see a pattern similar to what we described above for the notauli. However, when generally smooth and even (as in *A. typica*, *A. petiolata*, *A. immunis* and *A. minima*) or when

distinctly carinate (as in *A. ensifer*, *A. eucharoides*, *A. martinae*, *A. maxima* and *A. norvegica*), mesoscutellar sculpture can be of diagnostic value.

The propodeal sculpture is intraspecifically variable, especially in the median part of the propodeum. From our examination, it cannot be used diagnostically between species.

Especially if qualitative characters are difficult to find, multivariate morphometric analyses can be executed. Our results, however, show that – generally – morphometric characters in *Anacharis* are of very limited use (Figs 7, 8). Exceptions are the differentiation between species groups and the partial or full delimitation of *A. martinae* (Fig. 8B) and *A. maxima* (Fig. 8C) which showcase the power of multivariate statistics in delimiting taxonomically challenging species.

The analyses of molecular sequence data, implementing more than one automated species delimitation method as should be common practice (Meier et al. 2022), gave results widely congruent between methods and also congruent with morphological examinations, including morphometric analyses. When using only DNA barcode data, interspecific haplotype-sharing goes undetected. Accordingly, taxonomic acts should be taken integrating various traits into forming species hypotheses. Ideally, mitochondrial DNA barcode sequence data will be complemented by nuclear markers (e.g. Dietz et al. 2022), especially if diagnoses are weak or results from DNA barcodes and morphology are incongruent.

In addition to molecular sequence data, morphology and morphometrics, we further explored the use of WIPs in the alpha taxonomy of Figitidae. We found it to be useful for species group diagnostics and potentially also for separating species, as shown for the newly described species *A. martinae* and *A. maxima*. With an optimised protocol, the WIPs on areas like the radial and median areas of fore and hind wing could potentially emerge better and be further evaluated for their use in species delimitation. However, to do that reliably, larger series of better-quality images are required for each species. Once established, ideally on species level, WIPs might also be used for automated species recognition. This has great potential, especially when applying a trained AI to recognise the species (Cannet et al. 2022, 2023; Jin et al. 2023).

From our first steps in evaluating male genitalia for their specific diagnostic power in Figitidae, we report some interspecific differences, most notably between the *eucharoides* and *immunis* species groups. On the species level, we could find differences in male genitalia morphology in the cases of *A. eucharoides* and *A. maxima* only. The differences are however subtle and nowhere close to the diversity of male genitalia morphology of the Ceraphronoidea (Salden & Peters, 2023). Like in other groups of microhymenoptera, the dissection of the male genitalia is difficult and yet we would argue that consulting male genitalia generally is a strategy worth investigating in parasitoid wasp taxonomy when there is a shortage of diagnostic characters.

Hemerobiiform Neuroptera are comparably poor in natural enemies (Aspöck et al. 1980). Several taxa which are parasitoids of defensible hosts share similar adaptations, which are often striking in these neuropteran parasitoids, including a short compact mesosoma, a strongly petiolate metasoma and comparably long and slender legs. This facilitates quick movements in general and specifically those associated with “quick-strike” oviposition maintaining a distance to the host to avoid being injured by

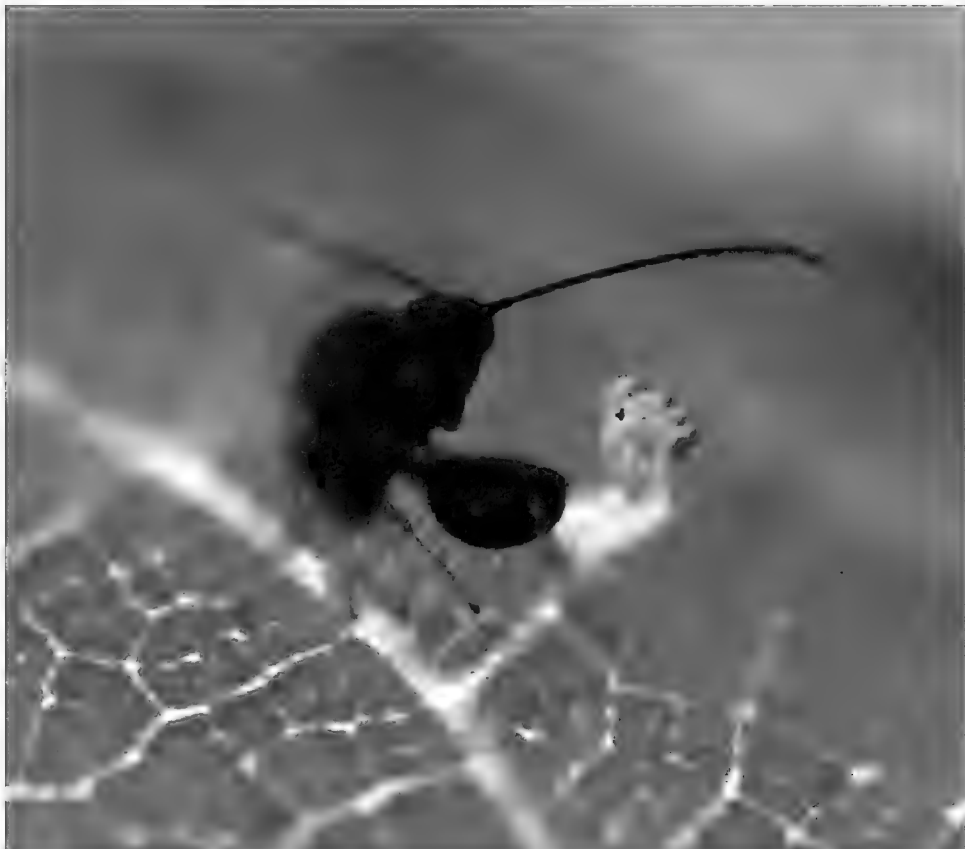


**Figure 20.** *Anacharis* sp. in action. A female *Anacharis* sp. attacking a hemerobiid early instar larva by bending its metasoma through the legs in the style of aphidiine braconids (photo by Kim Neubauer).

it (Buffington et al. 2007). Among these taxa are the A-wasps (Heloridae, larval-cocoon parasitoids of Chrysopidae), braconids in the genus *Chrysopophthorus* (adult parasitoids of Chrysopidae), Brachycyrtinae (Ichneumonidae, (pre-)pupal parasitoids of Chrysopidae) and the Anacharitinae. The Anacharitinae are the only group within the Cynipoidea that show these adaptations and are the only ones which are associated with obviously defensible hosts. Field observations in the US (Arizona) on *Anacharis* specimens of unknown species show a characteristic positioning of the metasoma for oviposition that resembles that of aphidiine braconids (aphid parasitoids). The metasoma is bent downwards through the prancing legs, pointing forward in the direction of the host (Fig. 20). In this instance, the wasp was striking about five times over the course of one full minute, taking less than three seconds per strike (Kim Neubauer, pers. comm.).

Among the Anacharitinae in Northwestern Europe, *Anacharis* is the most commonly occurring genus. Yet, the taxonomic turmoil (Fergusson 1986; Mata-Casanova et al. 2018 and this study) has blurred the knowledge about life history of each species significantly, i.e. it is impossible to assign the few existing host records beyond species group level. As parasitoids of brown lacewing larvae, they play an arguably important role as natural regulators of these common aphidivorous insects that are also of economic importance (Stelzl and Devetak 1999). In order to understand the trophic interactions of aphids, their predators and parasitoids, knowledge about host-parasitoid relationships is fundamental, which in turn requires taxonomically stable taxa and unambiguously vouchered host records.

The DNA barcode dataset we provide is currently the most comprehensive dataset of *Anacharis* sequences worldwide and enabled us to connect European barcode data

of *A. eucharioides*, *A. petiolata* and *A. typica* with that of Nearctic (mainly Canadian) records that are publicly available on BOLD. As the available data grows, along with continued revisionary work, the barcode datasets will become increasingly useful to accelerate the accumulation of life history and distribution knowledge about the species treated herein as well as of currently unknown species in Europe and worldwide.

## Acknowledgements

The Federal Ministry of Education and Research of Germany (Bundesministerium für Bildung und Forschung, BMBF) is funding the project “GBOL III: Dark Taxa” as Research for Sustainable Development (Forschung für Nachhaltige Entwicklung, FONA; [www.fona.de](http://www.fona.de)) under the funding reference 16LI1901A.

We sincerely appreciate the invaluable input from the reviews of Louis Nastasi and Simon van Noort that led to the final version of this manuscript.

We want to express our gratitude to Ximo Mengual, Tobias Salden and Santiago Jaume Schinkel for practical advice regarding the preparation of the male genitalia. Ximo Mengual proved most helpful for introducing and troubleshooting the camera setup. Juliane Vehof gave a comprehensive introduction into and was available for constant troubleshooting with the Zeiss imaging setup.

For the procession of the data into the GBOL and BOLD databases, we are indebted to the GBOL core team at the ZFMK and want to specifically thank Jana Thormann.

We thank the administrative body and the research department of the Kellerwald Edersee National Park, in particular Carsten Morkel, for allowing the sampling with ten Malaise traps over a long period that yielded many interesting specimens.

We are grateful for the provision of samples by Andrius Petrašiūnas for the Lithuanian samples, Fons Verheyde, Augustijn de Ketelaere and Wouter Dekoninck for the Belgian and Dutch samples and Alf Tore Mjös for the Norwegian samples. We thank the staff of the Swedish Malaise Trap Project, Martti Koponen in Otava, Thorkild Munk in Aarhus (+), and curators of several Swiss museums (Giulio Cuccodoro at MHNG, Anne Freitag at MZL, Hannes Baur at NMBE), who had all provided samples in other connections years ago which turned out useful here. For the kind loan of barcode voucher specimens, we want to thank Lars Vilhemsen (ZMUC) & Stefan Schmidt (ZSM). In short, we want to thank all the collectors and curators, specifically mentioned or not, that made the study of the material possible.

We want to thank Alexandra Popa (MGAB) for the gratuitous loan of the holotype and a paratype of *A. gracilipes* and the permission to mount the specimens, Joseph Monks (NHMUK) for organising images of the Walker type specimens, the team at the CNC, especially Andrew Bennett and Amber Bass, for making the type images of *A. fergussoni* accessible, the team of the entomology section at the MZLU, especially Rune Bygberg and Christoffer Fägerström for the images of the MZLU type material and Stefan Schmidt, Olga Schmidt and Jeremy Hübner (ZSM) for making the Hartig types accessible.

We want to express our thanks for the support by Hege Vårdal (NHRS) for her help at several different stages of the manuscript's development, including the utterly kind hospitality during JV's visits to Stockholm.

We are grateful to Göran Nordlander and Matt Buffington for the continuous and exciting discussions about Cynipoid taxonomy and more.

We thank Santiago Jaume Schinkel and Fons Verheyde for testing the key and their precious comments that lead to its much-improved state.

For sharing her observations and images with us and allowing us to further share one of her images within this manuscript, we want to sincerely thank Kim Neubauer.

We are grateful to the International Society of Hymenopterists for their support.

## References

van Achterberg C, Shaw MR (2016) Revision of the Western Palaearctic species of *Aleiodes* Wesmael (Hymenoptera, Braconidae, Rogadinae). Part 1: Introduction, key to species groups, outlying distinctive species, and revisionary notes on some further species. ZooKeys 639: 1–164. <https://doi.org/10.3897/zookeys.639.10893>

Aspöck H, Aspöck U, Hölzel H (1980) 1 Die Neuropteren Europas: Eine zusammenfassende Darstellung der Systematik, Ökologie und Chorologie der Neuropteroidea (Megaloptera, Raphidioptera, Planipennia) Europas. Goecke & Evers, Krefeld, 495 pp.

Astrin JJ, Stüben PE (2008) Phylogeny in cryptic weevils: molecules, morphology and new genera of Western Palaearctic Cryptorhynchinae (Coleoptera: Curculionidae). Invertebrate Systematics 22(5): 503–522. <https://doi.org/10.1071/IS07057>

Awad J, Höcherl A, Hübner J, Jafari S, Moser M, Parsa M, Vogel J, Schmidt S, Krogmann L, Peters RS (2020) Just launched! GBOL III: Dark Taxa, a large research initiative focusing on German and Central European parasitoid wasps (and lower Diptera). Hamuli 11(2): 5–8.

Baur H (2015) Pushing the limits – two new species of *Pteromalus* (Hymenoptera, Chalcidoidea, Pteromalidae) from Central Europe with remarkable morphology. ZooKeys 514: 43–72. <https://doi.org/10.3897/zookeys.514.9910>

Baur H, Leuenberger C (2011) Analysis of ratios in multivariate morphometry. Systematic Biology 60(6): 813–825. <https://doi.org/10.1093/sysbio/syr061>

Baur H, Leuenberger C (2020) Multivariate Ratio Analysis (MRA): R-scripts and tutorials for calculating Shape PCA, Ratio Spectra and LDA Ratio Extractor. <https://doi.org/10.5281/ZENODO.4250142>

Buffington ML, Nylander JAA, Heraty JM (2007) The phylogeny and evolution of Figitidae (Hymenoptera: Cynipoidea). Cladistics 23 (5): 403–431. <https://doi.org/10.1111/j.1096-0031.2007.00153.x>

Buffington ML, Sandler RJ (2011) The Occurrence and Phylogenetic Implications of Wing Interference Patterns in Cynipoidea (Insecta: Hymenoptera). Invertebrate Systematics 25(6): 586. <https://doi.org/10.1071/IS11038>

Buffington ML, Condon M (2013) The description and bionomics of *Tropideucoila blepharon-eurae* Buffington and Condon, new species (Hymenoptera: Figitidae: Zaeucoilini), para-

sitoid of *Blepharoneura* Loew Fruit Flies (Tephritidae). Proceedings of the Entomological Society of Washington 115(4): 349–357. <https://doi.org/10.4289/0013-8797.115.4.349>

Buffington ML, Forshage M (2014) The description of *Garudella* Buffington and Forshage, new genus (Hymenoptera: Figitidae: Eucoilinae). Proceedings of the Entomological Society of Washington 116(3): 225–242. <https://doi.org/10.4289/0013-8797.116.3.225>

Buuren SV, Groothuis-Oudshoorn K (2011) mice: Multivariate Imputation by Chained Equations in R. Journal of Statistical Software 45(3): 1–67. <https://doi.org/10.18637/jss.v045.i03>

Cameron P (1890) A monograph of the British phytophagous Hymenoptera (*Tenthredo*, *Sirex* and *Cynips*, Linné.) Vol. III. Ray Society, London, 341 pp.

Cannet A, Simon-Chane C, Akhoudi M, Histace A, Romain O, Souchaud M, Jacob P, Delaunay P, Sereno D, Bousses P, Grebaut P, Geiger A, De Beer C, Kaba D, Sereno D (2022) Wing Interferential Patterns (WIPs) and machine learning, a step toward automatized tsetse (*Glossina* spp.) identification. Scientific Reports 12(1): 20086. <https://doi.org/10.1038/s41598-022-24522-w>

Cannet A, Simon-Chane C, Akhoudi M, Histace A, Romain O, Souchaud M, Jacob P, Sereno D, Mouline K, Barnabe C, Lardeux F, Boussès P, Sereno D (2023) Deep learning and wing interferential patterns identify *Anopheles* species and discriminate amongst Gambiae complex species. Scientific Reports 13(1): 13895. <https://doi.org/10.1038/s41598-023-41114-4>

Cave RD, Miller GL (1987) Notes on *Anacharis melanoneura* (Hymenoptera: Figitidae) and *Charitopes mellicornis* (Hymenoptera: Ichneumonidae) Parasitizing *Micromus posticus* (Neuroptera: Hemerobiidae). Entomological News 98(5): 211–216.

Dalman JW (1823) Analecta entomologica. Typis Lindhianis, Holmiae, 104 pp. <https://doi.org/10.5962/bhl.title.66069>

Dal Pos D, Mikó I, Talamas EJ, Vilhelmsen L, Sharanowski BJ (2023) A revised terminology for male genitalia in Hymenoptera (Insecta), with a special emphasis on Ichneumonoidea. PeerJ 11: e15874. <https://doi.org/10.7717/peerj.15874>

von Dalla-Torre KW, Kieffer J-J (1910) Das Tierreich: Cynipidae. R. Friedländer und Sohn, Berlin. <https://doi.org/10.5962/bhl.title.1077>

De Queiroz K (2007) Species concepts and species delimitation. Systematic Biology 56(6): 879–886. <https://doi.org/10.1080/10635150701701083>

Dietz L, Eberle J, Mayer C, Kukowka S, Bohacz C, Baur H, Espeland M, Huber BA, Hutter C, Mengual X, Peters RS, Vences M, Wesener T, Willmott K, Misof B, Niehuis O, Ahrens D (2022) Standardized nuclear markers improve and homogenize species delimitation in Metazoa. Methods in Ecology and Evolution 14(2): 543–555. <https://doi.org/10.1111/2041-210X.14041>

Edgar RC (2004) MUSCLE: A multiple sequence alignment method with reduced time and space complexity. BMC Bioinformatics 5(1): 113. <https://doi.org/10.1186/1471-2105-5-113>

Fergusson NDM (1986) Handbook for the Identification of British Insects: Charipidae, Ibalidae & Figitidae. Royal Entomological Society of London, London, 55 pp.

Fontal-Cazalla FM, Buffington ML, Nordlander G, Liljeblad J, Ros-Farre P, Nieves-Aldrey JL, Pujade-Villar J, Ronquist F (2002) Phylogeny of the Eucoilinae (Hymenoptera: Cynipoidea: Figitidae). Cladistics 18(2): 154–199. <https://doi.org/10.1111/j.1096-0031.2002.tb00147.x>

German Barcode of Life Consortium [Wägele W, Haszprunar G, Eder J, Xylander W, Borsch T, Quandt D, Grobe P, Pietsch S, Geiger M, Astrin J, Rulik B, Hausmann A, Morinier J, Holstein J, Krogmann L, Monje C, Traunspurger W, Hohberg K, Lehmitz R, Müller K, Nebel M, Hand R] (2011) GBOL. <https://www.bolgermany.de>

Handlirsch A (1886) Die Metamorphose zweier Arten der Gattung *Anacharis* Dalm.

Harris RA (1979) A glossary of surface sculpturing. Occasional Papers in Entomology 28: 1–31.

Hausmann A, Krogmann L, Peters RS, Rduch V, Schmidt S (2020) GBOL III: DARK TAXA. iBOL Barcode Bulletin 10(1): 1–4. <https://doi.org/10.21083/ibol.v10i1.6242>

Hawkes MF, Duffy E, Joag R, Skeats A, Radwan J, Wedell N, Sharma MD, Hosken DJ, Troscianko J (2019) Sexual selection drives the evolution of male wing interference patterns. Proceedings of the Royal Society B: Biological Sciences 286(1903): 20182850. <https://doi.org/10.1098/rspb.2018.2850>

Hayat M (2009) Records and descriptions of Trichogrammatidae from India (Hymenoptera: Chalcidoidea). Oriental Insects 43 (1): 201–227. <https://doi.org/10.1080/00305316.2009.10417583>

Hoang DT, Chernomor O, Von Haeseler A, Minh BQ, Vinh LS (2018) UFBoot2: Improving the Ultrafast Bootstrap Approximation. Molecular Biology and Evolution 35 (2): 518–522. <https://doi.org/10.1093/molbev/msx281>

Hosseini F, Lotfalizadeh H, Norouzi M, Dadpour M (2019) Wing interference colours in *Eurytoma* (Hymenoptera: Eurytomidae): Variation in patterns among populations and sexes of five species. Systematics and Biodiversity 17(7): 679–689. <https://doi.org/10.1080/14772000.2019.1687603>

ICZN [International Commission on Zoological Nomenclature] (1999) International Code of Zoological Nomenclature. 4<sup>th</sup> edn. The International Trust for Zoological Nomenclature, London.

Ionescu MA (1969) Hymenoptera Cynipoidea. Fauna Republicii Socialiste Romania Vol. 9 Fasc. 6: 290 pp.

Janšta P, Delvare G, Baur H, Wipfler B, Peters RS (2020) Data-rich description of a new genus of praying mantid egg parasitoids, *Lasallegrion* gen. n. (Hymenoptera: Torymidae: Podagrionini), with a re-examination of *Podagrion* species of Australia and New Caledonia. Journal of Natural History 54(9–12): 755–790. <https://doi.org/10.1080/00222933.2020.1778112>

Jafari S, Müller B, Rulik B, Rduch V, Peters RS (2023) Another crack in the Dark Taxa wall: a custom DNA barcoding protocol for the species-rich and common Eurytomidae (Hymenoptera, Chalcidoidea). Biodiversity Data Journal 11: e101998: 1–13. <https://doi.org/10.3897/BDJ.11.e101998>

Jin S, Parks KS, Janzen DH, Hallwachs W, Dyer LA, Whitfield JB (2023) The wing interference patterns (WIPs) of *Parapanteles* (Braconidae, Microgastrinae): demonstrating a powerful and accessible tool for species-level identification of small and clear winged insects. Journal of Hymenoptera Research 96: 967–982. <https://doi.org/10.3897/jhr.96.111382>

Kapli P, Lutteropp S, Zhang J, Kober K, Pavlidis P, Stamatakis A, Flouri T (2017) Multi-rate Poisson tree processes for single-locus species delimitation under maximum likelihood and Markov chain Monte Carlo. [Valencia A (Ed.)] Bioinformatics 33(11): 1630–1638. <https://doi.org/10.1093/bioinformatics/btx025>

Katayama N, Abbott JK, Kjærandsen J, Takahashi Y, Svensson EI (2014) Sexual Selection on Wing Interference Patterns in *Drosophila melanogaster*. *Proceedings of the National Academy of Sciences* 111(42): 15144–15148. <https://doi.org/10.1073/pnas.1407595111>

Kierych E (1984) Notes on the Genus *Prosynapsis* D.T. et Kieff. (*Synapsis* Forst.), with a List of *Anacharis* Dalm. Species Occurring in Poland (Hymenoptera, Cynipoidea, Anacharitidae). *Annales Zoologici* 37 (11): 335–340.

Markmann M, Tautz D (2005) Reverse taxonomy: an approach towards determining the diversity of meiobenthic organisms based on ribosomal RNA signature sequences. *Philosophical Transactions of the Royal Society B: Biological Sciences* 360(1462): 1917–1924. <https://doi.org/10.1098/rstb.2005.1723>

Mata-Casanova N, Selfa J, Pujade-Villar J (2018) Three new species of *Anacharis* Dalman, 1823 (Hymenoptera: Figitidae), with revised taxonomy and distribution records of palaearctic and indomalayan species. *European Journal of Taxonomy* 414: 1–25. <https://doi.org/10.5852/ejt.2018.414>

Mata-Casanova N, Selfa J, Wang Y, Chen X-X, Pujade-Villar J (2016) Diversity of subfamily Anacharitinae (Hymenoptera: Cynipoidea: Figitidae) in China with description of a new species of *Xyalaspis* Hartig, 1843. *Journal of Asia-Pacific Entomology* 19(1): 9–14. <https://doi.org/10.1016/j.aspen.2015.11.007>

Meier R, Shiyang K, Vaidya G, Ng PKL (2006) DNA barcoding and taxonomy in diptera: A tale of high intraspecific variability and low identification success. [Hedin M (Ed.)] *Systematic Biology* 55(5): 715–728. <https://doi.org/10.1080/10635150600969864>

Meier R, Blaimer BB, Buenaventura E, Hartop E, vonRintelen T, Srivathsan A, Yeo D (2022) A re-analysis of the data in Sharkey et al.'s (2021) minimalist revision reveals that BINs do not deserve names, but BOLD Systems needs a stronger commitment to open science. *Cladistics* 38: 264–275. <https://doi.org/10.1111/cla.12489>

Mikó I, Masner L, Johannes E, Yoder MJ, Deans AR (2013) Male terminalia of Ceraphronoidea: morphological diversity in an otherwise monotonous taxon. *Insect Systematics & Evolution* 44(3–4): 261–347. <https://doi.org/10.1163/1876312X-04402002>

Miller GL, Lambdin PL (1985) Observations on *Anacharis melanoneura* (Hymenoptera: Figitidae), a Parasite of *Hemerobius stigma* (Neuroptera: Hemerobiidae). *Entomological News* 96(3): 93–97.

Minh BQ, Schmidt HA, Chernomor O, Schrempf D, Woodhams MD, Von Haeseler A, Lanfear R (2020) IQ-TREE 2: New Models and Efficient Methods for Phylogenetic Inference in the Genomic Era. *Molecular Biology and Evolution* 37(5): 1530–1534. <https://doi.org/10.1093/molbev/msaa015>

Moser M, Ulmer JM, Van De Kamp T, Vasilić C, Renninger M, Mikó I, Krogmann L (2023) Surprising morphological diversity in ceraphronid wasps revealed by a distinctive new species of *Aphanogmus* (Hymenoptera: Ceraphronoidea). *European Journal of Taxonomy* 864: 146–166. <https://doi.org/10.5852/ejt.2023.864.2095>

van Noort S, Buffington ML, Forshage M (2015) Afrotropical Cynipoidea (Hymenoptera). *ZooKeys* 494: 1–176. <https://doi.org/10.3897/zookeys.493.6353>

Polaszek A, Fusu L, Viggiani G, Hall A, Hanson P, Polilov AA (2022) Revision of the World Species of *Megaphragma* Timberlake (Hymenoptera: Trichogrammatidae). *Insects* 13(6): 561. <https://doi.org/10.3390/insects13060561>

Puillandre N, Brouillet S, Achaz G (2021) ASAP: assemble species by automatic partitioning. *Molecular Ecology Resources* 21(2): 609–620. <https://doi.org/10.1111/1755-0998.13281>

Ratnasingham S, Hebert PDN (2007) Barcoding BOLD: The Barcode of Life Data System ([www.barcodinglife.org](http://www.barcodinglife.org)). *Molecular Ecology Notes* 7(3): 355–364. <https://doi.org/10.1111/j.1471-8286.2007.01678.x>

Ratnasingham S, Hebert PDN (2013) A DNA-Based Registry for All Animal Species: The Barcode Index Number (BIN) System. [Fontaneto D (Ed.)] *PLoS ONE* 8(7): e66213. <https://doi.org/10.1371/journal.pone.0066213>

Reinhard H (1860) Die Figitiden des mittlern Europa. *Berliner Entomologische Zeitschrift* 4: 204–245.

Ronquist F, Nordlander G (1989) Skeletal morphology of an archaic cynipoid, *Ibalia rufipes* (Hymenoptera: Ibaliidae). *Entomologica Scandinavica Supplement No. 33*: 1–62.

Salden T, Peters RS (2023) Afrotropical Ceraphronoidea (Insecta: Hymenoptera) put back on the map with the description of 88 new species. *European Journal of Taxonomy* 884: 1–386. <https://doi.org/10.5852/ejt.2023.884.2181>

Schulmeister S, Wheeler WC, Carpenter JM (2002) Simultaneous analysis of the basal lineages of Hymenoptera (Insecta) using sensitivity analysis. *Cladistics* 18 (5): 455–484. <https://doi.org/10.1111/j.1096-0031.2002.tb00287.x>

Shevtsova E, Hansson C (2011) Species recognition through wing interference patterns (WIPs) in *Achrysocharoides* Girault (Hymenoptera, Eulophidae) including two new species. *ZooKeys* 154: 9–30. <https://doi.org/10.3897/zookeys.154.2158>

Shevtsova E, Hansson C, Janzen DH, Kjærandsen J (2011) Stable structural color patterns displayed on transparent insect wings. *Proceedings of the National Academy of Sciences* 108(2): 668–673. <https://doi.org/10.1073/pnas.1017393108>

Stelzl M, Devetak D (1999) Neuroptera in agricultural ecosystems. *Agriculture, Ecosystems and Environment* 74(1–3): 305–321. [https://doi.org/10.1016/S0167-8809\(99\)00040-7](https://doi.org/10.1016/S0167-8809(99)00040-7)

Thomson CG (1862) Försök Till Uppställning och Beskrifning af Sveriges Figiter. *Öfversigt af Kongl. Vetenskaps-akademiens förhandlingar* 18: 395–420.

Trietsch C, Mikó I, Notton D, Deans A (2018) Unique extrication structure in a new megaspilid, *Dendrocerus scutellaris* Trietsch & Mikó (Hymenoptera: Megaspilidae). *Biodiversity Data Journal* 6: e22676. <https://doi.org/10.3897/BDJ.6.e22676>

Verhandlungen Der Kaiserlich-Königlichen Zoologisch-Botanischen Gesellschaft in Wien 36: 235–238.

Walker F (1835) Description of Some British Species of *Anacharis*. *Entomological Magazine* 2: 518–522.

Weld LH (1952) Cynipoidea (Hym.) 1905–1950 Being a Supplement to the Dalla-Torre and Kieffer Monograph - the Cynipidae in *Das Tierreich*, Lieferung 24, 1910 and Bringing the Systematic Literature of the World up to Date, Including Keys to Families and Subfamilies and Lists of New Generic, Specific and Variety Names. Privately printed, Ann Arbor, Michigan, 351 pp.

Westwood JO (1833) Notice of the habits of a cynipideous insect, parasitic upon the rose louse (*Aphis rosae*); with descriptions of several other parasitic hymenoptera. *Magazine of Natural History* 6: 491–497.

Zetterstedt JW (1822) Resa genom Sveriges och Norriges lappmarker, förrättad år 1821. Berling, Lund, 1–2[: 266 + 232 pp].

Zetterstedt JW (1838) pt. 2. In: Insecta Lapponica. Lipsiae [Leipzig], 220 pp.

Žikić V, Van Achterberg C, Stanković SS, Ilić M (2011) The male genitalia in the subfamily Agathidinae (Hymenoptera: Braconidae): Morphological information of species on generic level. Zoologischer Anzeiger - A Journal of Comparative Zoology 250(3): 246–257. <https://doi.org/10.1016/j.jcz.2011.04.006>

## Supplementary material 1

### Material examined

Authors: Jonathan Vogel, Mattias Forshage

Data type: xlsx

Explanation note: Listing all material examined, including BOLD IDs if available.

Was used as a basis for the material examined sections of each respective species.

Contains all nine species.

Copyright notice: This dataset is made available under the Open Database License (<http://opendatacommons.org/licenses/odbl/1.0/>). The Open Database License (ODbL) is a license agreement intended to allow users to freely share, modify, and use this Dataset while maintaining this same freedom for others, provided that the original source and author(s) are credited.

Link: <https://doi.org/10.3897/jhr.97.131350.suppl1>

## Supplementary material 2

### Foreign BOLD IDs

Author: Jonathan Vogel

Data type: xlsx

Explanation note: BOLD IDs of the sequences accessed via BOLD that were neither examined morphologically, nor produced herein.

Copyright notice: This dataset is made available under the Open Database License (<http://opendatacommons.org/licenses/odbl/1.0/>). The Open Database License (ODbL) is a license agreement intended to allow users to freely share, modify, and use this Dataset while maintaining this same freedom for others, provided that the original source and author(s) are credited.

Link: <https://doi.org/10.3897/jhr.97.131350.suppl2>

## Supplementary material 3

### Morphometry analysis: Raw data

Authors: Jonathan Vogel, Christoph Braun

Data type: xlsx

Explanation note: The raw data that was used to run the morphometric analyses, prior to the imputation script.

Copyright notice: This dataset is made available under the Open Database License (<http://opendatacommons.org/licenses/odbl/1.0/>). The Open Database License (ODbL) is a license agreement intended to allow users to freely share, modify, and use this Dataset while maintaining this same freedom for others, provided that the original source and author(s) are credited.

Link: <https://doi.org/10.3897/jhr.97.131350.suppl3>

## Supplementary material 4

### Imputed morphometric data

Author: Christoph Braun

Data type: xlsx

Explanation note: The imputed morphometric data that was used for the morphometric analyses.

Copyright notice: This dataset is made available under the Open Database License (<http://opendatacommons.org/licenses/odbl/1.0/>). The Open Database License (ODbL) is a license agreement intended to allow users to freely share, modify, and use this Dataset while maintaining this same freedom for others, provided that the original source and author(s) are credited.

Link: <https://doi.org/10.3897/jhr.97.131350.suppl4>

## Supplementary material 5

### Additional results from morphometry

Author: Christoph Braun

Data type: pdf

Explanation note: Documentation of additional results from morphometry: PCA and ratio extractor results of the species-level analyses not shown in the manuscript as well as the results of the allometry tests of all species group- and species-level comparisons.

Copyright notice: This dataset is made available under the Open Database License (<http://opendatacommons.org/licenses/odbl/1.0/>). The Open Database License (ODbL) is a license agreement intended to allow users to freely share, modify, and use this Dataset while maintaining this same freedom for others, provided that the original source and author(s) are credited.

Link: <https://doi.org/10.3897/jhr.97.131350.suppl5>